SIMPLIFIED ASSESSMENT PROCEDURE TO DETERMINE THE SEISMIC VULNERABILITY OF REINFORCED CONCRETE BRIDGES IN INDIANA

by

Farida I. Mahmud

A Thesis

Submitted to the Faculty of Purdue University

In Partial Fulfillment of the Requirements for the degree of

Master of Science in Civil Engineering

Lyles School of Civil Engineering

West Lafayette, Indiana

August 2019

THE PURDUE UNIVERSITY GRADUATE SCHOOL
STATEMENT OF COMMITTEE APPROVAL

Dr. Shirley Dyke, Co-Chair

Department of Mechanical Engineering and Lyles School of Civil Engineering

Dr. Julio Ramirez, Co-Chair

Lyles School of Civil Engineering

Dr. Christopher Williams

Lyles School of Civil Engineering

Approved by:

Dr. Dulcy Abraham

Head of the Graduate Program

To my family

ACKNOWLEDGMENTS

Firstly, I would like to acknowledge the Joint Transportation Research Program (JTRP) for funding this project. Without them, my education at Purdue would not have been possible.

I would like to express my gratitude to my advisors, Dr. Shirley Dyke and Dr. Julio Ramirez for their support, guidance, and knowledge throughout this project. I am grateful for the opportunity to work with both of them, and my experience on this project exceeded my expectations. I would also like to thank Dr. Christopher Williams for being on my committee and for his insightful comments.

Additionally, I would like to recognize my lab mates, Leslie Bonthron and Corey Beck, for the continuous assistance during this project. Corey was instrumental in automating the Matlab code, and I am thankful for that. I am thankful for Leslie's help with various aspects of this project and the continuous exchange of ideas. Working with both of them has been a pleasant experience.

Special thanks to Sijia Wang for being a supportive friend during my time at Purdue. Without her, my experience at Purdue would have been different. I am ever so grateful for her friendship. I would also like to thank Herta Montoya, my friends of HAMP 1212, and my classmates for making my time at Purdue most memorable.

Lastly, I would like to thank my parents for teaching me to believe I could achieve anything, and their immense support and sacrifices throughout my academic career. Their love and encouragement continue to inspire me to pursue my dreams. Without them, I will not be where I am today.

TABLE OF CONTENTS

LIST OF TABLES viii
LIST OF FIGURES x
NOMENCLATURE xvi
ABSTRACT xviii
1. INTRODUCTION 1
1.1 Objective 1
1.2 Organization 2
2. LITERATURE REVIEW 3
2.1 Introduction 3
2.2 Seismicity in Indiana 3
2.2.1 New Madrid Seismic Zone 4
2.2.2 Wabash Valley Seismic Zone 5
2.3 Literature Review of the Seismic Vulnerability Assessment and Methods of Bridges 5
2.4 Lessons Extracted from the Literature Review 10
2.5 Summary 13
3. LEVEL 2 ASSESSMENT OF SELECTED BRIDGES 14
3.1 Introduction 14
3.2 Bridge Selection Process 14
3.2.1 Selected Bridges 15
3.3 Analysis of Single Span Bridges 16
3.4 2-D Finite Element Modelling Procedure 17
3.4.1 Finite Element Model of Bridges with Multi-Column Bents 19
3.4.2 Finite Element Model of Bridges with Wall-type Bents 26
3.4.3 Force and Displacement Demand 27
3.5 Capacity of Bridge Elements 28
3.5.1 Substructure 28
3.5.2 Bearing Support Length 31
3.6 Results from the Analysis of Selected Bridges 31
3.6.1 Bridge Asset Name: 067-42-07298 31

3.6.1.1 Results – Transverse Direction 33
3.6.1.2 Results – Longitudinal Direction 33
3.6.2 Bridge Asset Name: 041-42-5080 BNBL 34
3.6.2.1 Results – Transverse Direction 36
3.6.2.2 Results – Longitudinal Direction 37
3.6.3 Bridge Asset Name: 066-13-05443 A 38
3.6.3.1 Results – Transverse Direction 41
3.6.3.2 Results – Longitudinal Direction 42
3.7 Conclusions 44
3.8 Summary 45
4. LEVEL 1 ASSESSMENT PROCEDURE 46
4.1 Introduction 46
4.2 Level 1 Assessment Procedure 46
4.3 Initial Screening of Bridges 47
4.4 Information Available in BIAS 47
4.5 Assumptions and Validations 48
4.5.1 Mass Estimate for Slab Bridges 48
4.5.2 Substructure Height 51
4.5.3 Pile Size and Material Properties 53
4.5.4 Number of Piles 55
4.6 Bridge Vulnerability Criteria 56
4.7 Incremental Development of the Level 1 Assessment Procedure 57
4.7.1 Base Model 57
4.7.2 Results and Validation 58
4.8 Improved Models 60
4.8.1 Option A 60
4.8.2 Results and Validation 60
4.8.3 Option B 62
4.8.4 Results and Validation 62
4.8.5 Option C 64
4.8.6 Results and Validation 64

4.9 Summary 66
5. DEMONSTRATION OF THE LEVEL 1 ASSESSMENT OF SELECTED BRIDGES 68
5.1 Introduction 68
5.2 Simplified Assessment of the Selected bridges 68
5.2.1 Procedure for Determining Demand 68
5.2.2 Preliminary Screening Results 69
5.2.3 Results of the Simplified Assessment 69
5.3 Summary 70
6. CONCLUSIONS AND RECOMMENDATIONS 71
6.1 Conclusions 71
6.2 Implementation Recommendations for INDOT 72
6.3 Future Work 73
REFERENCES 74
APPENDIX. LEVEL 2 ASSESSMENT RESULTS 78

LIST OF TABLES

Table 3-1: Selected Reinforced Concrete Bridges 15
Table 3-2: Stiffness Matrix and Displacement Vector of a Beam Element 20
Table 3-3: Transverse Stiffness Matrix Corresponding to the Bent in Figure 3-2 21
Table 3-4: Stiffness Matrix and Displacement Vector of a Beam Element Including Shear Effects 23
Table 3-5: Deck Stiffness Matrix Corresponding to Figure 3-6 – Transverse Direction 24
Table 3-6: Mass Matrix of a Three Span Bridge in the Transverse Direction 25
Table 4-1: NBI Numbers of Bridges Used for Validation in this Chapter 49
Table 4-2: Comparison of Performance Using the Base Model to that of the Level 2 Assessment 59
Table 4-3: Comparison of Performance Using Improved Model A to that of the Level 2 Assessment 61
Table 4-4: Comparison of Performance Using Improved Model B to that of the Level 2 Assessment 63
Table 4-5: Comparison of Performance Using Improved Model B to that of the Level 2 Assessment 66
Table 5-1: Simplified Assessment Results Using Base Model 69
Table 5-2: Simplified Assessment Results Using Improved Model A 70
Table 5-3: Simplified Assessment Results Using Improved Model B 70
Table 5-4: Simplified Assessment Results Using Improved Model C 70
Table A.1: Specifications and Information on Bridge (237) 37-13-07277 78
Table A.2: Specifications and Information on Bridge 55-45-07366 81
Table A.3: Specifications and Information on Bridge 56-63-07286 84
Table A.4: Specifications and Information on Bridge 252-55-08713 87
Table A.5: Specifications and Information on Bridge 28-79-07672 90
Table A.6: Specifications and Information on Bridge 327-17-06419A 93
Table A.7: Table Specifications and Information on Bridge 44-55-06793 96
Table A.8: Specifications and Information on Bridge 57-14-06739 99
Table A.9: Specifications and Information on Bridge 252-24-06934A 102

Table A.10: Specifications and Information on Bridge 64-19-03723A 105
Table A.11: Specifications and Information on Bridge 67-55-03831ANBL 110
Table A.12: Specifications and Information on Bridge I69-334-04590BNB..... 114
Table A.13: Specifications and Information on Bridge 63-86-05970BNBL..... 118
Table A.14: Specifications and Information on Bridge I70-112-05137 DEBL..... 122
Table A.15: Specifications and Information on Bridge 18-05-06573 126
Table A.16: Specifications and Information on Bridge 22-27-04724 130
Table A.17: Specifications and Information on Bridge 75-06-04958A 135
Table A.18: Specifications and Information on Bridge 64-63-03590A 140
Table A.19: Specifications and Information on Bridge 41-56-03828 BSBL 145
Table A.20: Specifications and Information on Bridge 24-56-00899B..... 150
Table A.21: Specifications and Information on Bridge 67-28-00938A 151
Table A.22: Specifications and Information on Bridge I69-30-9187NB 152

LIST OF FIGURES

Figure 2-1: Earthquakes in the New Madrid and Wabash Valley Seismic Zones Prior to 2002 (USGS, 2002) 4
Figure 2-2: Selected Emergency Routes in the Vincennes District (Sozen et al., 2005) 6
Figure 2-3: Description of Bridge Damage States (after Choi et al., 2004) 9
Figure 2-4: Bridge Failure Due to Unseating at Support During the 1994 Northridge California Earthquake (Sozen et al., 2005) 11
Figure 2-5: Column Failure of a Bridge During the 1994 Northridge California Earthquake (Sozen et. al., 2005) 12
Figure 2-6: Failure of an Elastomeric Bearing Due to Excessive Longitudinal Displacement (Ramirez et al., 2000) 12
Figure 3-1: Displacement Response Spectra of a Site in Vincennes District 17
Figure 3-2: Multi-Column Bent Substructure (BIAS,2018) 18
Figure 3-3: Wall Type Substructure (BIAS, 2018) 19
Figure 3-4: Transverse Elevation of an Interior Bent with Degrees-of-Freedom Shown 20
Figure 3-5: INDOT Standard Pile Sections (INDOT, 2012) 22
Figure 3-6: Plan View of the Deck of a Three Span Bridge with Degrees of Freedom Shown ... 23
Figure 3-7: SDOF Model of the Bridge in the Longitudinal Direction 25
Figure 3-8: Mechanism 1 – Hinges Forming in the Columns/Piles Only 28
Figure 3-9: Mechanism 2 – Hinges Forming in Both the Beams and the Columns/Piles 28
Figure 3-10: Elevation View of the Bridge (INDOT, 1996) 32
Figure 3-11: Transverse Elevation View of the Interior Bents (INDOT, 1996) 32
Figure 3-12: Section C-C of Figure 3-9 (INDOT, 1996) 32
Figure 3-13: Elevation View of the Bridge (INDOT, 2009) 34
Figure 3-14: Transverse Elevation View of Interior Bents (INDOT, 2009) 35
Figure 3-15: Cross-Section of Column Members (INDOT, 2009) 35
Figure 3-16: Cross-Section of Bent Cap (INDOT, 2009) 35
Figure 3-17: Shear Demand Due to Applied Ground Motions – Transverse Direction 37
Figure 3-18: Shear Demand Due to Applied Ground Motions – Longitudinal Direction 38
Figure 3-19: Elevation View of the Bridge (INDOT, 1999) 39

Figure 3-20: Anchorage of Approach Slab and Bridge Deck (INDOT, 1999)..... 39
Figure 3-21: Transverse Elevation and Reinforcement Details of Bent #2 (INDOT,1999)..... 40
Figure 3-22: Transverse Elevation and Reinforcement Details of Bent #3 (INDOT, 1999)..... 40
Figure 3-23: Shear Demand Due to Applied Ground Motions – Transverse Direction 42
Figure 3-24: Shear Demand Due to Applied Ground Motions – Longitudinal Direction 43
Figure 4-1: Level 1 Assessment Procedure 46
Figure 4-2: Comparison of Mass Estimated Based on Assumed Deck Thickness with Mass Calculated Using the Level 2 Assessment 50
Figure 4-3: Comparison of Period Estimated Based on Assumed Mass with Period Calculated Using the Level 2 Assessment 50
Figure 4-4: Comparison of Stiffness Estimated Based on Assumed Height with Stiffness Calculated Using the Level 2 Assessment 52
Figure 4-5: Comparison of Period Estimated Based on Assumed Height with Period Calculated Using the Level 2 Assessment 52
Figure 4-6: Comparison of Stiffness Estimated Based on Assumed Pile Size and Properties with Stiffness Calculated Using the Level 2 Assessment 54
Figure 4-7: Comparison of Period Estimated Based on Assumed Pile Size and Properties with Period Calculated Using the Level 2 Assessment..... 54
Figure 4-8: Comparison of Stiffness Estimated Based on Assumed Pile Size Number of Piles with Stiffness Calculated Using the Level 2 Assessment 55
Figure 4-9: Comparison of Period Estimated Based on Assumed Pile Size Number of Piles with Period Calculated Using the Level 2 Assessment..... 56
Figure 4-10: Process for Development of the Level 1 Assessment Procedure..... 57
Figure 4-11: Information Used to Obtain Base Model 58
Figure 4-12: Comparison Between the Period Determined in the Level 2 Assessment with that of the Base Model 58
Figure 4-13: Information Used to Obtain Improved Model A 60
Figure 4-14: Comparison Between the Period Determined in the Level 2 Assessment with that of Improved Model A..... 61
Figure 4-15: Information Used to Obtain Improved Model B..... 62

Figure 4-16: Comparison Between the Period Determined in the Level 2 Assessment with that of Improved Model B 63
Figure 4-17: Information Used to Obtain Improved Model C 64
Figure 4-18: Comparison Between the Period Determined in the Level 2 Assessment with that of Improved Model C 65
Figure 5-1: NEHRP-2015 Design Spectra for 064-19-03723 A (USGS, 2015) 68
Figure A-1: Elevation View of the Bridge (INDOT, 1994) 79
Figure A-2: Transverse Elevation View of the Interior Bents (INDOT, 1994) 79
Figure A-3: Section D-D of Figure A-2 (INDOT, 1994) 79
Figure A-4: Elevation View of the Bridge (INDOT, 1992) 81
Figure A-5: Transverse Elevation View of the Interior Bents (INDOT, 1992) 82
Figure A-6: Section D-D of Figure A.5 (INDOT, 1992) 82
Figure A-7: Elevation View of the Bridge (INDOT, 1992) 84
Figure A-8: Transverse Elevation View of the Interior Bents (INDOT, 1992) 85
Figure A-9: Section View of Figure A-8 (INDOT, 1992) 85
Figure A-10: Elevation View of the Bridge (INDOT, 2013) 87
Figure A-11: Transverse Elevation View of the Interior Bents (INDOT, 2013) 88
Figure A-12: Section E-E of Figure A-11 (INDOT, 2013) 88
Figure A-13: Elevation View of the Bridge (INDOT, 1995) 90
Figure A-14: Transverse Elevation View of the Interior Bents (INDOT, 1995) 91
Figure A-15: Section B-B of Figure A-14 (INDOT, 1995) 91
Figure A-16: Elevation View of the Bridge (INDOT, 2016) 93
Figure A-17: Transverse Elevation View of the Interior Bents (INDOT, 2016) 94
Figure A-18: Section View of Figure A-17 (INDOT, 2016) 94
Figure A-19: Elevation View of the Bridge (INDOT, 1980) 96
Figure A-20: Transverse Elevation View of the Interior Bents to Center Line (INDOT, 1980) .. 97
Figure A-21: Section View of Figure A-19 (INDOT, 1980) 97
Figure A-22: Elevation View of the Bridge (INDOT, 1982) 99
Figure A-23: Transverse Elevation View of the Interior Bents (INDOT, 1982) 100
Figure A-24: Section View of Figure A-23 (INDOT, 1982) 100
Figure A-25: Elevation View of the Bridge (INDOT, 1985) 102

Figure A-26: Transverse Elevation View of the Interior Bents (INDOT, 1985) 103
Figure A-27: Section View of Figure A-26 (INDOT, 1985) 103
Figure A-28: Elevation View of the Bridge (INDOT, 1984) 105
Figure A-29: Transverse Elevation View of the Interior Bents (INDOT, 1984) 106
Figure A-30: Section B-B of Figure A-29 (INDOT, 1984) 106
Figure A-31: Bearing Support at Abutments (INDOT, 1984) 106
Figure A-32: Shear Demand Due to Applied Ground Motions – Transverse Direction 108
Figure A-33: Shear Demand Due to Applied Ground Motions – Longitudinal Direction 109
Figure A-34: Elevation View of the Bridge (INDOT, 1992) 110
Figure A-35: Transverse Elevation View of Interior Bents (INDOT, 1992) 111
Figure A-36: Section F-F of Figure A-35 (INDOT, 1992) 111
Figure A-37: Bearing Support at Abutments (INDOT, 1992) 111
Figure A-38: Shear Demand Due to Applied Ground Motions – Transverse Direction 112
Figure A-39: Shear Demand Due to Applied Ground Motions – Longitudinal Direction 113
Figure A-40: Elevation View of the Bridge (INDOT, 1997) 114
Figure A-41: Transverse Elevation View of Interior Bents (INDOT, 1997) 115
Figure A-42: Section B-B of Figure A-41 (INDOT, 1997) 115
Figure A-43: Bearing Support at Abutments (INDOT, 1997) 115
Figure A-44: Shear Demand Due to Applied Ground Motions – Transverse Direction 116
Figure A-45: Shear Demand Due to Applied Ground Motions – Longitudinal Direction 117
Figure A-46: Elevation View of the Bridge (INDOT, 2014) 118
Figure A-47: Transverse Elevation View of Interior Bents (INDOT, 2014) 119
Figure A-48: Bearing Support at Abutments (INDOT, 2014) 119
Figure A-49: Shear Demand Due to Applied Ground Motions – Transverse Direction 120
Figure A-50: Shear Demand Due to Applied Ground Motions – Longitudinal Direction 121
Figure A-51: Elevation View of the Bridge (INDOT, 1994) 122
Figure A-52: Transverse Elevation View of Interior Bents (INDOT, 1994) 123
Figure A-53: Bearing Support at Abutments (INDOT, 1994) 123
Figure A-54: Shear Demand Due to Applied Ground Motions – Transverse Direction 124
Figure A-55: Shear Demand Due to Applied Ground Motions – Longitudinal Direction 125
Figure A-56: Elevation View of the Bridge (INDOT, 1985) 126

Figure A-57: Transverse Elevation View of Interior Bents (INDOT, 1985)..... 127
Figure A-58: Bearing Support at Abutments (INDOT, 1985)..... 127
Figure A-59: Shear Demand Due to Applied Ground Motions – Transverse Direction 128
Figure A-60: Shear Demand Due to Applied Ground Motions – Longitudinal Direction 129
Figure A-61: Elevation View of the Bridge (INDOT, 1999)..... 130
Figure A-62: Transverse Elevation View of Interior Bents #3 and #5 (INDOT, 1999)..... 131
Figure A-63: Transverse Elevation View of Interior Bent #4 (INDOT, 1999) 131
Figure A-64: Elevation of Girder Section (INDOT, 1999)..... 131
Figure A-65: Bearing Support at Abutments (INDOT, 1999)..... 132
Figure A-66: Shear Demand Due to Applied Ground Motions – Transverse Direction 133
Figure A-67: Shear Demand Due to Applied Ground Motions – Longitudinal Direction 134
Figure A-68: Elevation View of the Bridge (INDOT, 1981)..... 135
Figure A-69: Transverse Elevation View of Interior Bents #2 and #4 (INDOT, 1981)..... 136
Figure A-70: Transverse Elevation View of Interior Bents #3 (INDOT, 1981)..... 136
Figure A-71: Cross-Section of the Column Members and Bent Cap (INDOT, 1981) 136
Figure A-72: Elevation View of Girders (INDOT, 1981) 137
Figure A-73: Shear Demand Due to Applied Ground Motions – Transverse Direction 138
Figure A-74: Shear Demand Due to Applied Ground Motions – Longitudinal Direction 139
Figure A-75: Elevation View of the Bridge (INDOT, 1979)..... 140
Figure A-76: Transverse Elevation View of Interior Bents (INDOT, 1979)..... 141
Figure A-77: Section U-U of Figure A-76 (INDOT, 1979)..... 141
Figure A-78:Cross-Section of Precast Concrete Piles (INDOT, 1940) 141
Figure A-79: Cross-Section of Bridge Superstructure (INDOT, 1979)..... 142
Figure A-80: Shear Demand Due to Applied Ground Motions – Transverse Direction 143
Figure A-81: Shear Demand Due to Applied Ground Motions – Longitudinal Direction 144
Figure A-82: Elevation View of the Bridge (INDOT, 1996)..... 145
Figure A-83: Transverse Elevation View of Interior Bents (INDOT, 1996)..... 146
Figure A-84: Section U-U of Figure A-89 (INDOT, 1996)..... 146
Figure A-85:Cross-Section of Precast Concrete Piles (INDOT, 1940) 146
Figure A-86: Cross-Section of Bridge Superstructure (INDOT, 1996)..... 147
Figure A-87: Shear Demand Due to Applied Ground Motions – Transverse Direction 148

Figure A-88: Shear Demand Due to Applied Ground Motions – Longitudinal Direction 149
Figure A-89: Elevation View of the Bridge (INDOT, 1991)..... 150
Figure A-90: Elevation View of the Bridge (INDOT, 1980)..... 151
Figure A-91: Elevation View of the Bridge (INDOT, 2010)..... 152

NOMENCLATURE

A	Gross plan area of elastomer (in^2)
A_s	Area of shear reinforcement (in^2)
A_v	Shear area (in^2)
b	Width of compression face of member (in)
C	Damping (kip*sec/in)
d_s	Distance from the extreme compression fiber to the centroid of longitudinal reinforcement (in)
d	Displacement vector of a beam element
E	Modulus of elasticity of column (ksi)
E_d	Modulus of elasticity of deck (ksi)
f'_c	Compressive strength of concrete (psi)
f_y	Yield strength of reinforcement (ksi)
F	Inertia force due to the ground motions (kips)
G	Shear modulus of concrete (ksi)
G_e	Effective shear modulus of elastomer (ksi)
h	Height of member (in)
h_r	Total thickness of elastomer (in)
I	Moment of inertia of a member (in^4)
H_J	Average height of columns supporting the bridge deck to the next expansion joint for abutments, and column or pier height for columns or piers (ft)
I_d	Moment of inertia of deck (in^4)
k_{00}	Elements in a stiffness matrix corresponding to pure rotation
k_{0t}	Elements in a stiffness matrix corresponding to rotation and translation
k_{t0}	Elements in a stiffness matrix corresponding to translation and rotation
k_{tt}	Elements in a stiffness matrix corresponding to pure translation
$\hat{k}_{tt}$	Condensed stiffness matrix
K	Stiffness (kips/in)
K_I	Stiffness of the bridge using the simplified assessment procedure (kips/in)
l_n	Clear span of member (ft)
l_p	Hinge length (in)
L	Length of a member (in)
L_{BS}	Minimum bearing support length (in)
L_J	Length of the bridge deck to the adjacent expansion joint or to the end of the bridge deck (ft)
L_s	Span length from bent to bent (in)
$mass_{bent1}$	Mass of the bridge supported by the first intermediate bent (kips/g)
$mass_{bent2}$	Mass of the bridge supported by the second intermediate bent (kips/g)
M	Mass of the bridge (kips/g)
M_I	Mass of the bridge using the simplified assessment procedure (kips/g)
M_p	Plastic moment of member (ft-kip)
N	Normal force (kips)
N_b	Number of intermediate bents

N_{bolts}	Number of anchor bolts at both abutments
N_c	Number of columns or piles per bent
S	Skew angle of support (degrees)
S_a	Spectral acceleration (g)
S_d	Spectral displacement (in)
T	Period of the bridge (seconds)
T_I	Period of the bridge using the simplified assessment procedure (seconds)
u	Modal displacement (in)
U	Total displacement (in)
V_c	Nominal shear strength from concrete (lb)
V_{cN}	Strength to overcome friction force associated with normal force (kips)
V_{conn}	Strength of shear friction connection (kips)
V_n	Nominal shear strength (lb)
V_s	Nominal shear strength from steel (lb)
V_{sf}	Strength of shear friction connection provided by reinforcement (kips)
V_u	Shear resultant (kips)
z	Distance to moment contra-flexure (in)
δ_u	Ultimate inelastic displacement (in)
η	Poisson's ratio
θ_u	Ultimate inelastic rotation (radians)
μ	Shear term
μ_f	Coefficient of friction for concrete on concrete = 0.6
φ_u	Ultimate curvature (1/in)
Φ	Mode shape
ω_n	Natural frequency (rad/s)

ABSTRACT

Author: Mahmud, Farida, I. MSCE
Institution: Purdue University
Degree Received: August 2019
Title: Simplified Assessment Procedure to Determine the Seismic Vulnerability of Reinforced Concrete Bridges in Indiana
Committee Chair: Shirley Dyke and Julio Ramirez

The possibility of earthquakes in Indiana due to the presence of the New Madrid Seismic Zone is well known. However, the identification of the Wabash Valley Seismic Zone has increased our understanding of the seismic hazard in the state of Indiana. Due to this awareness of the increased potential for earthquakes, specifically in the Vincennes District, the seismic vulnerability of Indiana's bridge network must be assessed. As such, the objective of this thesis is to develop a simplified assessment procedure that can be used to conduct a state-wide seismic vulnerability assessment of reinforced concrete bridges in Indiana.

Across the state, variability in substructure type, seismic hazard level, and soil site class influences the vulnerability of bridges. To fully understand the impact of this variation, a detailed assessment is completed on a representative sample. Twenty-five reinforced concrete bridges are selected across the state, and analyzed using information from the bridge drawings and a finite element analysis procedure. These bridges are analyzed using synthetic ground motions representative of the hazard level in Indiana. The results of the detailed analysis are used to develop a simplified assessment procedure that uses information that is available in BIAS or can be added to BIAS. At this time, BIAS does not contain all the necessary information required for accurate estimates of dynamic properties, thus, certain assumptions are made. Several candidate models are developed by incrementally increasing the level of information proposed to be added into BIAS, which resulted in an increase in the level of accuracy of the results. The simplified assessment is then validated through a comparison with the detailed analysis.

Through the development of the simplified assessment procedure, the minimum data item which must be added to BIAS to complete the assessment is the substructure type, and bridges with reinforced concrete columns in the substructure require a detailed assessment. Lastly, by increasing the level of information available in BIAS, the agreement between the results of the simplified assessment and the detailed assessment is improved.

1. INTRODUCTION

The possibility of earthquakes in Indiana due to the presence of the New Madrid Seismic Zone is commonly acknowledged. However, the identification of the Wabash Valley Seismic Zone has increased our understanding of the seismic hazard in the state of Indiana. The Indiana Department of Transportation (INDOT) is aware of this and has now funded SPR 4222 to study the seismic vulnerability of its bridge network, with special attention to the Vincennes District. Due to the awareness of the increased potential for earthquakes in Indiana, the seismic vulnerability across the bridge network must be updated, and information required to better facilitate this process must be included in the asset management database, BIAS.

INDOT would like a seismic vulnerability assessment tool that can be used to assess the vulnerability of the bridge inventory more frequently. The tool is envisioned to be an automated process that uses information stored in BIAS. BIAS is INDOT's asset management database, and contains inspection reports, photos and history, National Bridge Inventory (NBI) fields, maintenance requests, and some superstructure information (BIAS, 2018). Certain bridge drawings, geotechnical reports and load rating information can also be obtained manually through BIAS. Thus, to ensure an adequate and efficient assessment of the state bridge network, BIAS must be evaluated and if necessary, improved upon.

As such, the goal of this project is to develop a simplified seismic vulnerability assessment procedure, herein referred to as the Level 1 assessment, that can be made into a tool. The goal of the tool is to complete the seismic assessment procedure automatically using only information extracted from BIAS. The procedure developed in this thesis can be modified as necessary and be applied to other bridge types not discussed within this document.

1.1 Objective

The objectives of this thesis work are as follows:

- Conduct a detailed vulnerability assessment, the Level 2 assessment, of a representative sample of reinforced concrete bridges from the Indiana bridge network.
- Develop and validate a simplified assessment procedure, Level 1 assessment, with validation conducted through a comparison with the Level 2 assessment results.

- Identify gaps in BIAS that can improve the validity of the Level 1 assessment procedure, and
- Provide recommendations to INDOT for addressing these gaps.

1.2 Organization

This thesis is organized into six chapters plus one appendix. Chapter 2 provides a summary of research studies and literature relevant to seismic vulnerability of bridges in moderate seismic zones, and a discussion of the seismicity of Indiana. The Level 2 assessment procedure and results of the selected bridges representing various substructure types is discussed in Chapter 3. Chapter 4 outlines the development of the Level 1 assessment procedure and its validation, as well as the criteria for establishing vulnerability. Chapter 5 demonstrates the implementation of the Level 1 assessment procedure on the selected bridges. Conclusions from the results and recommendations for improving information in BIAS for seismic assessment is presented in Chapter 6. Lastly, the results of the Level 2 assessment are presented in the appendix.

2. LITERATURE REVIEW

2.1 Introduction

This chapter focuses on the seismic hazard in Indiana and the review of key literature relevant to the seismic behavior of bridges when subjected to ground motions. The seismicity of Indiana is discussed first. Following this, literature relevant to the seismic behavior of bridges in Indiana and areas of low to moderate hazard is presented, and concludes with a description of the potential damage to bridges due to earthquakes as it pertains to the bridge types considered in this thesis.

2.2 Seismicity in Indiana

Evidence of the seismic hazard in Indiana can be attributed to the occurrence of the New Madrid sequence of earthquakes in 1811 – 1812, and the presence of paleo liquefaction evidence which is evidence of the past occurrence of earthquakes. Indiana is located near the New Madrid Seismic Zone (NMSZ), and the Wabash Valley Seismic Zone (WVSZ). Figure 2-1 shows the earthquakes that have occurred in both seismic zones between 1974 to 2002 with a magnitude greater than 2.5 (red circles), and earthquakes that occurred before 1974 (green circles). Larger circles indicate larger magnitude events.

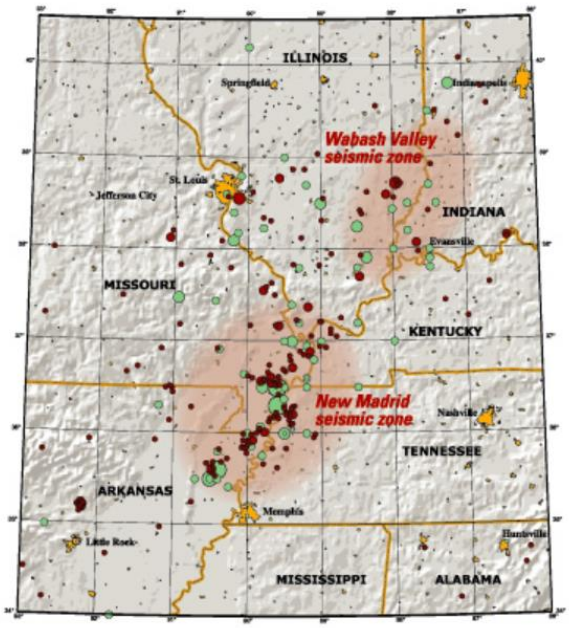

Figure 2-1: Earthquakes in the New Madrid and Wabash Valley Seismic Zones Prior to 2002 (USGS, 2002)

2.2.1 New Madrid Seismic Zone

The New Madrid fault is 240 km long, and extends into Illinois, Missouri, Arkansas, and Tennessee. Earthquakes in the fault system pose threats to Illinois, Indiana, Arkansas, Kentucky, Missouri, Tennessee, Oklahoma, and Mississippi. The faults in the NMSZ are embedded in the Reel foot rift, which formed when the supercontinent Rodina broke up. Although the Reel foot rift failed to split Rodina, the system remains a zone of weakness.

Furthermore, the NMSZ is responsible for the series of strong earthquakes that occurred in the Mississippi Valley in the early 19th century. The magnitude of these events are estimated to be as large as 7.0 and up to 7.5. The first of these earthquakes occurred on December 16, 1811 with its epicenter located in northeastern Arkansas. The next earthquake occurred on January 23, 1812 with its epicenter located around New Madrid, Missouri (Ramirez et. al., 2000). The third earthquake struck on February 7, 1812 with its epicenter located around New Madrid. According to details in newspapers, the third earthquake was the largest event and destroyed New Madrid. Hundreds of aftershocks were felt until 1817. Since the New Madrid sequence, frequent smaller events have occurred. The effects of these earthquakes have been felt in Indiana. The largest of these events that has struck in recent times is the magnitude 5.4 earthquake that occurred on November 9, 1968 near Dale, Illinois.

2.2.2 Wabash Valley Seismic Zone

Previously, the WVSZ was thought to be part of the NMSZ. However, geologic evidence has shown that the Wabash Valley Seismic Zone is an independent system. The Wabash Valley fault is 90 km long, and 50 km wide. The fault system is located in the valley of the Lower Wabash River, and spans from southeastern Illinois, southwestern Indiana and Northwestern Kentucky. The system is made up of subparallel high angle faults, with the dip angle of the major fault plain ranging from 50 to 85 degrees (Sozen et al., 2005).

While lesser magnitude earthquakes occur frequently, these events with a magnitude less than 3.5 are not usually felt. Some researchers have said that the WVSZ may pose greater threats to the region than the NMSZ. This is because the strongest earthquakes in the region in recent times have come from the WVSZ. Some of these earthquakes are the magnitude 5.0 June 10, 1987 event in Lawrenceville, Illinois, and the June 18, 2002 magnitude 4.6 earthquake in Evansville, Indiana. The strongest earthquake that has occurred is the magnitude 5.4 April 18, 2008 earthquake. The epicenter was located close to Vincennes in West Salem and Mount Carmel, Illinois. The effects of the event were felt in Indiana.

2.3 Literature Review of the Seismic Vulnerability Assessment and Methods of Bridges

Reinforced Concrete bridge superstructures consist of multiple simply supported spans separated by expansion joints and resting on bearings at the abutments and intermediate piers. Integral abutment bridges are bridges with the superstructure and abutments constructed together to form a continuous monolithic structure, thus move together. The bridges may be entirely integral with the intermediate piers, or may rest on bearings at the intermediate supports. Expansion joints are eliminated in these structures. Due to the absence of expansion joints, integral abutment bridges have increased resistance to seismic inputs. The most common problem associated with this type of bridge construction is the unseating of the superstructure at the supports. With integral abutments, this problem is eliminated because of the monolithic construction which allows the superstructure and abutments to move together. Thus, there is no differential displacement with the ground. However, the demand on the abutment and foundation is increased.

Frosch et. al. conducted a study to evaluate the earthquake resistance of integral abutments using INDOT design details and the seismic hazard associated with Indiana (Frosch et. al.,

2009). Field data collected from an existing instrumented integral abutment bridge was evaluated to determine the relationship between abutment displacements and earth pressures. Laboratory tests of current and proposed abutment-pile connection details were carried out to determine displacement capacity, and analytical models were used to estimate displacements of abutments due to ground motions. The major conclusion of the project is that for bridges spanning less than 500ft from abutment to abutment, INDOT design details for integral abutments are sufficient to provide seismic resistance.

Earlier, a two-part study was conducted, entitled Emergency Earthquake Routes for the State of Indiana, focused on determining critical routes for earthquake response in Indiana, and the seismic vulnerability of bridges in the Vincennes district (Sozen et al., 2005). The emergency routes presented in the report were based on minimizing the total travel time and maximizing the population reached, while considering the cost of retrofitting the selected bridges.

The second part of the study focused on establishing the seismic vulnerability of bridges. The seismic hazard in Indiana exists primarily in the Vincennes district. Thus, the project focused on establishing vulnerability in that area. At the time, there were 827 bridges in the district, with 230 on the emergency routes established in the first part of the study. Figure 2-2 shows the emergency routes in the Vincennes districts.

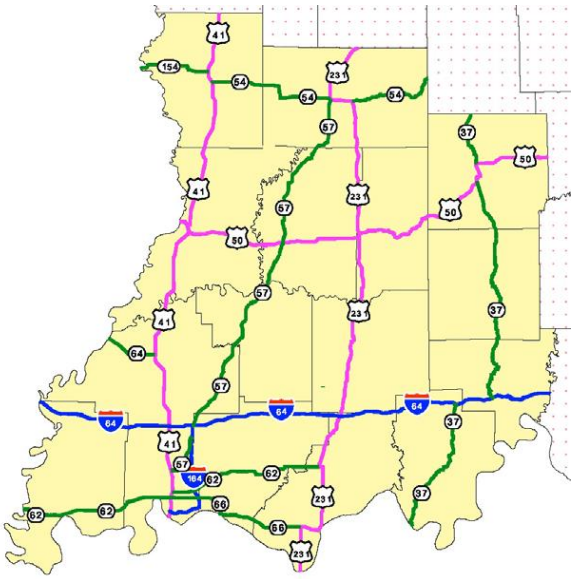

Figure 2-2: Selected Emergency Routes in the Vincennes District (Sozen et al., 2005)

In order to create an approximate assessment methodology, 69 bridges were selected to study their seismic behavior when subjected to ground motions of varying intensity, making the study independent of USGS requirements at the time. The sample was deemed representative of the material and superstructure type. These selected bridges were analyzed in detail using the bridge drawings, and vulnerability was established for each acceleration level based on excessive displacement or insufficient shear capacity to resist the shear demand. The results from these bridges were extrapolated and applied to approximate assessments of the remaining bridges in Vincennes using only the information available in INDOT's maintenance database. Thus, two levels of confidence and vulnerability of the entire bridge inventory were established (Sozen et. al., 2005).

For the approximate assessment, the dynamic properties of the bridges were calculated using only information in the maintenance database. The mass was estimated using the superstructure dimensions and material properties. Due to a lack of substructure information, lateral stiffness was estimated on the low side and lateral force demand was established (Sozen et. al., 2005). The level of toughness required for nonlinear response and the lateral load strength of the substructure was directly related to the year of construction and the assumed dimensions.

The vulnerability of the bridges was established using three damage levels: green tag indicated no vulnerability, yellow tag was marginal vulnerability, and red tag was vulnerable. Using the assessment procedure, 7% of the bridges were red tagged when AASHTO Standard Specifications were used and 15% were red tagged when AASHTO LRFD Specifications were used (Sozen et. al., 2005). Additionally, 65% of red tagged bridges were assessed in this category due to unseating at the supports. Overturning of steel expansion bearings in steel bridges were the cause of most unseating cases even for cases with PGA as low as 10%.

The Seismic Vulnerability Manual of the New York State Department of Transportation outlines the approach to assess the seismic vulnerability of each bridge in its inventory (NYSDOT, 2004). The approach applies to both new and existing bridges, and comprises of a series of screening and classification steps. This approach results in a seismic vulnerability rating for each bridge. The objective of the manual is to identify seismically deficient bridges and to establish an order for corrective action based on the level of vulnerability, probability of failure, and the consequence.

NYSDOT uses a three step procedure. The first step is screening. Preliminary rankings of the bridges are developed using only information available in the Bridge Inventory and Inspection System, (BIIS), database. The information used are the seismic acceleration coefficient, date of construction, importance, bearing details, span configuration, and abutment and pier types. The bridges are then assigned a susceptibility group.

The second step is classifying. Each of the bridges identified in the screening step as potentially being seismically deficient is evaluated in detail using as built plans and inspection report. One or more site visits may be carried out to confirm or obtain additional data. The evaluation is based on capacity to demand (C/D) ratios and the push over method. C/D ratio is determined for each element and elements less than unity are identified for corrective actions. This method is on the conservative side because it ignores the interaction between elements and the redistribution of loads. However, the push over method addresses these issues, but is time consuming. The result of the evaluation is a "classification score" which estimates the vulnerability of the bridge with respect to the other bridges in the inventory. The result is used to designate a "seismic vulnerability class" of high, medium or low to each bridge.

The last step in the procedure is establishing a vulnerability rating. The goal is to provide a measure of vulnerability in relation to the "seismic vulnerability class" and consequence of failure. The "seismic vulnerability rating" is designed to be compatible with other Bridge Safety Assurance, (BSA), failure modes. It also designates the need and urgency of rehabilitation measure. NYSDOT has developed corrective measures for the common problems associated with inadequate seismic details and capacity of bridge elements.

Choi et. al. presented a collection of fragility curves for typical bridges found in Central and Southeastern United States (CSUS) (Choi et. al., 2004). The bridge classes used in this study were identified from an inventory analysis of bridges found in CSUS. According to the inventory analysis, 95% of bridges in CSUS are single span bridges, multi-span simply supported girder bridges, or multi-span continuous girder bridges. Since research has shown that single span bridges are highly resistant to earthquakes, the four classes of bridges used in this study are:

1. Multi-span simply supported steel girder bridge (MSSS-SG),
2. Multi-span continuous steel girder bridge (MSC-SG),
3. Multi-span simply supported prestressed concrete girder bridge (MSSS-PSC)
4. Multi-span continuous prestressed concrete girder bridge (MSC-PSC)

For each bridge class, 10 nominally identical but statically different sample bridges were developed using a Latin Hypercube technique (Choi et. al, 2004). The details regarding bridge configurations were deemed representative of their respective bridge class. Variability and uncertainty in material properties and bridge stiffness were included in the bridge models.

2-D analytical models of the bridges were developed in DRAIN-2DX with nonlinear behavior of bridge elements incorporated. The superstructure was modelled using linear beam-column elements, columns were modeled using fiber elements, bearings were modeled using truss and link elements, and pile foundations were modeled using a combination of linear translational and rotational springs. For ground motions, 100 synthetic ground motions developed by Hwang et al. were used (Choi et. al., 2004). The peak ground acceleration ranged from 0.07 to 0.51, moment magnitude ranged from 6.0 to 8.0, and the distance to the epicenter ranged from 40 to 100 km. To describe the damage to the bridge, damage states were defined for column ductility demand, steel fixed and expansion bearing deformations, and elastomeric bearing deformations. The damage states are shown in Figure 2-3. Analytical fragility curves were developed for each component and the combined system using first-order reliability theory.

Table 2
Description of bridge damage states (taken from HAZUS 97)

Damage states	Description
No damage (N)	No damage to a bridge
Slight/minor damage (S)	Minor cracking and spalling to the abutment, cracks in shear keys at abutments, minor spalling and cracks at hinges, minor spalling at the column (damage requires no more than cosmetic repair) or minor cracking to the deck
Moderate damage (M)	Any column experiencing moderate cracking and spalling (column structurally still sound), any connection having cracked shear keys or bent bolts, or moderate settlement of the approach
Extensive damage (E)	Any column degrading without collapse (column structurally unsafe), any connection losing some bearing support, or major settlement of the approach
Complete damage (C)	Any column collapsing and connection losing all bearing support, which may lead to imminent deck collapse

Figure 2-3: Description of Bridge Damage States (after Choi et al., 2004)

2.4 Lessons Extracted from the Literature Review

The lessons from the literature review and the damage to bridges due to earthquake forces are presented in this section. The major conclusions from the literature are as follows:

1. For bridges less than 500ft, INDOT design details for integral abutments are sufficient to provide seismic resistance (Frosch et. al., 2009).
2. Overturning of steel expansion bearings in steel bridges can be the cause of unseating of the superstructure even with PGA as low as 10% (Sozen et. al., 2005).
3. For the slight damage state defined in Choi e.t al., the fixed bearings were the controlling component for all bridges (Choi et. al., 2004).
4. For the moderate damage state, MSSS-SG and MSC-SG bridges are more vulnerable and the fixed bearings are the controlling component for MSSS-SG bridges (Choi et. al., 2004).
5. For the extensive damage state, expansion bearings control for all but MSSS-SG bridges (Choi et. al., 2004).
6. For the complete damage state, the results show that MSSS-SG bridge is the most vulnerable and MSC-PSC bridge is the least vulnerable (Choi et. al., 2004).

The level of damage sustained by a bridge after an earthquake depends on the intensity of the ground motion, structural system, and type of soil. One of the most common damage is the unseating of the superstructure, as shown in Figure 2-4. Short seat lengths at abutments or at simple supports can lead to partial or complete collapse of the superstructure if the displacement of the superstructure exceeds the available seat length. In bridges with steel rollers, overturning of the support may cause collapse of the superstructure. To mitigate this problem, integral abutments or restrainers can be used.

Figure 2-4: Bridge Failure Due to Unseating at Support During the 1994 Northridge California Earthquake (Sozen et al., 2005)

Additionally, bridges may experience column failure due to inadequate amount and detail of transverse reinforcement or under developed splice lengths (shear failure), or insufficient flexural deformation capacity. Figure 2-5 shows an example of a flared column failure. Abutments may also be damage due to soil conditions or increased demands, like in the case of integral abutment bridges.

Figure 2-5: Column Failure of a Bridge During the 1994 Northridge California Earthquake (Sozen et. al., 2005)

Excessive displacement of superstructure may cause bearing failure, as shown in Figure 2-6. Bearings are also susceptible to failure under the lateral load demand of the earthquake. The lateral load may cause failure of the shear friction connection between the superstructure and the substructure when the capacity of the connection is exceeded.

Figure 2-6: Failure of an Elastomeric Bearing Due to Excessive Longitudinal Displacement (Ramirez et al., 2000)

Lastly, the age of the structure influences the amount of damage experienced. Due to changing design specifications, older bridges may not have been designed to provide adequate performance for seismic demand. Deterioration may affect the performance of the bridge during an earthquake. Studies have shown a correlation between poor performance and old bridges (Sozen et al., 2005).

2.5 Summary

This chapter presented information regarding the seismic hazard in Indiana, and multiple studies on seismic assessment of bridges in areas of moderate seismic risk. The main conclusions from the literature review is that integral abutment bridges in the state of Indiana may be excluded from a seismic vulnerability analysis due to the adequacy of INDOT's abutment pile detailing. Additionally, steel girder bridges and simply supported bridges can be very vulnerable during earthquakes, while prestressed continuous bridges are typically of low vulnerability. State DOTs and other agencies in areas of low to moderate seismic risk are establishing vulnerability of their bridge inventory and implementing retrofit procedures to deficient bridges. The type of damge observed in bridges located in areas of similar seismic risk as Indiana due to the seismic action can be of unseating of superstructure, column shear failure, shear friction failure or abutment damage.

3. LEVEL 2 ASSESSMENT OF SELECTED BRIDGES

3.1 Introduction

This chapter discusses the bridge selection process, and the Level 2 procedure used to determine the response of the bridges to ground motion. The analysis is carried out in two phases; the forces acting on the bents and the displacement of the bridge due to the ground motions (demand) are first determined. The capacity of the bridge elements is calculated next. Information from bridge drawings is used to build a 2-D finite element model of the bridge to determine the dynamic properties of the bridge. The Level 2 assessment is completed using Matlab. This detailed assessment will serve as a basis of comparison to validate the results from the Level 1 assessment to be discussed in a subsequent chapter.

3.2 Bridge Selection Process

The determination of seismic vulnerability for bridges in the state of Indiana is conducted by first analyzing a representative sample of bridges using site specific ground motions. With few ground motions recorded in Indiana, it is necessary to generate synthetic ground motions based on geotechnical conditions at the desired sites. However, geotechnical information is limited in bridge sites in Indiana. Representative sites were selected with respect to the seismic hazard potential, bridge characteristics, and geological and geographical diversity.

Additionally, attention was placed to select bridges on emergency routes. The emergency routes used for the selection process were the routes proposed in JTRP project SPR-2480 (Sozen et al., 2005). A representative sample of 100 bridges, including 25 reinforced concrete bridges, were selected from the state bridge inventory with respect to variation in physical and dynamic characteristics.

As geotechnical information was not available for any of the reinforced concrete bridges, generic site amplification factors are used for the de-aggregation analysis to generate the respective ground motions for site class A to D. Generic site amplification factors provide an approximation to the true soil conditions of the site. The ground motions synthesized by the project research team members can be found in Deliverable 1 of this project (Cao et. al., 2019).

3.2.1 Selected Bridges

Of the 5895 state bridges that INDOT maintains, 25 reinforced concrete bridges were selected to be assessed in detail. These bridges are representative of the superstructure type and the number of spans for concrete bridges in the state of Indiana. The selected bridges along with the location, superstructure type (material and construction), substructure type, and number of spans are shown in Table 3-1. The sample includes eighteen Continuous Reinforced Concrete Slab (CRCS) bridges, three Continuous Reinforced Concrete Girder (CRCG) bridges, one Reinforced Concrete Girder (CG) bridge, and three Single Span bridges. The slab deck bridges represent 75% of the reinforced concrete bridge inventory.

Table 3-1: Selected Reinforced Concrete Bridges

Asset Name	NBI Number	District	Number of Spans	Kind of Material	Construction	Abutment Type
024-56-00899 B	5880	La Porte	1	Concrete	Girder	Integral
I69-030-09187 NB	80114	Vincennes	1	Concrete	Slab	Integral
067-28-00938 A	23770	Vincennes	1	Concrete	Slab	Non Integral
064-63-03590 A	22950	Vincennes	3	Concrete	Girder	Non Integral
063-86-05970 BNBL	22810	Crawfordsville	3	Concrete Continuous	Slab	Non Integral
028-79-07672	7640	Crawfordsville	3	Concrete Continuous	Slab	Integral
067-55-03831 ANBL	24100	Crawfordsville	3	Concrete Continuous	Slab	Non Integral
075-06-04958 A	24860	Crawfordsville	4	Concrete Continuous	Girder	Non Integral
018-05-06573 B	4880	Fort Wayne	3	Concrete Continuous	Slab	Non Integral
(35)22-27-04724 B	11170	Fort Wayne	3	Concrete Continuous	Girder	Non Integral
327-17-06419 A	31350	Fort Wayne	3	Concrete Continuous	Slab	Integral
I69-334-04590 BNB	40720	Fort Wayne	3	Concrete Continuous	Slab	Non Integral
I70-112-05137 DEBL	42960	Greenfield	3	Concrete Continuous	Slab	Non Integral
055-45-07366	19880	La Porte	3	Concrete Continuous	Slab	Integral
041-56-03828 BSBL	15440	La Porte	3	Concrete Continuous	Girder	Non Integral
044-55-06793	16310	Seymour	3	Concrete Continuous	Slab	Integral
252-55-08713	30721	Seymour	3	Concrete Continuous	Slab	Integral
252-24-06934 A	30780	Seymour	3	Concrete Continuous	Slab	Integral
066-13-05443 A	23670	Vincennes	3	Concrete Continuous	Slab	Non Integral
041-42-05080 BNBL	14650	Vincennes	3	Concrete Continuous	Slab	Non Integral
(237)37-13-07277	11840	Vincennes	3	Concrete Continuous	Slab	Integral
056-63-07286	19933	Vincennes	3	Concrete Continuous	Slab	Integral
057-14-06739	20690	Vincennes	3	Concrete Continuous	Slab	Integral
067-42-07298	23760	Vincennes	3	Concrete Continuous	Slab	Integral
064-19-03723 A	22960	Vincennes	4	Concrete Continuous	Slab	Non Integral

3.3 Analysis of Single Span Bridges

In most studies, single span bridges are excluded from seismic vulnerability analysis due to low vulnerability to earthquakes (Choi, 2004). To demonstrate this concept and validate that it is acceptable to exclude single span bridges from a vulnerability assessment, the ground motions corresponding to a bridge site in Vincennes is used to assess the vulnerability of typical single span bridge.

The period of a single span bridges is dependent on the mass of the bridge and the stiffness of its bearings. The mass of the bridge is estimated using the deck dimensions and the material properties of reinforced concrete. The stiffness of the bridge is obtained from the stiffness of the bearings. In the case of elastomeric bearing pads, the stiffness of each bearing can be calculated using Eq. 3.1. The variables are defined in the nomenclature section of the thesis.

$$K = \frac{G_e A}{h_r} \tag{3.1}$$

The stiffness of the bearing pads is independent of direction, hence the period of the bridge in both the longitudinal and transverse direction is assumed to be the same.

Additionally, due to the lack of intermediate bents, the displacement of the bridge in response to the ground motion is the only concern. Thus, the vulnerability of single span bridges is dependent on the available seat length at the abutments. This concern can be eliminated by using integral end bents, which allows the bridge and the abutments to move together. In bridges without integral end bents, the seat length must be compared to the maximum displacement due to the expected ground motions.

Using the ground motions generated for a bridge site in Vincennes, the displacement response spectra is obtained and is shown in Figure 3-1. 50 ground motions corresponding to site class D, representing the worst case scenario, are used in generating the displacement response spectra shown in Figure 3-1.

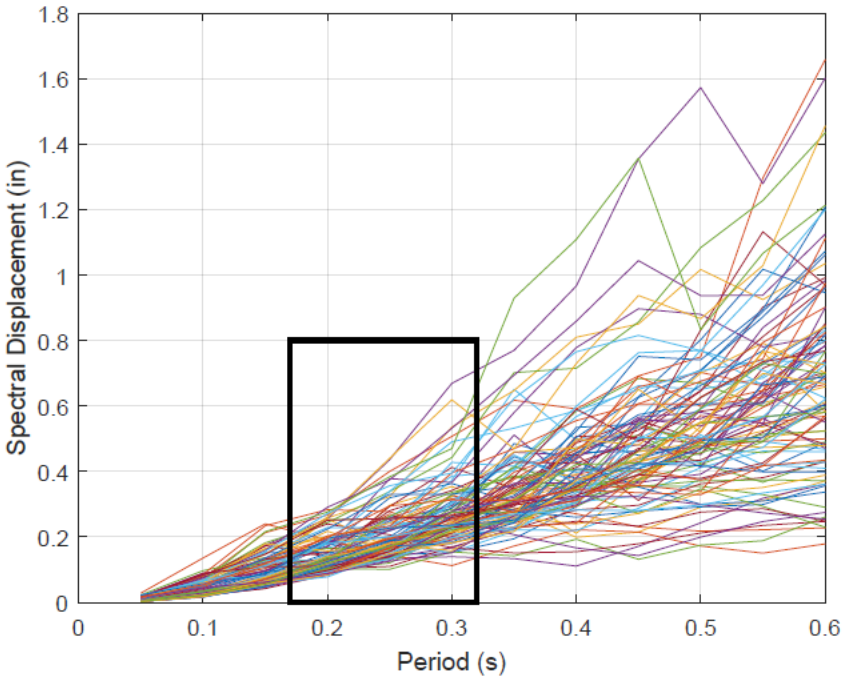

Figure 3-1: Displacement Response Spectra of a Site in Vincennes District

According to Nielson, the period of a typical reinforced concrete single span bridge found in Central and Southeastern United States is 0.32s, and 0.17s for a single span steel girder bridge (Nielson, 2005). Using these periods along with the displacement response spectra, the maximum displacement the structures will experience due to the ground motions is between 0.05” and 0.70”. The minimum bearing support length required by AASHTO LRFD Specifications is much greater than 1”, thus these bridges are highly resistant to the level of ground motions that are expected in Vincennes and across Indiana. Therefore, single span bridges can be eliminated from the analysis in this project due to the low potential for damage if damage of the abutment foundation is prevented.

3.4 2-D Finite Element Modelling Procedure

The detailed vulnerability assessment is carried out in two phases. First, the forces acting on the bents and the displacement of the bridge due to ground motions (demand) are computed, and then the demand is compared to the strength of the bridge elements (capacity). To calculate the demand on the bridge due to earthquake forces, the dynamic properties of the structure must be

determined. Thus, a 2-D finite element modelling procedure is developed to determine the fundamental dynamic characteristics of the bridges and the equations of motion.

The bridge is modelled in the longitudinal and transverse directions. The transverse direction is defined as the direction in plane with the bent, while the longitudinal direction is defined as out of plane with the bent. The finite element modelling procedure varies based on the substructure type. The modelling procedure shall be presented separately for bridges with multi-column bents and those with wall-type bents.

Figure 3-2: Multi-Column Bent Substructure (BIAS,2018)

Figure 3-3: Wall Type Substructure (BIAS, 2018)

3.4.1 Finite Element Model of Bridges with Multi-Column Bents

Multi-column bents typically have either reinforced concrete columns or pile sections that make up the substructure. In the transverse direction, multi-column bents are modelled as frames with the bent cap acting as beam elements that span from column to column or pile to pile. The columns are assumed to be fixed at the base of the crash wall, or at the ground level in the case of piles. Typically, the multi-column bents have their bent cap connected to the deck. The bent cap is connected to the deck either by reinforcing steel dowel bars, or by monolithic concrete pours of the bent cap and the slab deck. The bent is assumed to only displace in its plane. Thus, it can be modelled as a planar moment resisting frame with rotation at each beam-column node and translation at the end, as shown in Figure 3-4.

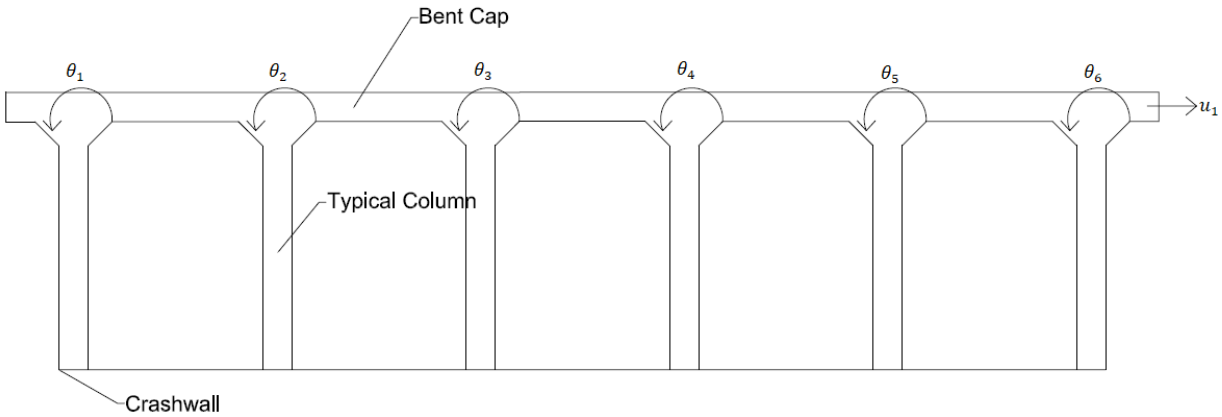

Figure 3-4: Transverse Elevation of an Interior Bent with Degrees-of-Freedom Shown

The stiffness of the bent is calculated by developing the stiffness matrix of each bent using the stiffness matrix of a beam element as the originating matrix. The originating matrix, and the assembled bent stiffness matrix corresponding to Figure 3-4 are shown in Tables 3-2 and 3-3.

Table 3-2: Stiffness Matrix and Displacement Vector of a Beam Element

$$k = \frac{EI}{L^3}\begin{bmatrix} 12 & 6L & -12 & 6L \\ 6L & 4L^2 & -6L & 2L^2 \\ -12 & -6L & 12 & -6L \\ 6L & 2L^2 & -6L & 4L^2 \end{bmatrix} \qquad d = \begin{bmatrix} v_1 \\ \theta_1 \\ v_2 \\ \theta_2 \end{bmatrix}$$

Table 3-3: Transverse Stiffness Matrix Corresponding to the Bent in Figure 3-4

Degrees of Freedom	u_1	θ_1	θ_2	θ_3	θ_4	θ_5	θ_6
u_1	$N_c\frac{12A}{h^3}$	$\frac{6A}{h^2}$	$\frac{6A}{h^2}$	$\frac{6A}{h^2}$	$\frac{6A}{h^2}$	$\frac{6A}{h^2}$	$\frac{6A}{h^2}$
θ_1	$\frac{6A}{h^2}$	$\frac{4A}{h}+\frac{4B}{l}$	$\frac{2B}{l}$	0	0	0	0
θ_2	$\frac{6A}{h^2}$	$\frac{2B}{l}$	$\frac{4A}{h}+2\frac{4B}{l}$	$\frac{2B}{l}$	0	0	0
θ_3	$\frac{6A}{h^2}$	0	$\frac{2B}{l}$	$\frac{4A}{h}+2\frac{4B}{l}$	$\frac{2B}{l}$	0	0
θ_4	$\frac{6A}{h^2}$	0	0	$\frac{2B}{l}$	$\frac{4A}{h}+2\frac{4B}{l}$	$\frac{2B}{l}$	0
θ_5	$\frac{6A}{h^2}$	0	0	0	$\frac{2B}{l}$	$\frac{4A}{h}+2\frac{4B}{l}$	$\frac{2B}{l}$
θ_6	$\frac{6A}{h^2}$	0	0	0	0	$\frac{2B}{l}$	$\frac{4A}{h}+\frac{4B}{l}$

$$A = E_c I_c \quad B = E_b I_b$$

The relative stiffness, EI, for the column or piles vary depending on the section. According to INDOT representatives, INDOT has two standard pile sections that are used in the multi-column bents with pile substructures. The cross-sections corresponding to these shapes are shown in Figure 3-5.

A)

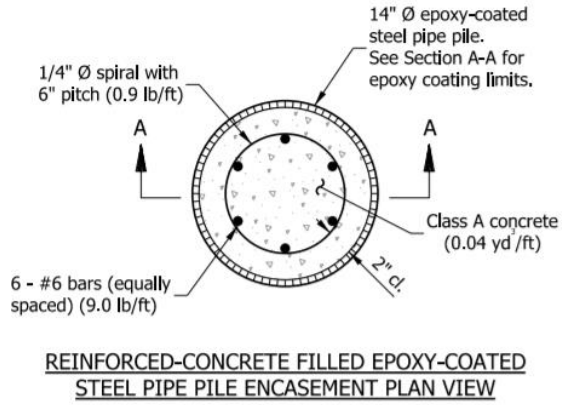

B)

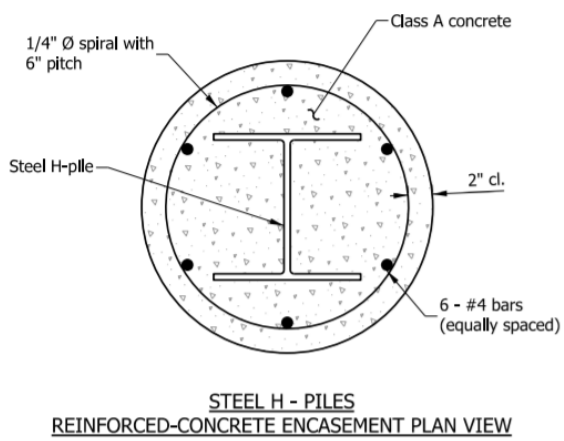

TABLE OF MATERIALS

Steel H-Pile designation	Minimum pile diameter	Reinforcing bars, lb/ft	Class A concrete, yd³/ft
HP 14	2'-3"	5.8	0.12
HP 12	2'-0"	5.6	0.10
HP 10	1'-9"	5.4	0.08

Figure 3-5: INDOT Standard Pile Sections (INDOT, 2012)

The stiffness of the entire bent corresponding to pure translation is needed to determine the bridge stiffness. As such, the rotation degrees of freedom in the bent stiffness matrix must be condensed (Chopra, 1995). This is done using the static condensation technique shown in Eq. 3.2 and 3.3. Refer to the nomenclature section for the definition of the variables.

$$K = \begin{bmatrix} k_{tt} & k_{t0} \\ k_{0t} & k_{00} \end{bmatrix} \tag{3.2}$$

$$\hat{k}_{tt} = k_{tt} - {k_{0t}}^{T} {k_{00}}^{-1} k_{0t} \tag{3.3}$$

Due to the connection of the bent cap to the bridge deck, the deck contributes to the stiffness of the bridge in the transverse direction. The bridge deck is modelled as a deep girder spanning from abutment to bent and from bent to bent. The depth of the girder corresponds to the deck width and the breadth of the girder corresponds to the deck thickness. To model the deck, rotation and translation are allowed at the intermediate bents, and rotation is only allowed at the abutments, as shown in Figure 3-6. The deck is assumed to be simply-supported at the abutments.

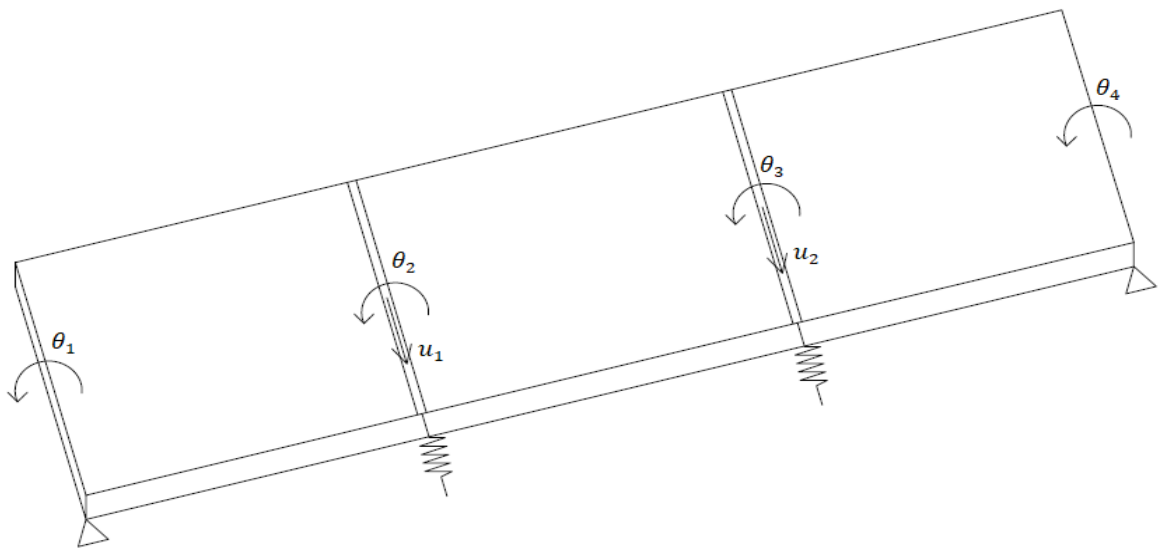

Figure 3-6: Plan View of the Deck of a Three Span Bridge with Degrees of Freedom Shown

To assemble the deck stiffness matrix, the beam element matrix that includes shear effect is used as the originating matrix. The shear term is added to include the effects of shear deformation.

Table 3-4: Stiffness Matrix and Displacement Vector of a Beam Element Including Shear Effects

$$k = \frac{EI}{(1+\mu)L^3}\begin{bmatrix} 12 & 6L & -12 & 6L \\ 6L & (4+\mu)L^2 & -6L & (2-\mu)L^2 \\ -12 & -6L & 12 & -6L \\ 6L & (2-\mu)L^2 & -6L & (4+\mu)L^2 \end{bmatrix} \qquad d = \begin{bmatrix} v_1 \\ \theta_1 \\ v_2 \\ \theta_2 \end{bmatrix}$$

Here, the value of μ is given by:

$$\mu = \frac{12E_d I_d}{GA_v L_s^2}$$

and the value of G is given by:

$$G = \frac{E_d}{2 * (1 + \eta)}$$

When calculating the shear modulus, a Poisson's ratio of 0.15 is assumed, with typical values for concrete ranging from 0.15 to 0.20.

Table 3-5: Deck Stiffness Matrix Corresponding to Figure 3-6 – Transverse Direction

Degrees of Freedom	u_1	u_2	θ_1	θ_2	θ_3	θ_4
u_1	$\frac{12E_dI_d}{(1+\mu)l_1^3} + \frac{12E_dI_d}{(1+\mu)l_2^3}$	$-\frac{12E_dI_d}{(1+\mu)l_2^3}$	$-\frac{6E_dI_d}{(1+\mu)l_1^2}$	$-\frac{6E_dI_d}{(1+\mu)l_1^2} + \frac{6E_dI_d}{(1+\mu)l_2^2}$	$\frac{6E_dI_d}{(1+\mu)l_2^2}$	0
u_2	$-\frac{12E_dI_d}{(1+\mu)l_2^3}$	$\frac{12E_dI_d}{(1+\mu)l_2^3} + \frac{12E_dI_d}{(1+\mu)l_2^3}$	0	$-\frac{6E_dI_d}{(1+\mu)l_2^2}$	$-\frac{6E_dI_d}{(1+\mu)l_2^2} + \frac{6E_dI_d}{(1+\mu)l_3^2}$	$\frac{6E_dI_d}{(1+\mu)l_3^2}$
θ_1	$-\frac{6E_dI_d}{(1+\mu)l_1^2}$	0	$\frac{(4+\mu)E_dI_d}{(1+\mu)l_1}$	$\frac{(2-\mu)E_dI_d}{(1+\mu)l_1}$	0	0
θ_2	$-\frac{6E_dI_d}{(1+\mu)l_1^2} + \frac{6E_dI_d}{(1+\mu)l_2^2}$	$-\frac{6E_dI_d}{(1+\mu)l_2^2}$	$\frac{(2-\mu)E_dI_d}{(1+\mu)l_1}$	$\frac{(4+\mu)E_dI_d}{(1+\mu)l_1} + \frac{(4+\mu)E_dI_d}{(1+\mu)l_2}$	$\frac{(2-\mu)E_dI_d}{(1+\mu)l_2}$	0
θ_3	$\frac{6E_dI_d}{(1+\mu)l_2^2}$	$-\frac{6E_dI_d}{(1+\mu)l_2^2} + \frac{6E_dI_d}{(1+\mu)l_3^2}$	0	$\frac{(2-\mu)E_dI_d}{(1+\mu)l_2}$	$\frac{(4+\mu)E_dI_d}{(1+\mu)l_2} + \frac{(4+\mu)E_dI_d}{(1+\mu)l_3}$	$\frac{(2-\mu)E_dI_d}{(1+\mu)l_3}$
θ_4	0	$\frac{6E_dI_d}{(1+\mu)l_3^2}$	0	0	$\frac{(2-\mu)E_dI_d}{(1+\mu)l_3}$	$\frac{(4+\mu)E_dI_d}{(1+\mu)l_3}$

With the deck stiffness matrix assembled (as shown in Table 3-5) and the condensed bent stiffness calculated, the bridge stiffness in the transverse direction can be obtained using a mixed modelling technique. In this case, mixed modelling refers to the use of a lumped parameter model and a finite element model. This is achieved by treating the intermediate bents as lumped springs with their stiffness added to the pure translation degrees-of-freedom in the deck stiffness matrix. After this lumped spring is added, the matrix is condensed using static condensation to

reflect only translation. The resulting matrix is the stiffness of the bridge in the transverse direction.

In the longitudinal direction, the bridge is modelled as a single-degree-of-freedom system with the intermediate bents acting as springs in parallel, as shown in Figure 3-7. In the bents, the columns are assumed to be fixed at both the top of the crash wall or ground, and at the bottom of the bent cap, allowing for only translation at the top. The columns in the bent are parallel to each other, and thus the stiffness of the bridge is:

$$K = N_b * N_c * \frac{12EI}{h^3} \tag{3.4}$$

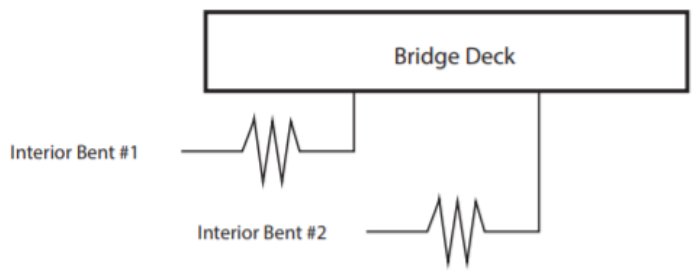

Figure 3-7: SDOF Model of the Bridge in the Longitudinal Direction

The mass of the bridge is calculated using the superstructure geometry, barrier dimensions, and the material properties of concrete. In the transverse direction, the mass matrix is determined using the tributary mass supported by each bent (lumped mass model).

Table 3-6: Mass Matrix of a Three Span Bridge in the Transverse Direction

$$M = \begin{bmatrix} mass_{bent1} & 0 \\ 0 & mass_{bent2} \end{bmatrix}$$

The entire mass of the bridge is used in calculating the dynamic properties in the longitudinal direction as the model is a single degree of freedom. With the mass and stiffness known in both directions, the equations of motion of the bridge when subjected to ground motion can be written, as shown in Eq. 3.5.

$$\boldsymbol{M\ddot{x} + C\dot{x} + Kx = -M\ddot{x}_g} \tag{3.5}$$

Solving the eigenvalue problem shown in Eq. 3.6, the periods and mode shapes of the bridge is determined.

$$Det(\boldsymbol{K} - \boldsymbol{\omega_n}^2\boldsymbol{M}) = \boldsymbol{0} \tag{3.6}$$

3.4.2 Finite Element Model of Bridges with Wall-type Bents

In the transverse direction, the walls act in both bending and shear, with both components contributing to the stiffness. To capture both the bending and shear deformations, the stiffness of the wall in the transverse direction is obtained from the deformation of the wall in its plane due to an applied unit load. Due to the presence of fixed connections between the walls and the superstructure (extended longitudinal reinforcement from the wall into the deck), the walls are modelled as fixed-fixed walls. The stiffness of the wall in the transverse direction is calculated using Eq. 3.7.

$$K = \frac{12EI}{h^3} + \frac{GA_v}{1.2h} \tag{3.7}$$

In cases in which the longitudinal reinforcement does not extend into the deck and the superstructure seats on bearings, the stiffness of the wall is neglected. This is because the wall, in this case, is not connected to the superstructure by any means, therefore it cannot be included in the dynamic model.

Due to the fixed connection between the walls and the superstructure, the stiffness of the deck contributes to the bridge stiffness. Similar to bridges with multi-column substructures, the deck is modelled as a deep girder spanning from abutment to bent and from bent to bent. The deck stiffness matrix is assembled using the procedure presented previously. After assembling the matrix, the stiffness of the walls is added to the pure translational degrees-of-freedom in the deck stiffness matrix. This matrix is then condensed to reflect only translation. The resulting matrix is the stiffness of the bridge in the transverse direction.

In the longitudinal direction, the bridge is modelled as a single degree of freedom system with the walls acting as parallel springs. Because the walls are acting in bending only in their out of plane direction, the walls can be treated as unit widths of columns totaling to the overall width of the wall. Due to the presence of extended reinforcing steel dowel bars between the walls and the deck, the walls are treated as fixed-fixed walls. As in the transverse direction, walls without

extended longitudinal reinforcement into the superstructure are excluded from the dynamic model. Equation 3.8 is used to calculate the stiffness of the bridge in the longitudinal direction.

$$K = N_b * \frac{12EI}{h^3} \tag{3.8}$$

The masses used to calculate the dynamic properties of the bridge are obtained using the same procedure for bridges with multi-column bents.

3.4.3 Force and Displacement Demand

In general, to determine the vulnerability of a bridge, the displacement of the bridge and the forces acting on the intermediate bents due to the applied ground motions must be compared to the strength of the bridge elements. To obtain the demand, a state space model in Simulink is used. The first step is to decouple the equations-of-motions (EOMs) using the mode shapes. After decoupling the EOMs, the state space model can be written.

Additionally, damping is incorporated into the EOMs by assuming proportional damping with a damping ratio of 5% which is typical for dynamic analysis of bridges (Chopra, 1995). The ground motions applied to each bridge is dependent on the seismic hazard and site class at the bridge location. The site class is determined using the bridge coordinates and a site class map for the state of Indiana, which was developed by the Indiana Geological and Water Survey (IGS, 2011). The ground motion corresponding to the site class at the bridge location is then applied to the state space model by simulating the response using Simulink, which produces displacement results in all modes. To obtain the total displacement of each bent, the mode shape is used together with the displacement for each mode as shown.

$$\{U\} = [\Phi]\{u\} \tag{3.9}$$

Furthermore, with the displacement of the bridge known, the lateral force on each bent is calculated using the force-displacement relationship,

$$\{F\} = [K]\{U\} \tag{3.10}$$

In the longitudinal direction, the displacement of the bridge is obtained directly from the Simulink results. The lateral force acting on the bridge is also calculated using the force-displacement relationship. With the demand on the bridge known, the next step in the analysis is to determine the capacity of the bridge elements.

3.5 Capacity of Bridge Elements

3.5.1 Substructure

The capacity of the bent must be determined in each direction. In the transverse direction, a limit analysis is used to determine the controlling mechanism for collapse of each bent, and two mechanisms are considered. Here, Mechanism 1 is used to describe the formation of plastic hinges at the base and the top of each column/pile, and Mechanism 2 is used to describe the formation of plastic hinges at the base of each column/pile and at ends of each beam, as shown in Figure 3-8 and Figure 3-9.

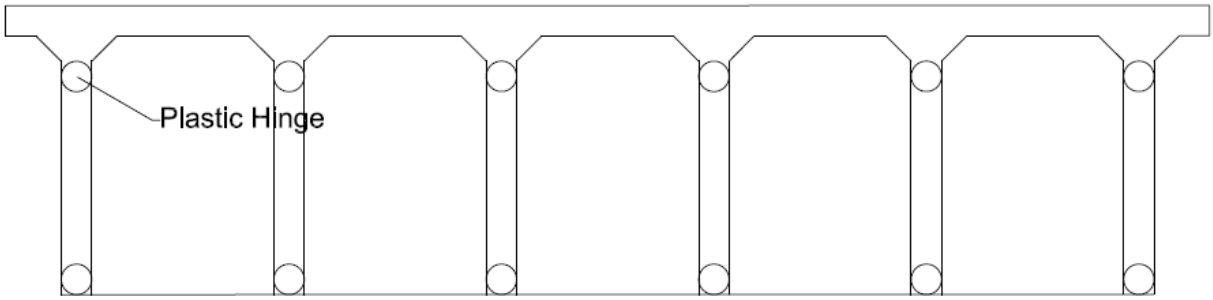

Figure 3-8: Mechanism 1 – Hinges Forming in the Columns/Piles Only

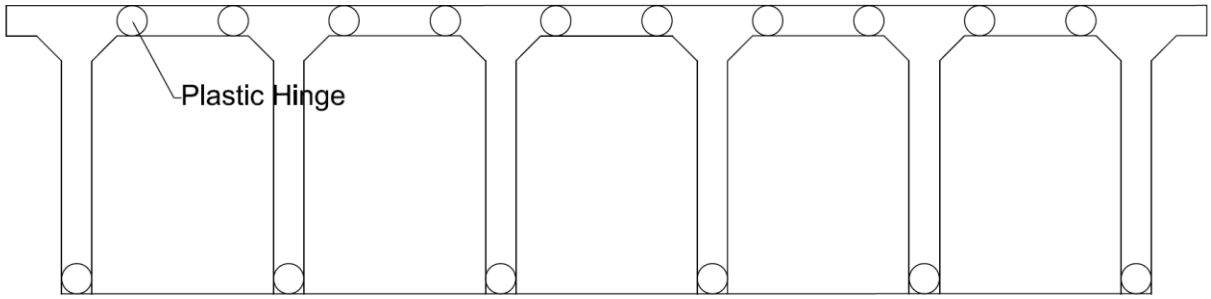

Figure 3-9: Mechanism 2 – Hinges Forming in Both the Beams and the Columns/Piles

For the limit analysis, the plastic moment is obtained using the moment-curvature relationship of the columns, walls, and beams. In bents with pile sections, the plastic stress distribution method is used to calculate the plastic moment of the sections. With the plastic moments applied at the hinges, the shear resultant (shear corresponding to the formation of plastic hinges on the elements) is calculated using equilibrium. The shear resultant is calculated by summing the moments about one end of the member, which results in Eq. 3.11. The shear resultant is also the flexural capacity, in terms of force, of the elements. Refer to the nomenclature section for the definition of the variables.

$$V_u = \frac{\sum M_p}{l_n} \tag{3.11}$$

The shear strength of reinforced concrete columns and beams are calculated in accordance to AASHTO LRFD specifications (AASHTO, 2017), using the following equations:

$$V_n = V_c + V_s \tag{3.12}$$

$$V_c = 2 * \sqrt{f'_c} * b * d_s \tag{3.13}$$

$$V_s = A_v * f_y * \frac{d_s}{s} \tag{3.14}$$

where, f_y is in psi.

For composite pile sections, the shear strength of the elements is calculated in accordance to Chapter G of the AISC Steel Construction Manual (AISC, 2016). The shear strength of the section is conservatively taken as the shear strength of the steel section, and the concrete contribution is ignored.

If the shear resultant from the plastic moment is greater than the shear strength of the member, the member will fail in shear. If the shear strength is greater, hinges will form in the member and the substructure will continue to deform. The formation of plastic hinges in the members allows for maximum rotation in the elements. The limit on the available rotation capacity can be used to displacements. The limiting rotation can be determined as:

$$l_p = 0.5d + 0.05z \tag{3.15}$$

$$\theta_u = \varphi_u * l_p \tag{3.16}$$

$$\delta_u = \theta_u * h \tag{3.17}$$

The force corresponding to the limiting rotation can be calculated using the force-displacement relationship and assuming that the elastic and inelastic displacement are approximately equal, limiting the shear demand to that corresponding to the yield moment of the section.

In the longitudinal direction, the bent is modeled as fixed-fixed. The model assumes that the connection between the column/wall and the crash wall or ground, and the connection between the column and the bent cap were properly designed. The plastic moment is calculated using the same procedure presented for the transverse direction. For a wall, the plastic moment is calculated by taking a unit width of the wall and using moment curvature analysis. The shear resultant on the column or pile corresponding to the plastic moment is obtained using equilibrium as

$$V_u = \frac{M_p}{l_n} \tag{3.18}$$

The shear strength, limiting rotation, and the force corresponding to the limiting rotation of the bent are calculated the same way as in the transverse direction using the correct dimensions.

Furthermore, the strength of the connection between the deck and the bent due to the extended reinforcing dowel bars must be calculated. The shear strength of the connection between the bent and the deck is dependent on the shear friction connection of the dowel bars, and the friction resistance from the normal force provided by the tributary weight of the deck carried along the length of the shear connection. Equations 3.19 to 3.21 are used to calculate the strength of the connection, and all variables are defined in the nomenclature.

$$V_{sf} = \mu * A_v * f_y \tag{3.19}$$

$$V_{cN} = \mu_f * N \tag{3.20}$$

$$V_{conn} = V_{sf} + V_{cN} \tag{3.21}$$

The coefficient of friction is dependent on the contact surface preparation. In the cases in which concrete was not intentionally roughened, the coefficient is 0.6.

3.5.2 Bearing Support Length

The bearing support length provided at the support must be checked. According to AASHTO LRFD specifications (AASHTO, 2017), the minimum bearing support length required is:

$$L_{BS} = \left(8 + 0.02 * L_J + 0.08 * H_J\right) * (1 + 0.000125S^2) \tag{3.22}$$

With the seismic demand on bridge and the capacity of the bridge both known, the vulnerability of the bridge can be determined. The forces acting on the bents due to the applied ground motion must be compared to the flexural capacity of the bents, shear strength of the bents, ultimate inelastic force, and the strength of the connection between bent and the deck. Lastly, the displacement of the bridge in response to the ground motion is compared to the available seat length at the supports.

3.6 Results from the Analysis of Selected Bridges

From the 25 selected concrete bridges, the detailed assessment results of three bridges corresponding to the main types of substructure for RC bridges, multi-column with piles, multi-column with RC columns, and wall-type bents are shown in detail to demonstrate the procedure fully. The results for the remaining 22 bridges can be found in Appendix.

3.6.1 Bridge Asset Name: 067-42-07298

The selected bridge has an NBI number of 023760, and is located in Knox County of the Vincennes District. Constructed in 1997, the superstructure of the bridge is a continuous reinforced concrete slab, with two spans of 24’-9.25” (7.55m), and a middle span of 32’-9.70” (10.00m). The deck has a width of 39’-8.30” (12.1m) and is 17.7” (450mm) thick. The bridge has a skew of 45-degrees.

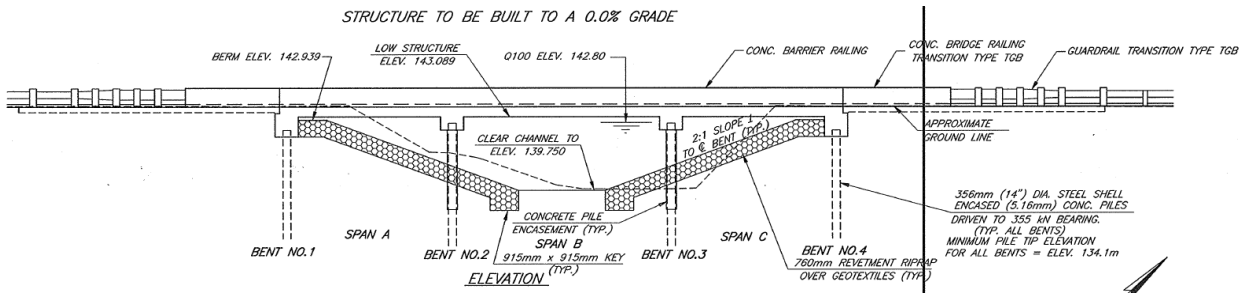

Figure 3-10: Elevation View of the Bridge (INDOT, 1996)

The bridge is supported by two end abutments and two interior bents. Each interior bent consists of a bent cap, and 11 piles. The piles are concrete filled tubes (CFT) with 14” (356 mm) diameter and have a wall thickness of 0.2” (5.16mm). The piles have a height of above ground of approximately 9’-0”. The bent cap has dimensions of 23.6” (600mm) by 29.5” (750mm). In both bents, the piles are spaced at 5’-1.7” (1560mm) on center. Additionally, the bridge has integral abutments, and the bent cap and the deck are monolithically poured.

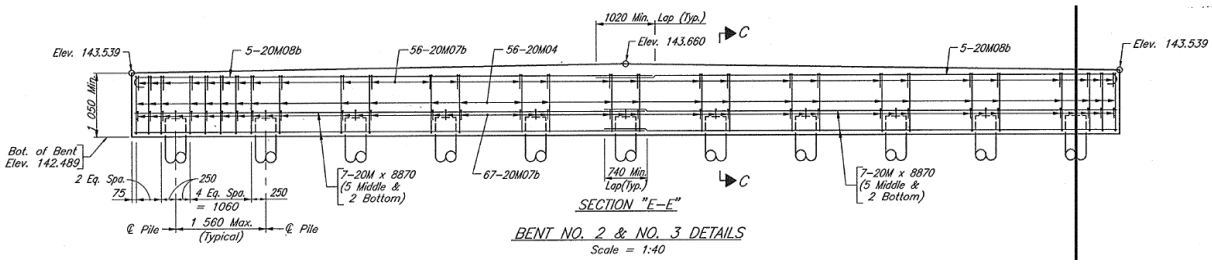

Figure 3-11: Transverse Elevation View of the Interior Bents (INDOT, 1996)

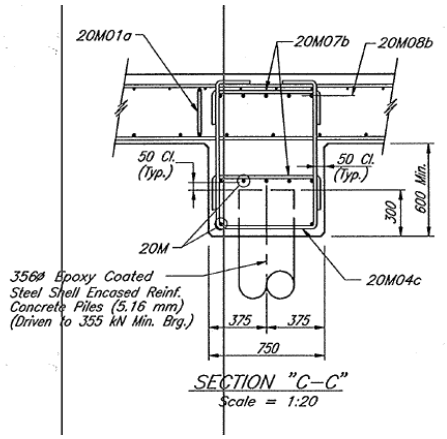

Figure 3-12: Section C-C of Figure 3-11 (INDOT, 1996)

According to the bridge drawings, the concrete used in the substructure has a compressive strength of 3500 psi, and 4000 psi for the concrete in the superstructure, while the reinforcing steel bars and piles have a yield strength of 60,000 psi. An ultimate strain for concrete of 0.003 is assumed for strength calculations.

3.6.1.1 Results – Transverse Direction

Using the modelling procedure presented in this chapter, the bent was modelled as a 10-bay portal frame. Due to the monolithic construction of the deck and bent cap, the deck contributes to the stiffness of the bridge. The mass, stiffness, period, and mode shape of the bridge calculated in the transverse direction are:

$$M = \begin{bmatrix} 0.72 & 0 \\ 0 & 0.72 \end{bmatrix} \frac{kips}{g}$$

$$K = \begin{bmatrix} 46900 & -31600 \\ -31600 & 46900 \end{bmatrix} kips/in$$

$$T = \begin{bmatrix} 0.04 \\ 0.02 \end{bmatrix} seconds$$

$$\Phi = \begin{bmatrix} -0.707 & -0.707 \\ -0.707 & 0.707 \end{bmatrix}$$

Due to the monolithic construction of the superstructure and the substructure, and integral end abutments, the bridge moves together with the ground during earthquakes. Thus, there are no differential displacement or inertial forces on the bridge, and it is not vulnerable.

3.6.1.2 Results – Longitudinal Direction

Using the modelling procedure presented in Section 3.4, the piles are acting in parallel and modelled as fixed at the top of the bent cap and at the ground. This assumes that the soil is compacted properly to provide fixity at the base. The bridge is modelled as a single degree of freedom system, so the entire mass is used to obtain the period. The mass, stiffness, and period of the bridge in the longitudinal direction are 2.1 $kips/g$, 680 $kips/in$, and 0.35 $seconds$, respectively.

Due to the use of integral end abutments, the bridge moves together with the ground during earthquakes. Thus, there are no differential displacement or inertial forces on the bridge, and it is not vulnerable.

3.6.2 Bridge Asset Name: 041-42-5080 BNBL

The selected bridge has an NBI number of 014650, and is located in Knox County of the Vincennes District. Constructed in 1967 and reconstructed in 1999, the superstructure of the bridge is a continuous reinforced concrete slab, with two spans of 38’-6”, and a middle span of 43’-0”. The deck has a width of 55’-5” and is 24” thick. The bridge has a skew of 8-degrees.

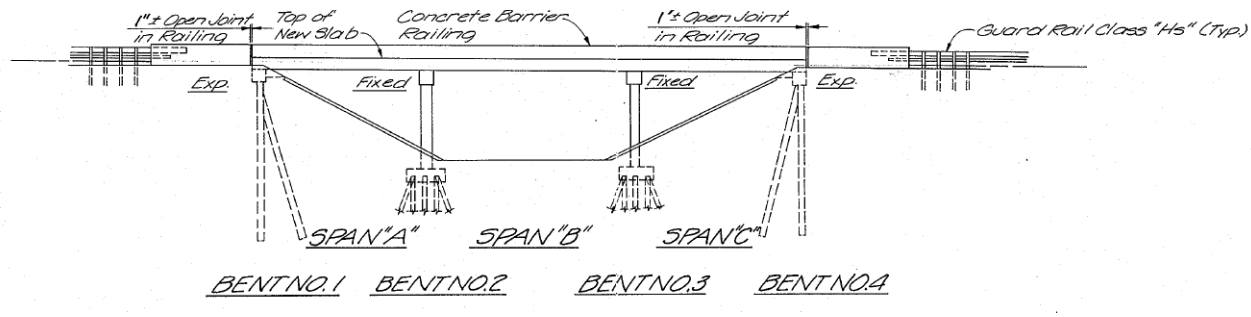

Figure 3-13: Elevation View of the Bridge (INDOT, 2009)

The bridge is supported by two end abutments and two interior bents. Each interior bent consists of a bent cap, and 6 RC columns. The columns are 24” by 36”, and have a height of 11’-3” above the crash wall. The bent cap has dimensions of 24” by 30”. The columns are spaced at 9’-6” on center. Additionally, the bridge has a bearing support length of 2’-0”, and the bent cap and the deck are connected by (7) #5 dowel bars extending from each interior bent into the deck.

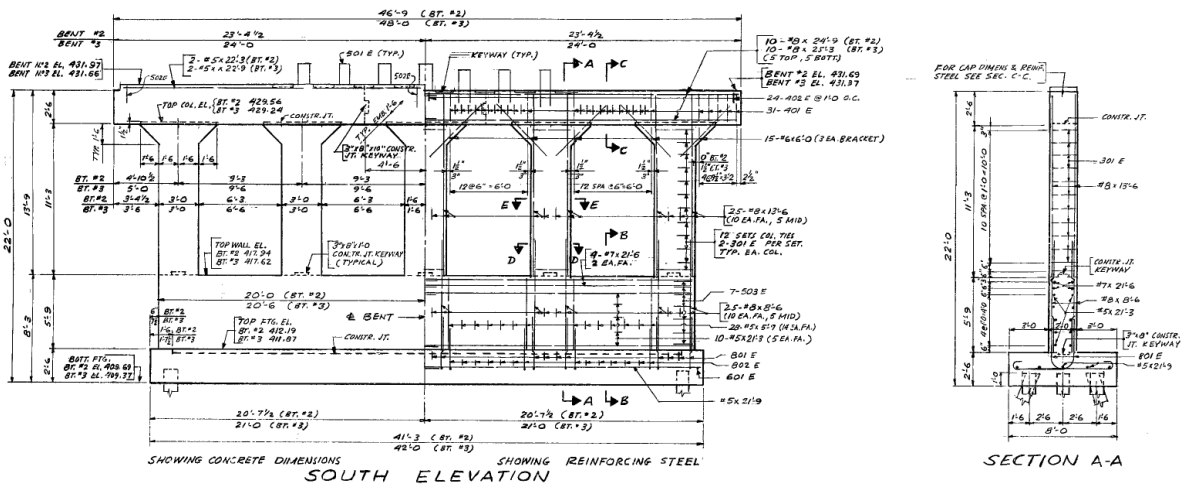

Figure 3-14: Transverse Elevation View of Interior Bents (INDOT, 2009)

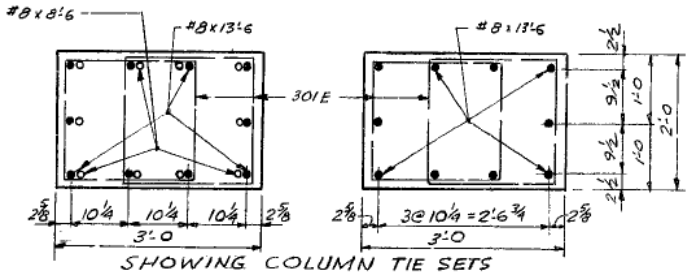

Figure 3-15: Cross-Section of Column Members (INDOT, 2009)

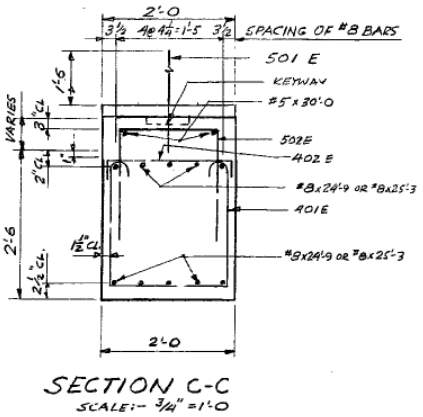

Figure 3-16: Cross-Section of Bent Cap (INDOT, 2009)

According to the bridge drawings, the concrete has a compressive strength of 3000 psi, while the reinforcing steel bars and piles have a yield strength of 40,000 psi. An ultimate strain for concrete of 0.003 is assumed for strength calculations.

3.6.2.1 Results – Transverse Direction

Each bent was modelled as a 5-bay portal frame. Due to presence of extended longitudinal bars from the bent cap into the deck, the deck contributes to the stiffness of the bridge. The mass, stiffness, period, and mode shape of the bridge calculated in the transverse direction are:

$$M = \begin{bmatrix} 1.86 & 0 \\ 0 & 1.86 \end{bmatrix} \frac{kips}{g}$$

$$K = \begin{bmatrix} 60700 & -38300 \\ -38300 & 60700 \end{bmatrix} kips/in$$

$$T = \begin{bmatrix} 0.06 \\ 0.03 \end{bmatrix} seconds$$

$$\Phi = \begin{bmatrix} -0.71 & -0.71 \\ -0.71 & 0.71 \end{bmatrix}$$

The plastic moment capacity and shear resultant of each column are 440 ft-kip, and 90 kips, respectively. Each bent has a shear strength of 675 kips, which is greater than the shear resultant of the six columns at each bent (540 kips). Thus, plastic hinges will form prior to collapse. The strength of the shear friction connection between each bent and the deck is 305 kips. Applying the 100 ground motions generated at this bridge site (site class D) to the bridge model, the shear demand at each bent from the ground motions (50 per fault orientation) is plotted on the vertical axis of Figure 3-17 against the peak ground acceleration (PGA) of each earthquake. The substructure capacity is shown using limit values (horizontal lines) corresponding to the flexural capacity, strength of the shear friction connection, and the shear strength, as shown in Figure 3-17.

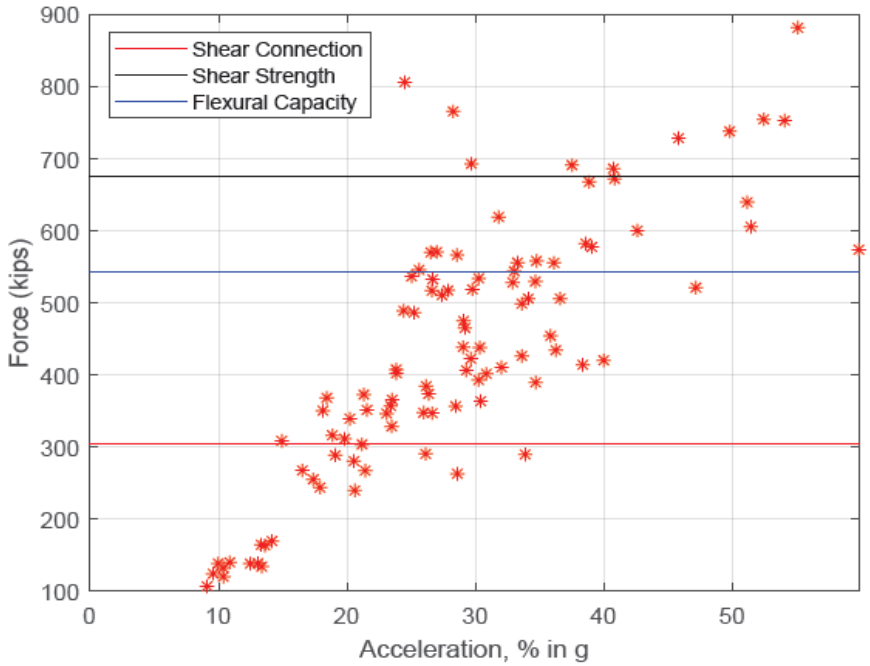

Figure 3-17: Shear Demand Due to Applied Ground Motions – Transverse Direction

Based on the plot, the shear capacity of the substructure is exceeded by the demand from some of the ground motions. The maximum displacement of the bridge due to the ground motions is less than 0.05”. However, since the capacity of the shear strength is exceeded, the bridge is deemed vulnerable in the transverse direction at level of ground motions expected at its location.

3.6.2.2 Results – Longitudinal Direction

The columns are acting in parallel and modelled as fixed at the top of the bent cap and at the crash wall. This assumes that the connection between the columns and the crash wall were designed properly. The bridge is modelled as a single degree of freedom system, so the entire mass is used to obtain the period. The mass, stiffness, and period of the bridge in the longitudinal direction are 5.50 $kips/g$, 7660 $kips/in$, and 0.17 $seconds$, respectively.

In the longitudinal direction, the plastic moment and shear resultant of each column are 325 ft-kip, and 30 kips, respectively. The substructure has a total shear strength of 1395 kips which is greater than the total shear resultant (340 kips). The strength of the shear friction connection between the substructure and the deck is 610 kips. Applying the 100 ground motions

generated at this bridge site (site class D) to the bridge model, the shear demand from the ground motions (50 per fault orientation) is plotted against the peak ground acceleration (PGA) of each earthquake. The substructure capacity is shown using threshold values corresponding to the flexural capacity, strength of the shear friction connection, and the shear strength, as shown in Figure 3-18.

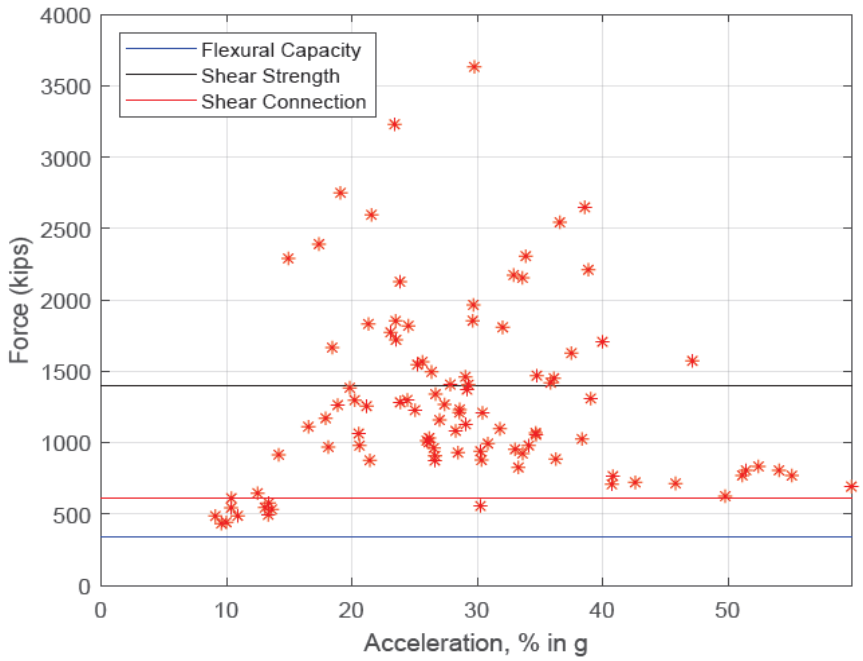

Figure 3-18: Shear Demand Due to Applied Ground Motions – Longitudinal Direction

From the plot, the base shear demand acting on the bridge from the ground motions exceeds the flexural capacity, and shear strength of the substructure. The maximum displacement of the bridge due to the set of ground motions is less than 0.5”. Additionally, since the shear strength of the substructure is exceeded, the bridge is vulnerable at the level of ground motions expected at its location.

3.6.3 Bridge Asset Name: 066-13-05443 A

The selected bridge has an NBI number of 023670, and is located in Crawford County of the Vincennes District. Initially, the bridge was constructed in 1968, but the deck was replaced in 2000. The superstructure of the bridge is a continuous reinforced concrete slab, with two spans of 24’-0”, and a middle span of 32’-0”. The deck has a width of 44’-6” and is 16” thick. The

bridge has a skew of 30-degrees. The approach slab is anchored to the deck using 29 #6 bars with a minimum pullout of 26.5 kips (117.9 kN) per bolt at each abutment.

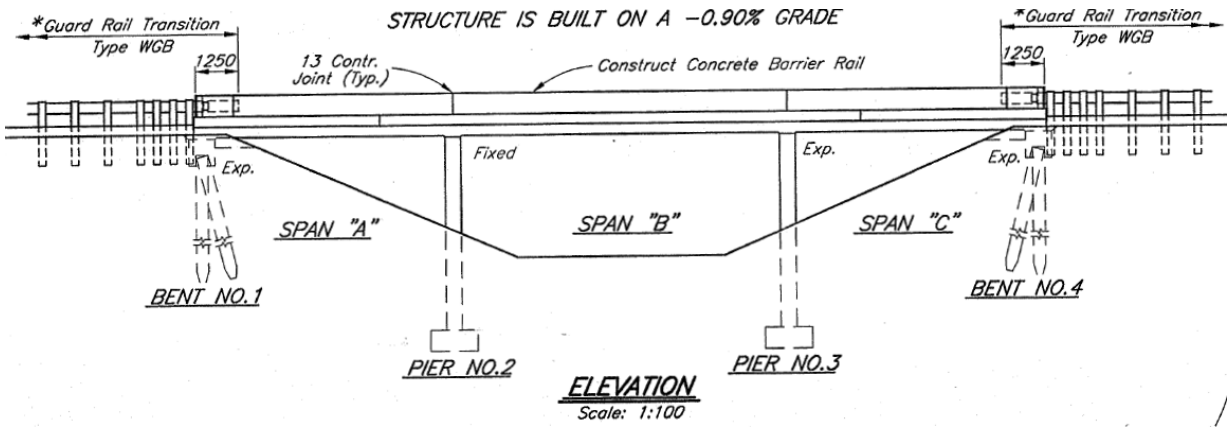

Figure 3-19: Elevation View of the Bridge (INDOT, 1999)

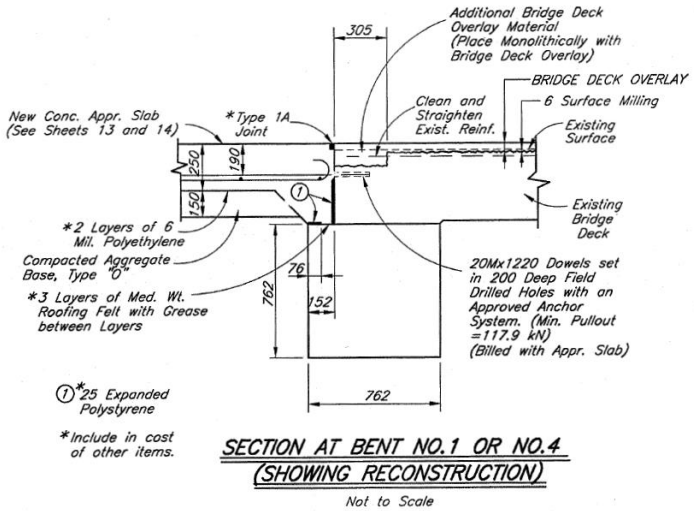

Figure 3-20: Anchorage of Approach Slab and Bridge Deck (INDOT, 1999)

The bridge is supported by two end abutments and two interior bents. Each bent consists of a wall and a single footing. Each wall is 52’-6” long and 1’-6” thick. In bent #2, the height of the wall measured from the base of the footing to the bottom of the bridge slab is 19’-6”, and the height in bent #3 is 17’-3”. Approximately half of the height of each wall is above the ground. Thus the shear deformation addition is justified by the wall aspect ratio of 0.20 in the direction of

transverse shear. Bent #2 has a shear friction connection to the deck consisting of ten (10) #5 bars, while the deck sits on a 1” by 6” neoprene pad at bent #3.

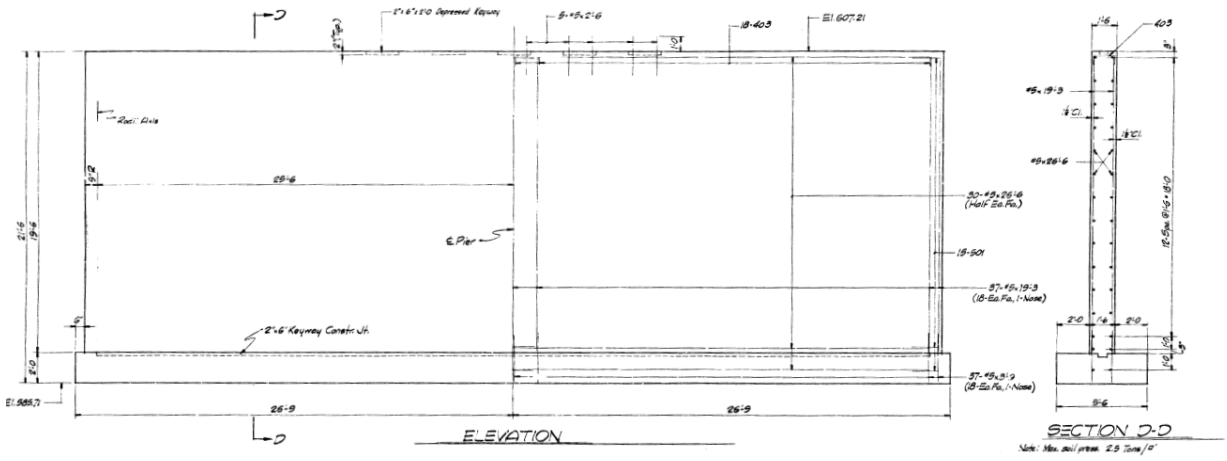

Figure 3-21: Transverse Elevation and Reinforcement Details of Bent #2 (INDOT,1999)

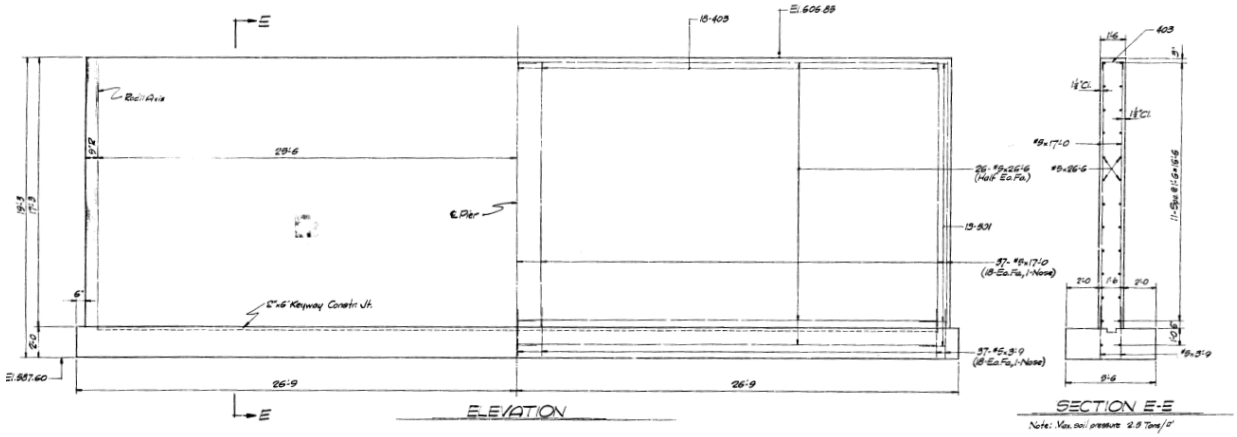

Figure 3-22: Transverse Elevation and Reinforcement Details of Bent #3 (INDOT, 1999)

According to the bridge drawings, the concrete has a compressive strength of 3000 psi, while the reinforcing steel bars have a yield strength of 40,000 psi. An ultimate strain for concrete in compression of 0.003 is assumed for strength calculations.

3.6.3.1 Results – Transverse Direction

The bridge is modelled assuming one bent integral with the deck is capable of resisting the earthquake demand based on the lack of a connection between the deck and bent #2. The deck sits on neoprene bearing pad, thus the wall at bent #2 can be excluded from the dynamic model. However, due to the presence of extended longitudinal bars from the wall in bent #3 into the deck, the deck contributes to the stiffness of the bridge. The mass, stiffness, and period of the bridge calculated in the transverse direction are $2.01\,\frac{kips}{g}$, $2.35 \times 10^6\ kips/in$, and $0.004\ seconds$, respectively.

The period of the bridge is low because of the additional stiffness from the deck due to the presence of extended longitudinal bars. Following the procedure for calculating the capacity of the bridge elements in Section 3.5, the plastic moment capacity and shear force on the substructure are 23325 ft-kip, and 2390 kips, respectively. The wall has a shear strength of 1210 kips which is less than the shear corresponding to the plastic moment. Thus, plastic hinges will not form and the flexural moment acting on the bent is limited by that corresponding to the shear strength. The strength of the shear friction connection between the substructure and the superstructure is 260 kips. This indicates that depending on the level of earthquakes, it is possible that prior to reaching the shear capacity of the wall, the connection would fail and the deck would be free to move in the transverse direction after the friction between the deck and the wall is overcome. Applying the 100 ground motions generated at this bridge site to the bridge model, the shear demand from the earthquakes (50 per fault orientation) is plotted against the peak ground acceleration (PGA) of each earthquake. The substructure capacity is shown using two threshold values corresponding to the strength of the shear friction connection and the shear strength of the wall, as shown in Figure 3-23.

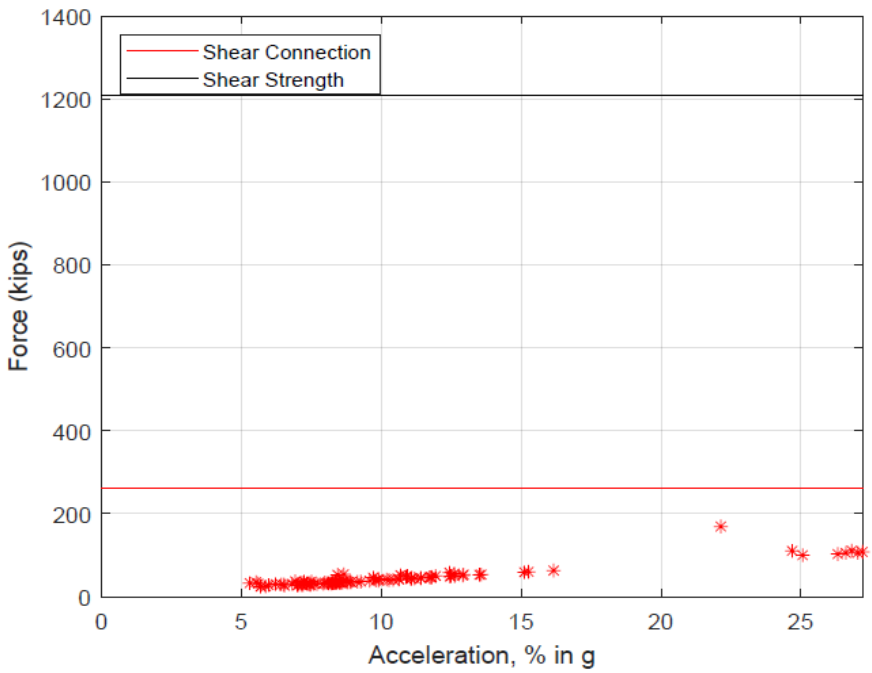

Figure 3-23: Shear Demand Due to Applied Ground Motions – Transverse Direction

Based on the plot, the capacity of the shear friction connection (red line) is not exceeded by the demand for any ground motions determined for this site. Additionally, the maximum displacement of the bridge due to the ground motions is approximately zero. Therefore, the bridge is not vulnerable in the transverse direction at level of ground motions determined at its location (Cao et. al., 2019).

3.6.3.2 Results – Longitudinal Direction

As with the transverse direction, the bridge is modelled as a two span bridge in this direction. The wall is modelled as fixed at the footing and at the top. This assumes that the footing and the extended longitudinal bars into the deck are properly anchored. The bridge is modelled as a single degree of freedom system, so the entire mass is used to obtain the period. The mass, stiffness, and period of the bridge in the longitudinal direction are 1.0 $kips/g$, 7240 $kips/in$, and 0.10 $seconds$, respectively.

In the longitudinal direction, the plastic moment and shear demand of the substructure are 600 ft-kip, and 60 kips, respectively. The wall has a shear strength of 1210 kips, which is greater than the shear demand. Thus, plastic hinges will form. The flexural capacity of the bent is 60

kips. The strength of the shear friction connection between the substructure and the superstructure is 260 kips. Applying the 100 ground motions generated for this bridge site to the bridge model, the shear demand from the earthquakes (50 per fault orientation) is plotted against the peak ground acceleration (PGA) of each earthquake. The substructure capacity is shown using three threshold values corresponding to the flexural capacity, strength of the shear friction connection and the shear strength, as shown in Figure 3-24.

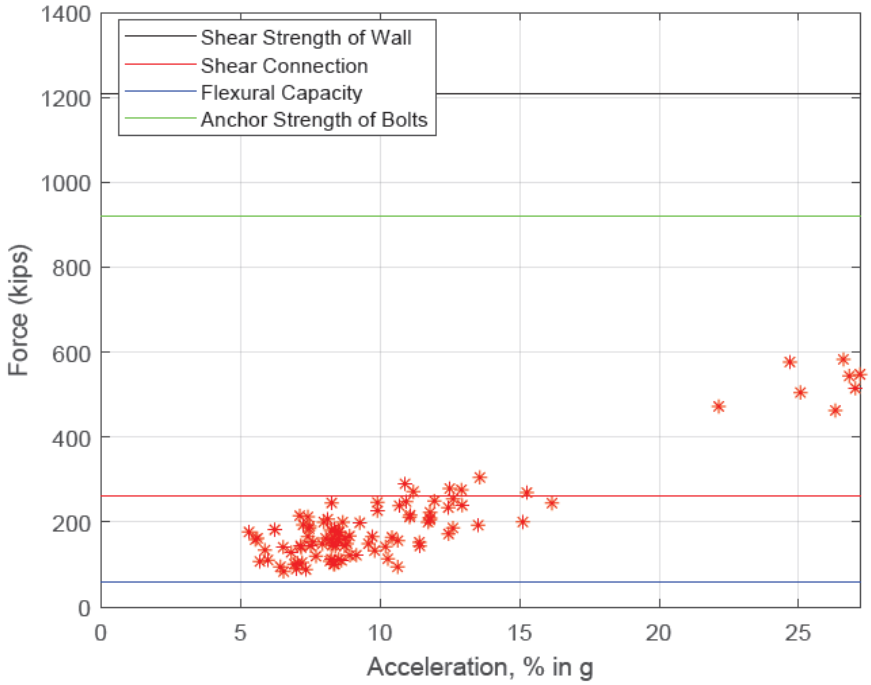

Figure 3-24: Shear Demand Due to Applied Ground Motions – Longitudinal Direction

From the plot, the shear demand from the ground motions does result in reaching the flexural capacity of the wall and strength of shear friction connection. The maximum displacement of the bridge due to the set of earthquakes is 0.08”. This bridge would be classified as marginally vulnerable because the strength of the shear friction connection is exceeded for the higher levels of acceleration at this location. However, due to the presence of anchor bolts that tie the bridge deck to the approach slab, the bridge will experience no differential displacement or inertial force except if the strength of the anchor bolts is exceeded by the shear demand. The strength of the anchor bolts is calculated as the sum of the anchoring forces of the bolts taking into account the coefficient of friction, $\mu_f = 0.6$, as shown in Eq. 3.23.

$$Anchor\ Strength = \mu_f * Anchor\ strength\ of\ each\ bolt * N_{bolts} \quad (3.23)$$

The anchor strength of each bolt was provided on the bridge drawings as shown in Figure 3-20. The total strength of the anchor bolts is 920 kips, which exceeds the shear demand of all the applied ground motions. Therefore, the bridge is not vulnerable at the level of ground motions expected at its location.

3.7 Conclusions

Using the results presented in this chapter and Appendix A, conclusions from the detailed assessment can be categorized by substructure type, and are as follows:

- Multi-column bents with piles: 10 out of 13 of these bridges had integral end abutments. Due to the use of integral end abutments in a bridge, the bridge moves together with the ground during earthquakes assuming the same ground motion at all supports. This is reasonable for the type of bridges in this class. Thus, there are no differential displacement or inertial forces on the bridge, and it is not vulnerable. For the non-integral bridges, the inertial force on the bridge due to the ground motions did not exceed the shear strength of each bridge in both the transverse and longitudinal directions. Additionally, the maximum displacement experienced by each bridge was less than ¼" in the transverse direction, and less than 1" in the longitudinal direction. Therefore, bridges of this type were determined to be of low vulnerability at the level of hazard in Indiana.
- Multi-column bents with RC columns: The maximum displacement experienced by each bridge was less than ¼" in the transverse direction, and less than 1" in the longitudinal direction. The inertial forces due to the ground motions exceeded the shear strength and flexural capacity of each of these bridges. Thus, these bridges were identified as being of high vulnerability at the level of ground motions expected in Indiana.
- Multi-column bents with precast concrete piles: In one of the bridges, the substructure had a high stiffness due to a low substructure height. The bridge experienced a displacement due the ground motions of less than ¼" in both directions, and the shear strength of the substructure was not exceeded. In the other bridge, the maximum displacement experienced was less than ¼" in the transverse direction, and less than 2" in the longitudinal direction. The inertial forces due to the ground motions exceeded the

shear strength, and the bridge was identified as being of high vulnerability at the level of ground motions expected in Indiana.

- Wall substructures: The maximum displacement experienced by each bridge was approximately zero in the transverse direction, and less than ½" in the longitudinal direction. The inertial forces due to the ground motions did not exceed the shear strength of each bridge. Thus, these bridges were identified as being of low vulnerability at the level of ground motions expected in Indiana.

3.8 Summary

In this chapter, the Level 2 assessment procedure for the case of the reinforced concrete bridge type structures is presented, and its application is demonstrated using three bridges located in the Vincennes district. The shear demand from the ground motions are determined and compared to the strength of the bridge load resisting elements. The displacement of the bridge is compared to the available seat length, and the results from the analysis are presented. The results from the assessment of the remaining 22 bridges are presented in the appendix. The results from the detailed assessment will be used to develop the Level 1 assessment procedure presented in the following chapters.

4. LEVEL 1 ASSESSMENT PROCEDURE

4.1 Introduction

In the Level 2 assessment, the bridge drawings were used to determine the dynamic properties of the bridges. For the Level 1 assessment, only information in BIAS shall be used. At this time, BIAS does not contain all the necessary information required for accurate estimates, and assumptions will be made to illustrate the procedure and levels of accuracy in the assessment. This chapter presents the Level 1 procedure and the assumptions made in several candidate models and their validation, as well as an incremental approach to improving the simplified assessment procedure by adding more information into BIAS. From this process, the approach to be used in determining the seismic vulnerability of the bridges will be selected. The analysis is carried out using Microsoft Excel.

4.2 Level 1 Assessment Procedure

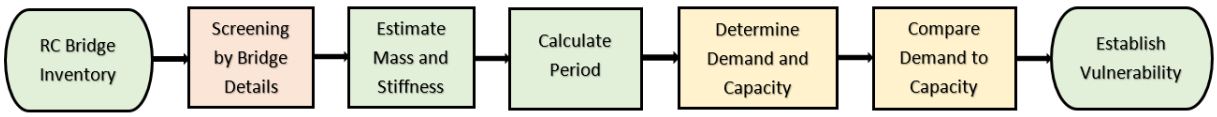

Figure 4-1: Level 1 Assessment Procedure

The first step in the assessment is the identification of the reinforced concrete bridges. Following the identification, some bridges can be excluded from the Level 1 assessment based on their details as being of low vulnerability or requiring a Level 2 assessment. From the Level 2 assessment in Chapter 3, the reinforced concrete bridges were not found vulnerable in the transverse direction except for bridges with RC columns in the substructure for the seismic hazard in Indiana. With this information, the only concern (in terms of demand) for establishing vulnerability in the Level 1 assessment procedure after the initial screening is the determination of the displacement of the bridge in the longitudinal direction. The procedure proposed in Figure 4-1 will be used in establishing the vulnerability of the bridges.

4.3 Initial Screening of Bridges

Prior to performing the Level 1 assessment, a screening is conducted of some bridges identified as having low or high vulnerability based on bridge details and the trends observed in the Level 2 analysis in Chapter 3. The preliminary screening criteria are as follows:

- Integral abutment bridges: Bridges with integral abutments considered in this study are assumed to experience no differential displacement or inertial forces from seismic loading. Thus, these bridges are not vulnerable and can be excluded from the assessment.
- Single span bridges: Based on the available literature (Choi, 2004) and the analysis completed on single span bridges in Chapter 3, single span bridges are of low vulnerability and can be eliminated from the analysis.
- Wall substructures: Bridges with wall substructures have a large stiffness and transverse capacity. The large stiffness results in a low period and at the level of ground motions expected in Indiana, these bridges have low vulnerability.
- Multi-column bents with RC columns and precast concrete piles: Using the detailed assessment results, it can be observed that the inertial forces induced by the ground motions exceeds the shear strength of the substructures in both directions for all the bridges with RC column substructures. Due to the high potential for exceedance of shear strength, bridges with this type of substructures have been identified as being more vulnerable at the intensity of ground motions expected in Indiana, and must be analyzed using the detailed assessment procedure.

4.4 Information Available in BIAS

The information available in BIAS that can be extracted and used to determine the dynamic properties and establish the vulnerability of the bridge are as follows:

- Asset name
- NBI number
- Latitude and Longitude
- Superstructure type (material and construction)
- Year of construction
- Number of spans in main unit

- Structure length
- Deck width, out-to-out

BIAS does not contain any data relevant to the substructure. This information is necessary to determine the stiffness of the bridge to properly assess its seismic vulnerability. To carry out the assessment, the most basic requirement is that substructure type must be known in order to obtain any reasonable estimate of the period. The period is calculated as follows:

$$T = \frac{2\pi}{\sqrt{\frac{K}{M}}} \tag{4.1}$$

The procedure presented in this chapter assumes that the substructure type is known, but not the dimensions. Thus, in the simplest candidate model, assumptions must be made regarding the height, cross sectional dimensions, number of piles or columns, and material properties. Furthermore, the thickness of the deck for the slab bridges is not available in the database. These values must be assumed in order to estimate the mass of the bridge.

4.5 Assumptions and Validations

4.5.1 Mass Estimate for Slab Bridges

To obtain an estimate of the mass of the bridge, a deck thickness must be assumed. From the bridges analyzed in detail in the previous chapter, the thickness of the deck ranges from 1’-3” to 2’- 0”. Due to the wide range of values, the average value for the sample (1.55’) and the average value less one standard deviation, low deck thickness (1.33’), were used to calculate the mass of the bridge. The effect of using each of these values on the period were plotted and examined for 13 bridges to determine the best estimate.

Additionally, the mass of the barriers and railings must be accounted for. To obtain an estimate for this mass, the average difference between the mass values estimated in the detailed assessment, and the mass of the bridge using only the deck geometry was calculated. This yielded a value of 0.20 kips/g, which is included in the mass estimate to account for the presence of the barriers and railings. The mass is calculated using Eq. 4.2.

$$M = \frac{\gamma_c * L_d * w_d * t_d}{g} + 0.2 kips/g \tag{4.2}$$

To check the validity of this assumption, the actual deck thickness together with 0.20 kips/g were used to calculate the mass and period for 13 bridges. The stiffness obtained in the detailed assessment is used, and the only variable is mass. Figure 4-2 shows the comparison between the estimated mass values, while Figure 4-3 shows the corresponding period. The NBI numbers corresponding to the 13 bridges used for validation and in all plots in this chapter are shown in Table 4-1.

Table 4-1: NBI Numbers of Bridges Used for Validation in this Chapter

Bridge Number	**Asset Name**	**NBI Number**
1	(237) 37-13-07277	11840
2	055-45-07366	19880
3	056-63-07286	19933
4	067-55-03831 ANBL	24100
5	252-55-08713	30721
6	064-19-03723 A	22960
7	067-42-07298	23760
8	028-79-07672	7640
9	327-17-06419 A	31350
10	044-55-06793	16310
11	057-14-06739	20690
12	252-24-06934 A	30780
13	I69-334-04590 BNB	40720

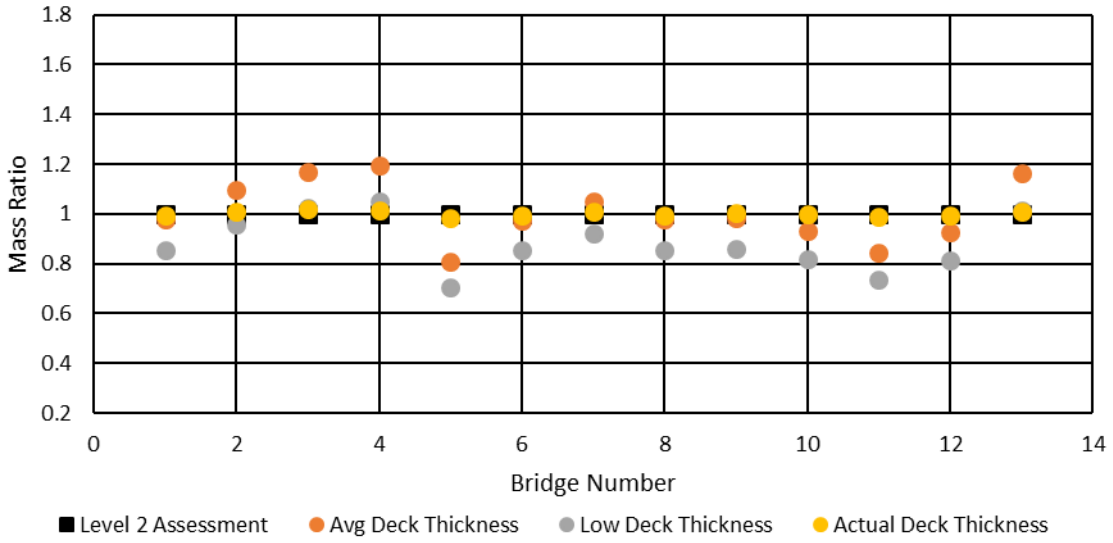

Figure 4-2: Comparison of Mass Estimated Based on Assumed Deck Thickness with Mass Calculated Using the Level 2 Assessment

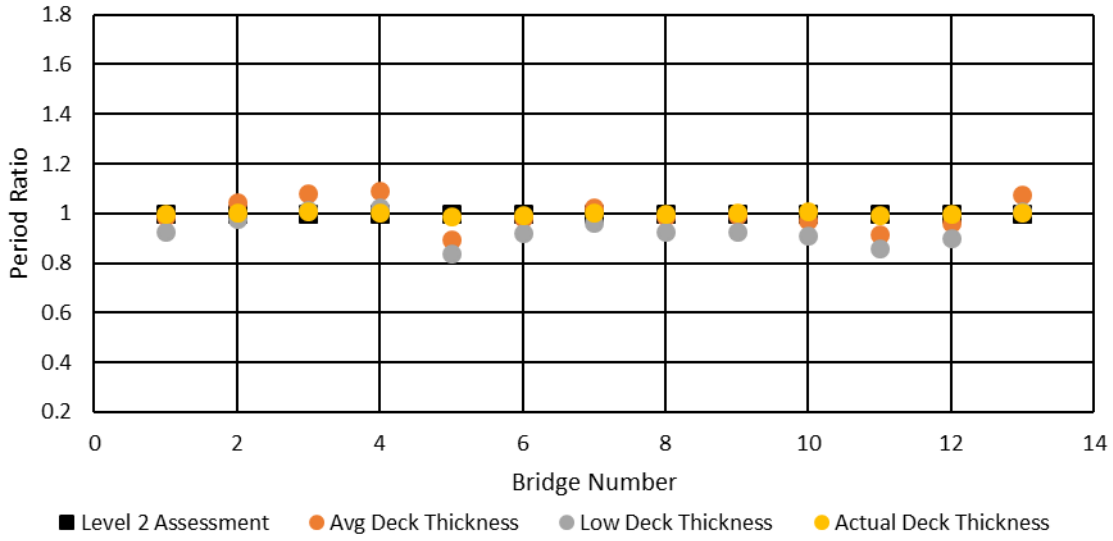

Figure 4-3: Comparison of Period Estimated Based on Assumed Mass with Period Calculated Using the Level 2 Assessment

From the plots, when the actual deck thickness is used together with the estimate for the barriers and railings, the mass and periods obtained are approximately the same as those from the detailed analysis. Regarding the assumed deck thickness values, the average thickness produced better period estimates compared to the low thickness. Using the average deck thickness did not produce the best mass estimate (±20%), but the period values are within ±10% of the detailed assessment results. This shows that the model is not as sensitive to mass, and the average deck thickness is a valid assumption.

4.5.2 Substructure Height

In the detailed assessment, the height of the substructure was based on the bridge drawings, and does not take into account erosion and scour. BIAS does contain information on the scour channel profile for most bridges over waterways. Although this information cannot currently be extracted automatically, it can be used to obtain an estimate of the height of the substructure. The values may not exactly match those obtained from the bridge drawings, but this provides a good estimate for height due to lack of information in BIAS. Additionally, in cases where the scour channel profile is not available, the average substructure height (10.68’) from the sample is used. Figure 4-4 and Figure 4-5 show the stiffness and period values obtained using the scour channel profile to estimate the substructure height. The points corresponding to bridges where the average substructure height are used are represented by red markers, and all bridges used in generating the figures are over waterways. For bridges over roadways, the vertical clearance under the bridge, as recorded in BIAS, is used.

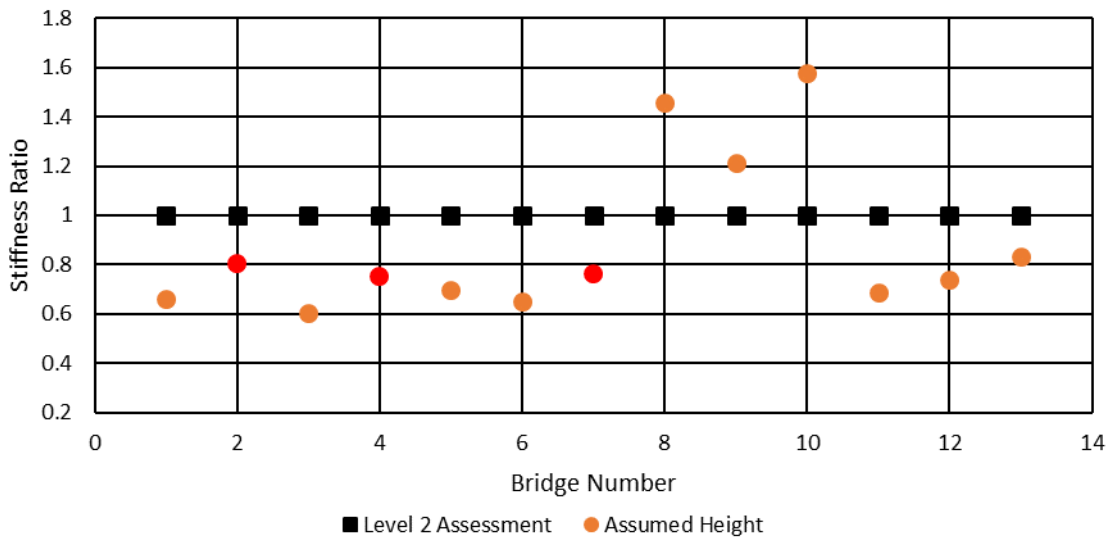

Figure 4-4: Comparison of Stiffness Estimated Based on Assumed Height with Stiffness Calculated Using the Level 2 Assessment

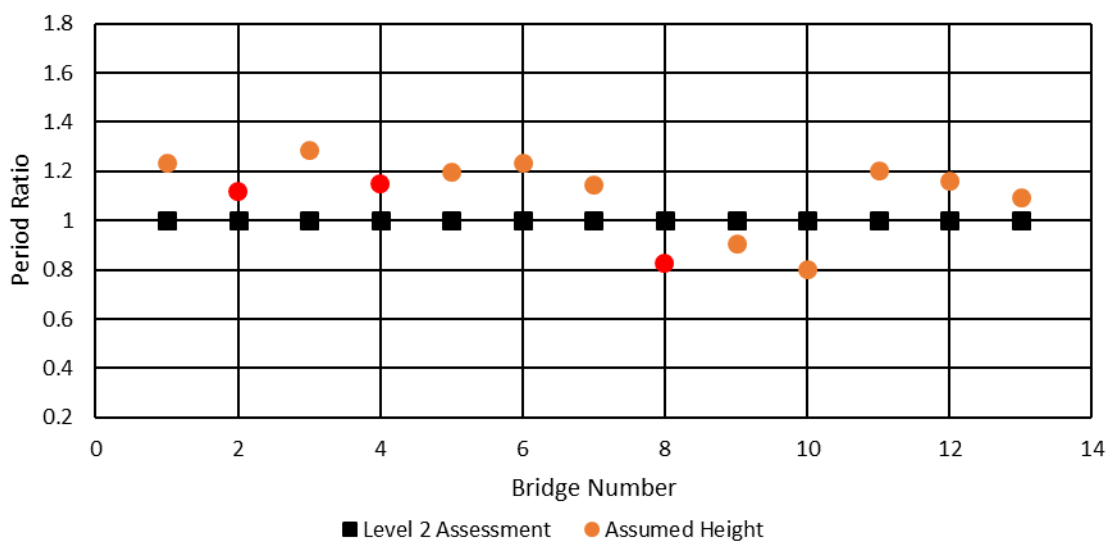

Figure 4-5: Comparison of Period Estimated Based on Assumed Height with Period Calculated Using the Level 2 Assessment

From the plots, the assumed height does not produce results that match well with the Level 2 assessment because scour was not included in the Level 2, but using the scour channel profile is the only information available for estimating the substructure height for bridges over waterways and is thus used for the simplified analysis.

4.5.3 Pile Size and Material Properties

INDOT uses certain standard pile sizes and sections in multi-column bents. For concrete filled steel piles, a 14” diameter steel tube with a wall thickness of 0.2” is typically used. This is demonstrated in the selected bridges that were analyzed in detail. For encased steel piles, HP 12x53 shape encased in a 2’-0” diameter concrete section is typically used. In the sample analyzed, only one bridge had a different pile section. Therefore, HP 12x53 piles can be assumed as the size of the piles. This is the most common detail used by INDOT.

In the current standard detail drawings provided by INDOT, the compressive strength of concrete of 3500 psi is specified. In bridges built prior to the 1990’s, a compressive strength of 3000 psi was typical. Using the year of construction, the material properties of steel and concrete can be estimated. Typically reinforcing steel with a yield strength of 60000 psi is used in bridges built after 1990, and 40000 psi is used in bridges built before 1990. For the H pile sections, a yield strength of 36000 psi is assumed in older bridges, and 50000 psi is assumed in recently constructed bridges. Lastly, for steel tubes, a yield strength of 40000 psi is assumed for older bridges, while 60000 psi steel is used for bridges constructed after 1990.

Using these assumptions, the relative stiffness, *EI*, of the substructure can be estimated. To demonstrate the validity of these assumptions, the stiffness and period for the sample of 13 bridges are calculated using the assumptions, and are then compared to the values obtained from the detailed assessment. The comparison is shown in Figure 4-6 and Figure 4-7.

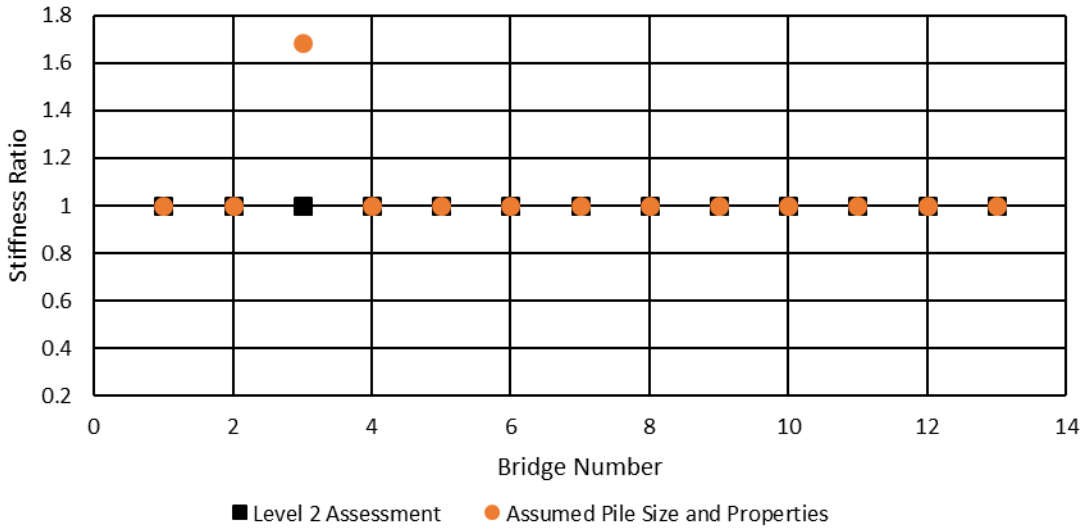

Figure 4-6: Comparison of Stiffness Estimated Based on Assumed Pile Size and Properties with Stiffness Calculated Using the Level 2 Assessment

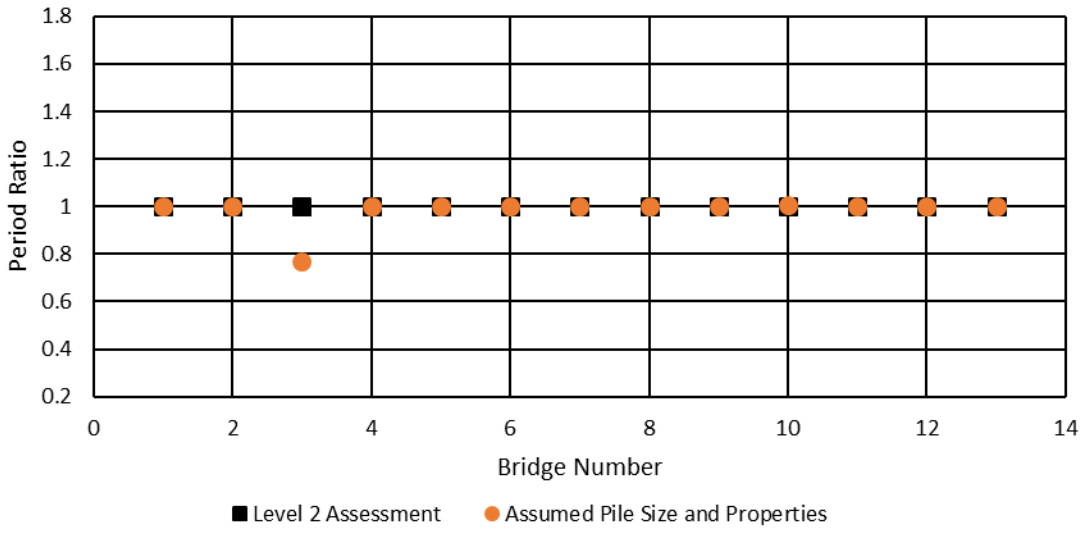

Figure 4-7: Comparison of Period Estimated Based on Assumed Pile Size and Properties with Period Calculated Using the Level 2 Assessment

According to Figure 4-6 and Figure 4-7, the assumptions used for the pile size and material properties accurately capture the results of the detailed analysis in all but one case. In this case, the pile is actually an HP 10x42 encased in a 1'-9" diameter concrete section. Without looking at the bridge drawings, one would not know that a different pile size is used. The error in period in this case is approximately 20%. Thus, the assumed pile sizes proposed in this section are adequate for estimating stiffness in most cases, and can be used in the simplified analysis. Note that if the substructure information was provided, it would improve the assessment.

4.5.4 Number of Piles

The number of piles varies from bridge to bridge. The ratio of the deck width to number of piles is examined separately for the concrete encased steel piles and the concrete filled steel piles. The average of the ratios for each pile type is calculated, 4.9 for the concrete encased steel pile and 4.4 for the concrete filled steel pile. Using these ratios along with the width of the deck, the number of piles in each bent is estimated and used to calculate the stiffness and period of the 13 bridges. The results are shown in Figure 4-8 and Figure 4-9.

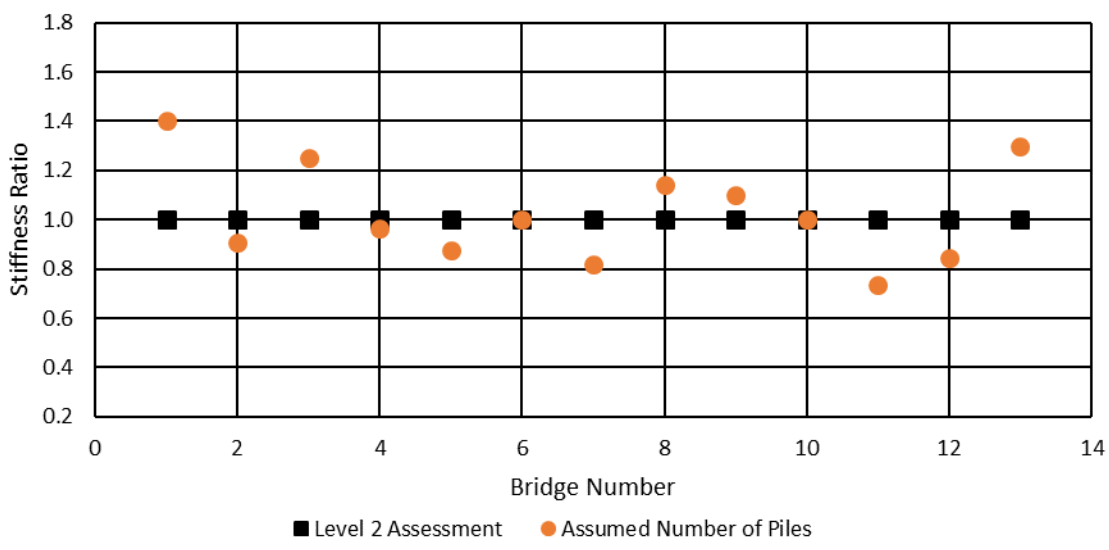

Figure 4-8: Comparison of Stiffness Estimated Based on Assumed Pile Size Number of Piles with Stiffness Calculated Using the Level 2 Assessment

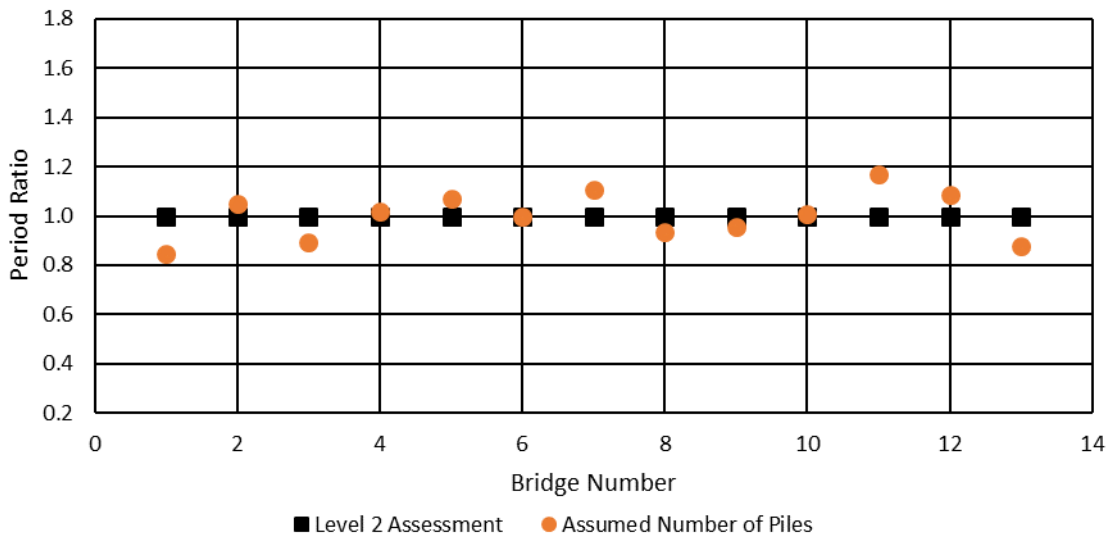

Figure 4-9: Comparison of Period Estimated Based on Assumed Pile Size Number of Piles with Period Calculated Using the Level 2 Assessment

Although these ratios do not accurately estimate the exact number of piles in each bent, it provides a reasonable estimate for stiffness. In Figure 4-8 and Figure 4-9, the first 5 bridges have concrete encased steel piles, and the others have concrete filled steel piles. Using the ratios is a practical way to estimate the number of piles.

4.6 Bridge Vulnerability Criteria

The criteria used in this project for establishing vulnerability is based on the Handbook for the Post Earthquake Safety Evaluation of Bridges and Roads, and the National Cooperative Highway Research Program (NCHRP) Project 12-49 (Ramirez, 2000 and NCHRP, 2002). The vulnerability levels are as follows:

- **Green vulnerability level (Low vulnerability)**
    - Displacement of the bridge is less than 1”
    - Column drift is less than 0.5% in the transverse direction
    - Longitudinal reinforcement has not yielded in the transverse direction
- **Yellow vulnerability level (Marginal vulnerability)**
    - Displacement of the bridge is between 1” to 6”

    - Column drift is between 0.5% to 1.5% in the transverse direction
    - Longitudinal reinforcement has yielded in the transverse direction
- **Red vulnerability level (High vulnerability)**
    - Displacement of the bridge is greater than 6”
    - Column drift is greater than 1.5% in the transverse direction
    - Column shear strength is exceeded

4.7 Incremental Development of the Level 1 Assessment Procedure

The process for developing and validating the Level 1 assessment procedure is shown in Figure 4-10. The validation of the procedure is necessary to ensure that both levels of analysis produce the similar vulnerability results for each bridge. By gradually increasing the level of information and reducing the number of assumptions used, the accuracy of the results can be improved. Moreover, the value of such added information can be quantified, as done in the following sections.

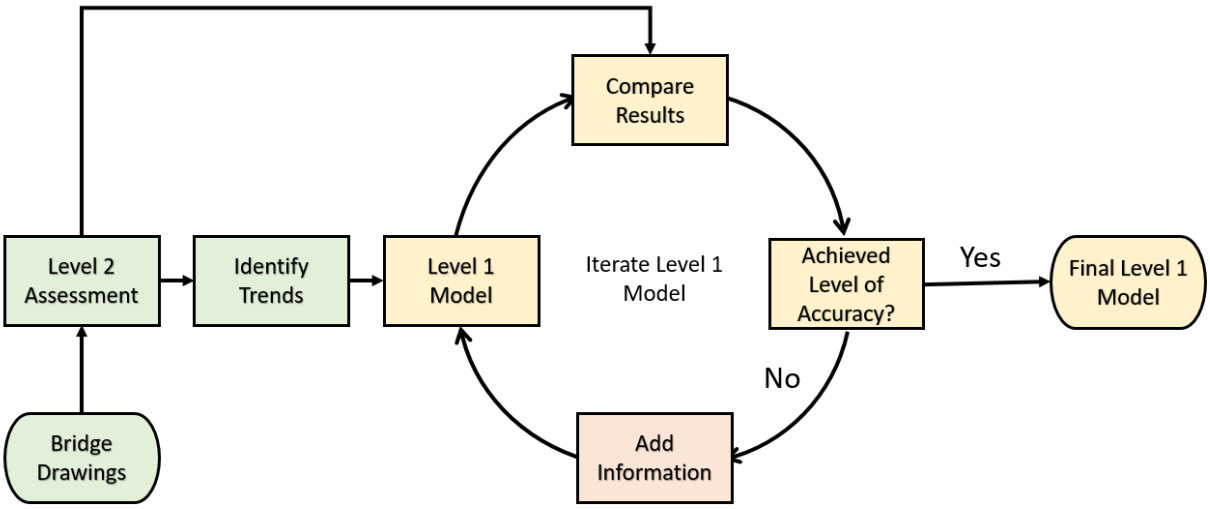

Figure 4-10: Process for Development of the Level 1 Assessment Procedure

4.7.1 Base Model

The base model is the basic model for the simplified assessment. This model is built using the information available in BIAS plus the substructure type. All other necessary information are defined based on the assumptions presented in Section 5. The substructure type is the minimum

level of information in addition to the BIAS data items that is necessary to estimate the period of the structure. Figure 4-11 presents the information used in calculating the period.

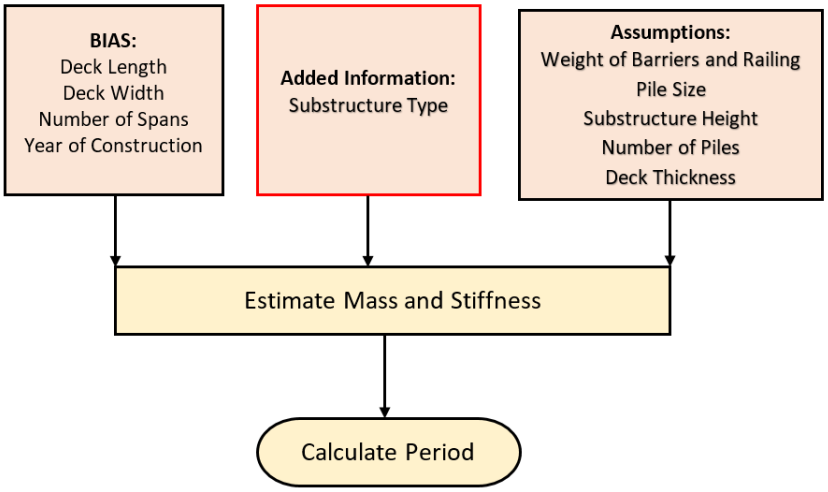

Figure 4-11: Information Used to Obtain Base Model

4.7.2 Results and Validation

Using the procedure presented in Figure 4-1 and the base model, the period of each of the 13 bridges is calculated and compared to the results of the Level 2 assessment. The comparison is shown in Figure 4-12.

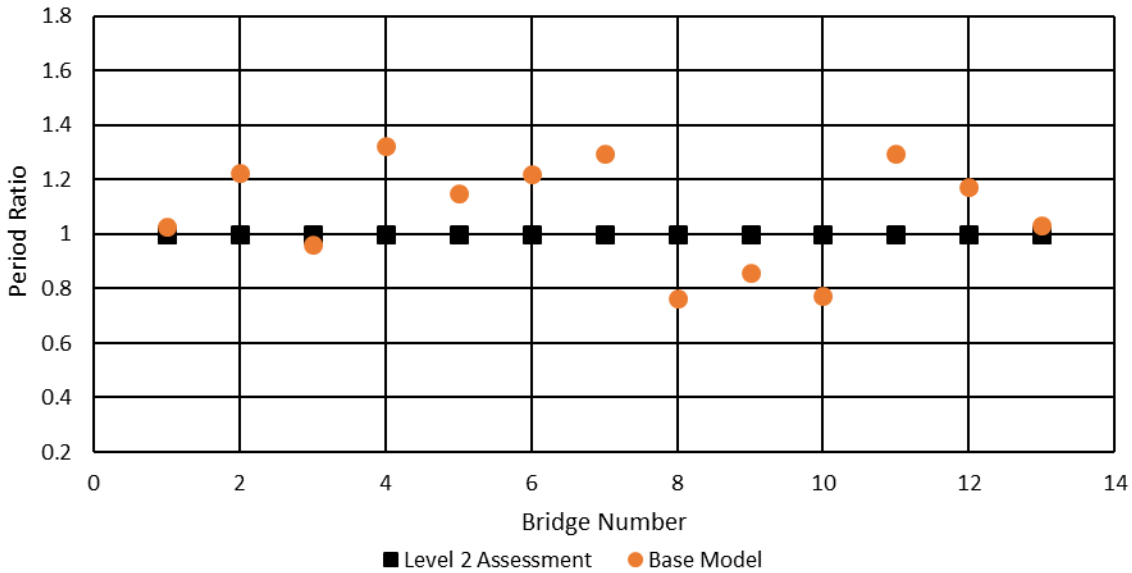

Figure 4-12: Comparison Between the Period Determined in the Level 2 Assessment with that of the Base Model

The period obtained using the base model ranges from 0.75 to 1.4 times the Level 2 assessment period. To understand the effect of using the approximate periods, the displacement response spectra corresponding to the same 100 synthetic ground motions are used to determine the response of each bridge, and the results from both models are directly compared. The 100 ground motions were used to validate that both models produce the same results for each bridge. Ideally, both models should always produce the same results for a given ground motion. The results from the comparison are shown in Table 4-2.

Table 4-2: Comparison of Performance Using the Base Model to that of the Level 2 Assessment

		Level 2 Assessment		
		Green	Yellow	Red
Base Model	Green	917	67	0
	Yellow	95	218	2
	Red	0	1	0

In Table 4-2, the diagonal (grey cells) represent the number of times that both the Level 2 assessment and base model yield the same results, while the terms below the diagonal (light blue cells) represent the conservative results. Conservative results refer to the cases where the base model is underestimating the performance of the bridge. The terms above the diagonal (navy blue cells) overestimate the performance of the bridges. The results indicate that the base model is predicting the bridges to not reach the increased limit state in 69 instances in which the Level 2 assessment resulted in the bridges having worse performance. To increase the agreement between both models thus reducing the number of cases where the Level 1 model overestimates results compared to the Level 2, the number of assumptions is incrementally reduced to understand the influence of this information and select an appropriate candidate model.

4.8 Improved Models

4.8.1 Option A

To improve the accuracy of the base model, the substructure height from the bridge drawings is added to the known data. The substructure height is selected to be added next because it has the largest influence on the stiffness after the substructure type. The details of this approach are shown in Figure 4-13.

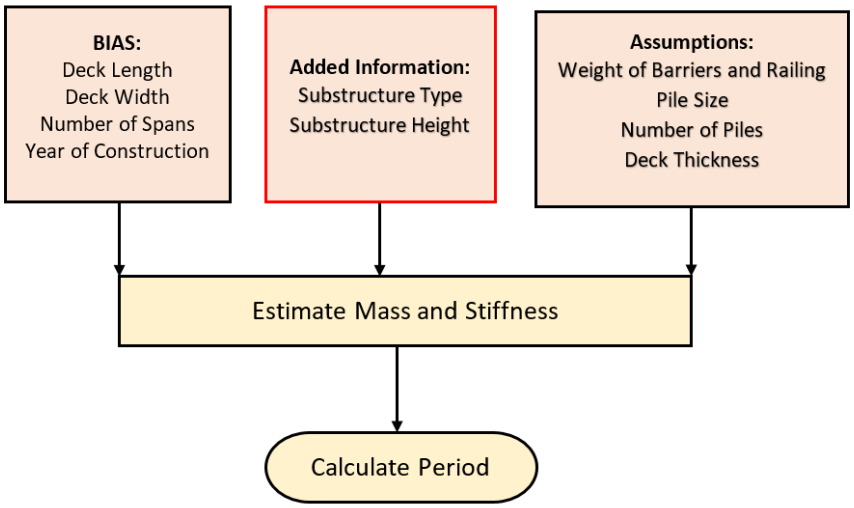

Figure 4-13: Information Used to Obtain Improved Model A

4.8.2 Results and Validation

Applying the process described in Figure 4-13 to develop improved model A for the same 13 bridges yields the periods shown in Figure 4-14.

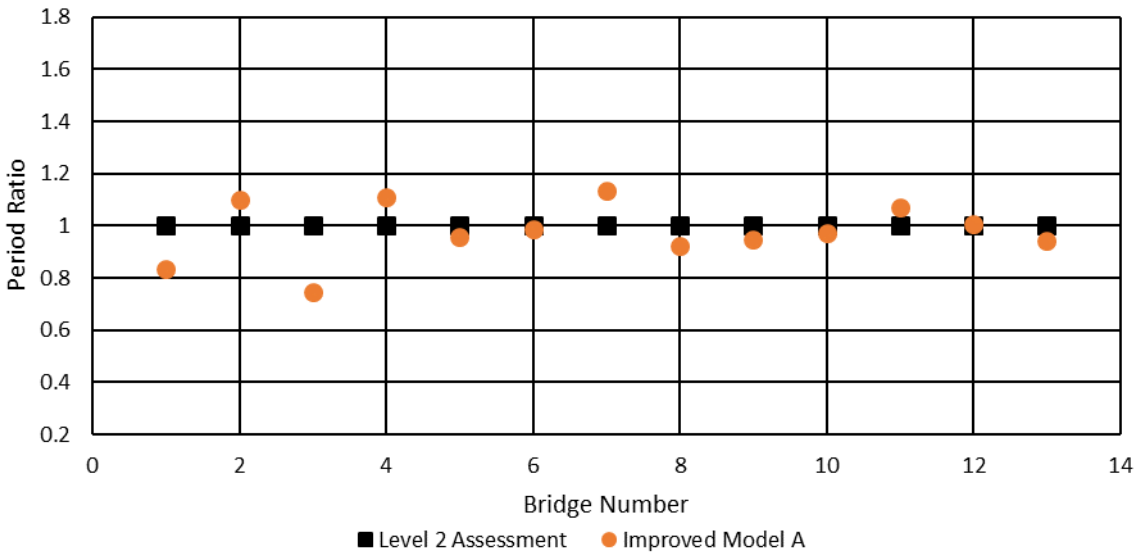

Figure 4-14: Comparison Between the Period Determined in the Level 2 Assessment with that of Improved Model A

The period obtained from this model ranges from 0.75 to 1.2 times that of the period obtained in the Level 2 assessment. Using the displacement response spectra of the same 100 ground motions used previously, the results with this model and with the Level 2 assessment are compared.

Table 4-3: Comparison of Performance Using Improved Model A to that of the Level 2 Assessment

		Level 2 Assessment		
		Green	Yellow	Red
Improved Model A	Green	981	33	0
	Yellow	18	264	2
	Red	0	2	0

Based on Table 4-3, the number of times that improved model A is overestimating the performance of the bridges is reduced by 50% as compared to the base model. This is a significant improvement already. The results of the analysis can be further improved by adding more information and reducing the assumptions.

4.8.3 Option B

By adding the actual number of piles to the known information, the simplified assessment results can be improved further. The number of piles is chosen to be added next because it has a larger influence on the stiffness and period compared to the other assumptions. The details of the model are shown in Figure 4-15.

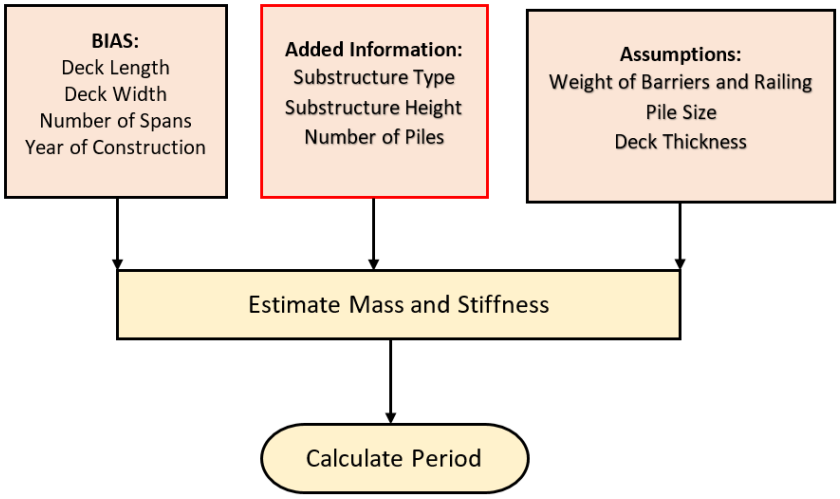

Figure 4-15: Information Used to Obtain Improved Model B

4.8.4 Results and Validation

The comparison of period obtained using the improved model B and the Level 2 assessment is shown in Figure 4-16. The period calculated using this model ranges from 0.8 to 1.1 times that of the Level 2 assessment results.

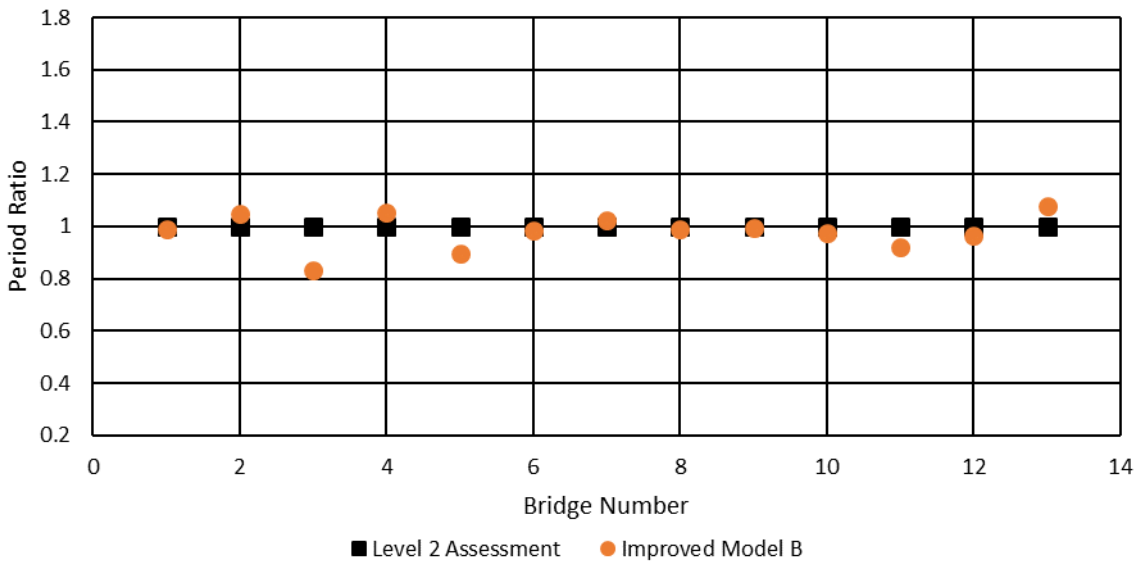

Figure 4-16: Comparison Between the Period Determined in the Level 2 Assessment with that of Improved Model B

The response spectra corresponding to the same100 ground motions are used to determine the performance of each bridge, and the results from the Level 2 assessment and this model are compared. The results are shown in Table 4-4.

Table 4-4: Comparison of Performance Using Improved Model B to that of the Level 2 Assessment

		Level 2 Assessment		
		Green	Yellow	Red
Improved Model B	Green	988	21	0
	Yellow	13	276	0
	Red	0	0	2

Based on Table 4-4, the number of times that improved model B is over predicting the performance of the bridges is reduced by 33% as compared to improved model A, and 70% as compared to the base model. The results of the analysis can be further improved by adding more information and reducing the assumptions.

4.8.5 Option C

Lastly, the actual deck thickness is added to the known information and the model is used to estimate the period of the bridges. The details of the model are presented in Figure 4-17.

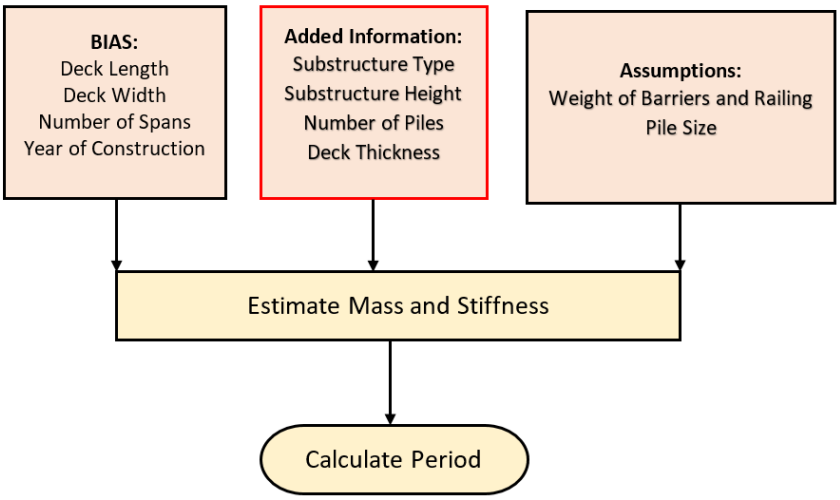

Figure 4-17: Information Used to Obtain Improved Model C

4.8.6 Results and Validation

Using Figure 4-17, the period of the 13 bridges is calculated and compared to the results of the detailed assessment. The comparison between the period obtained using this model and that of the detailed assessment is shown in Figure 4-18.

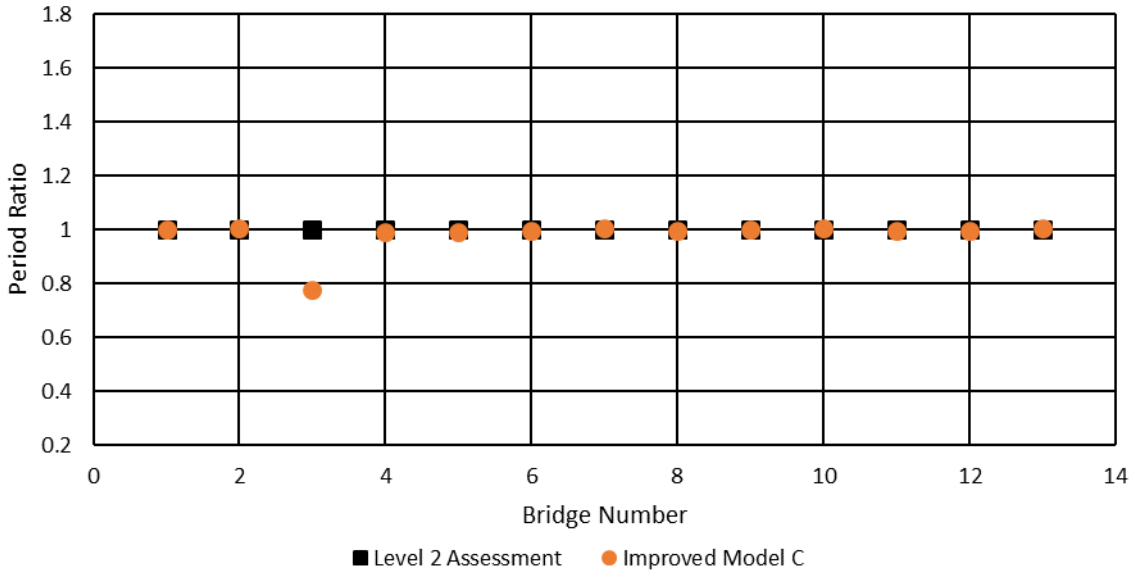

Figure 4-18: Comparison Between the Period Determined in the Level 2 Assessment with that of Improved Model C

Improved model C accurately estimates the period of the bridges as compared to the Level 2 assessment, except in one case. The reason for the discrepancy in this case is due to the assumption that HP 12x53 piles are typically used for encased pile section. In this bridge, a HP 10x42 pile was used. However, this information would not be known without the bridge drawings. This assumption results in the improved model C underestimating the period of the bridge by approximately 20%.

Using the displacement response spectra for the same 100 ground motions used previously, the performance of the bridges determined using this model and the Level 2 assessment are compared. The comparison is shown in Table 4-5.

Table 4-5: Comparison of Performance Using Improved Model B to that of the Level 2 Assessment

		Level 2 Assessment		
Improved Model C		Green	Yellow	Red
	Green	1001	2	0
	Yellow	0	295	0
	Red	0	0	2

According to Table 4-5, all of the conservative results have been eliminated, and the number of times the model is over predicting the number of exceedances is reduced by over 95% as compared to the base model. The results show that increasing the level of information available increases the accuracy of the model.

4.9 Summary

The criteria for establishing vulnerability levels were presented in this chapter. The process of validating the simplified assessment procedure, and the influence of increasing the level of available information on the analysis were developed and discussed. The major conclusions from this chapter are as follows:

- The initial screening of the RC bridges indicates that bridges with RC columns or precast concrete piles, due to the likelihood of shear strength being exceeded by the inertial forces from the ground motions, should be analyzed using the Level 2 assessment described in Chapter 3 to establish its vulnerability
- The minimum data item that must be added to BIAS to use the simplified assessment procedure (Level 1) is the substructure type. Improved agreement with the Level 2 results can be obtained by adding information to BIAS as described in Section 4.8.

- Adding information about the bridge details such as abutment and bearing types can be used for a more robust preliminary screening process as in Section 4.3 to identify bridges of low and high vulnerability.

5. DEMONSTRATION OF THE LEVEL 1 ASSESSMENT OF SELECTED BRIDGES

5.1 Introduction

In this chapter, the simplified assessment procedure is implemented to demonstrate how one would establish the vulnerability of the selected bridges presented in Chapter 3. The bridges are modelled using each of the models discussed in Chapter 4 and the results are provided and discussed.

5.2 Simplified Assessment of the Selected bridges

5.2.1 Procedure for Determining Demand

For the simplified assessment, the seismic demand on the bridges is calculated using the NEHRP-2015 design spectrum for each bridge location and its corresponding site class. The NEHRP-2015 design spectra are used because access to the AASHTO-2014 design spectra was unavailable at the time of completion of this report. NEHRP was chosen over ASCE 7 because the site classes used in the ground motion generation were based in NEHRP site classification.

An example of the design spectra is shown in Figure 5-1 (USGS, 2015). The spectra shown is the design spectra corresponding to bridge 064-19-03723 A, which has a site class D.

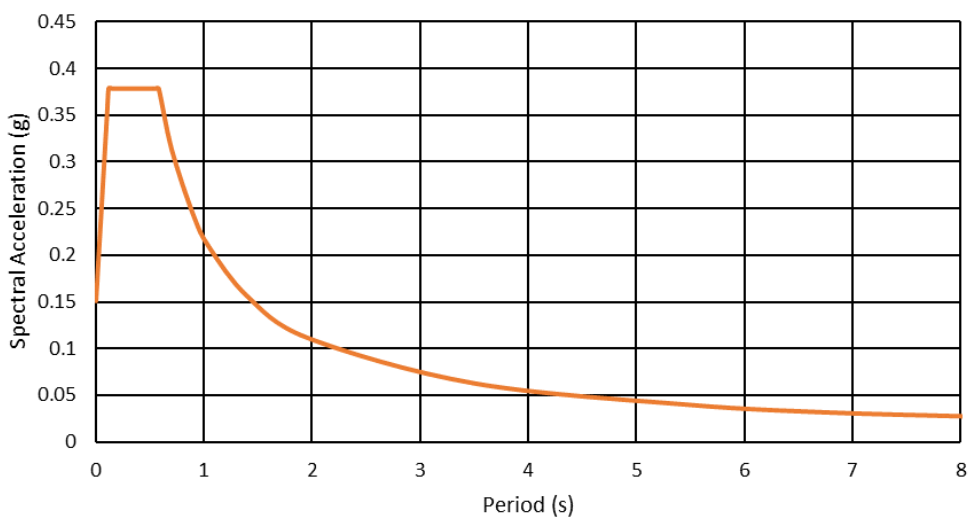

Figure 5-1: NEHRP-2015 Design Spectra for 064-19-03723 A (USGS, 2015)

The design spectrum is used to obtain the spectral acceleration at the period of the bridge, which is used to calculate the equivalent spectral displacement.

$$S_d = \frac{S_a}{{\omega_n}^2} \tag{5.1}$$

Here, the value of ω_n is given by:

$$\omega_n = \frac{2\pi}{T}$$

The bridges are modelled as single-degree-of-freedom systems, which means the spectral displacement is the displacement demand on the structure. Using Figure 5-1 and a period of 0.42 seconds for the bridge, the spectral acceleration obtained is 0.372g. Therefore, the spectral displacement and demand on the bridge is 0.62”. Based on the criteria presented in Section 4.6, this bridge is classified as having low vulnerability (Green).

5.2.2 Preliminary Screening Results

Applying the preliminary screening procedure discussed in Section 4.2 to the 25 selected representative sample of RC bridges in Indiana, the results are as follows:

- 3 single span bridges – Green (low vulnerability)
- 10 bridges with integral end abutments – Green (low vulnerability)
- 5 bridges with wall-type substructures – Green (low vulnerability)
- 2 bridges with RC columns in the bents – Detailed assessment required
- 2 bridges with precast concrete piles in the bents – Detailed assessment required

5.2.3 Results of the Simplified Assessment

After the preliminary screening, 3 out of the 25 bridges remain of those to be analyzed using the simplified assessment procedure. The vulnerability of each bridges using the base and improved models are presented in Table 5-1 to Table 5-4.

Table 5-1: Simplified Assessment Results Using Base Model

Asset Name	District	M_I (kip/g)	K_I (kips/in)	T_I (s)	S_a (g)	S_d (in)	Vulnerability
064-19-03723 A	Vincennes	2.10	466	0.42	0.378	0.65	**Green (Low)**
067-55-03831 ANBL	Crawfordsville	2.28	1995	0.21	0.218	0.09	**Green (Low)**
I69-334-04590 BNB	Fort Wayne	2.90	386	0.54	0.142	0.40	**Green (Low)**

Table 5-2: Simplified Assessment Results Using Improved Model A

Asset Name	District	M_I (kip/g)	K_I (kips/in)	T_I (s)	S_a (g)	S_d (in)	Vulnerability
064-19-03723 A	Vincennes	2.10	715	0.34	0.378	0.43	**Green (Low)**
067-55-03831 ANBL	Crawfordsville	2.28	2834	0.18	0.218	0.07	**Green (Low)**
I69-334-04590 BNB	Fort Wayne	2.90	462	0.50	0.142	0.35	**Green (Low)**

Table 5-3: Simplified Assessment Results Using Improved Model B

Asset Name	District	M_I (kip/g)	K_I (kips/in)	T_I (s)	S_a (g)	S_d (in)	Vulnerability
064-19-03723 A	Vincennes	2.10	715	0.34	0.378	0.43	**Green (Low)**
067-55-03831 ANBL	Crawfordsville	2.28	2939	0.17	0.218	0.06	**Green (Low)**
I69-334-04590 BNB	Fort Wayne	2.90	356	0.57	0.142	0.45	**Green (Low)**

Table 5-4: Simplified Assessment Results Using Improved Model C

Asset Name	District	M_I (kip/g)	K_I (kips/in)	T_I (s)	S_a (g)	S_d (in)	Vulnerability
064-19-03723 A	Vincennes	2.15	715	0.34	0.378	0.43	**Green (Low)**
067-55-03831 ANBL	Crawfordsville	1.93	2939	0.16	0.218	0.05	**Green (Low)**
I69-334-04590 BNB	Fort Wayne	2.52	356	0.53	0.142	0.39	**Green (Low)**

5.3 Summary

The results from a demonstration of the simplified assessment of the selected bridges were presented in this chapter. Applying the methodology to the 25 selected reinforced concrete bridges, 21 of the bridges were identified as being of low vulnerability at the level of seismic hazard in Indiana. Four bridges were required to have a Level 2 assessment completed to determine the level of vulnerability. Each of the simplified assessment models used produces the same level of vulnerability for each bridge with the selected hazard level. The vulnerability results determined in both the Level 1 and Level 2 assessment of the overall sample were the same.

6. CONCLUSIONS AND RECOMMENDATIONS

The conclusions of the thesis are summarized in this chapter. Recommendations for INDOT on how to incorporate the proposed additional information into BIAS are also presented.

6.1 Conclusions

The major conclusions from the Level 2 assessment of the selected bridges (Chapter 3) are as follows:

- Based on the results presented in Chapter 3 and Appendix A, the vulnerability of the bridges can be screened if the substructure type is added to BIAS.
- Single span bridges are of low vulnerability and do not need to be analyzed, as shown in Section 3.3.
- Integral end abutments allow the bridges considered in this study to be assumed to move together with the ground during earthquakes in a synchronous motion at all supports. Thus, there is no differential displacement or inertial force on these bridges, and they are not vulnerable.
- Using the detailed assessment results, bridges having multi-column bents with piles, or wall substructures were determined to be of low vulnerability at the level of ground motions expected in Indiana. The shear demand from the ground motions did not exceed the shear strength of the bridges, and the bridges experienced displacements less than 1”.
- Lastly, bridges with multi-column bents that consist of reinforced concrete columns or precast concrete piles were identified as being vulnerable at the level of hazard in Indiana, and screened for Level 2 vulnerability assessment.

The major conclusions from the development and validation of the Level 1 assessment procedure (Chapter 4) are as follows:

- Bridges with RC columns or precast concrete piles, due to the likelihood of shear strength being exceeded by the shear demand from the ground motions, are screened for Level 2 assessment as illustrated in Chapter 3.

- The minimum data item that must be added to BIAS to use the Level 1 assessment procedure is the substructure type.
- Adding information about the bridge details such as abutment and bearing types is important for the preliminary screening process to identify bridges as having low vulnerability or requiring a Level 2 assessment based on the bridge details and trends observed in the Level 2 analysis.
- Increasing the level of information available in BIAS improves the agreement between the results of the Level 1 assessment process and the Level 2. Adding substructure information, such a substructure type and height can improve the agreements between the results of the assessment by over 50%. And adding deck thickness in addition to the substructure information results in a 95% agreement between the results of the Level 1 and Level 2 assessment.

The simplified assessment procedure (Level 1) developed here was applied to the 25 selected representative sample of the reinforced concrete bridges in Indiana. 21 of the bridges were identified as being of low vulnerability at the level of seismic hazard in Indiana. Based on the screening, four bridges required a detailed assessment to determine the level of vulnerability. Each of the simplified assessment models used produced the same level of vulnerability for each bridge for the level of hazard used, NEHRP-2015 design spectra, for the appropriate site class at each bridge location which was determined using the site class map developed by IGS.

In applying the Level 1 procedure developed to the 2600 reinforced concrete bridges managed by INDOT, one would expect the results obtained to be similar to the results of the 25 RC bridges analyzed in this report. Based on the results observed in this report, RC bridges (excluding those with multi-column bents having RC columns) in all but the Vincennes district would be classified as having low vulnerability (Green) for the level of hazard in the state of Indiana. Due to the increased hazard in the Vincennes district, this is the area where bridges may be identified as being of all vulnerability levels.

6.2 Implementation Recommendations for INDOT

The simplified assessment procedure developed and discussed in this thesis requires that substructure type be added into INDOT's asset management database, BIAS, at a minimum.

Consistent information regarding the substructure type, substructure height, and number of piles can be collected during the routine inspection of the bridges with some modifications to the visual inspection forms. Currently, the inspection of each bridge is carried out every 24 months. If such information is collected during these inspections, the database can be updated with the additional data needs for all the bridges.

Prior to 2012, the predecessor to BIAS had a data item for the deck thickness, and some information is still available in previous inspection reports. If INDOT chooses to implement the addition of deck thickness, this can be achieved by uploading this data field back into BIAS. For bridges constructed after 2012, the bridge drawings may have to be examined to obtain the deck thickness information.

6.3 Future Work

The Level 1 assessment procedure developed in this report will be implemented into a tool that INDOT employees can use to determine the seismic vulnerability of its bridge network. Although this report focused on reinforced concrete bridges in Indiana, with some modifications the procedure can be adapted for steel and prestressed concrete bridges. The priority in which information is proposed to be added for other bridge types may vary based on the results and trends from the Level 2 assessment, which shall be completed by other project team members at Purdue University. Lastly, the results from the vulnerability assessment can be improved upon and retrofits can be recommended if more detailed information regarding the current condition of the bridges are known.

REFERENCES

AASHTO LRFD (2017). *AASHTO LRFD Bridge Design Specifications 8th Ed.* American Association of State Highway and Transportation Officials, Washington, D.C.

ACI Committee 318. (2014). *Building Code Requirements for Structural Concrete: (ACI 318-14); and Commentary (ACI 318R-14).* American Concrete Institute, Farmington Hills, MI.

AISC Committee 360. (2016). *Steel Construction Manual 15th Ed*. American Institute of Steel Construction, Chicago, IL

BIAS (2018). *Bentley® InspectTech™*, INDOT, indot-it.bentley.com/login.aspx.

Cao, Y., & Mavroeidis, G. (2019). *Seismic Hazard Assessment and Simulation of Ground Motions.* Deliverable 1 JTRP No. 4222, University of Notre Dame, IN.

Choi, E. (2002). *Seismic Analysis and Retrofit of Mid-America Bridges* (Doctoral dissertation). Retrieved from Georgia Tech Library.

Choi, E., Desroches, R., & Nielson, B. (2004). *Seismic Fragility of Typical Bridges in Moderate Seismic Zones.* Engineering Structures, 26(2), 187-199.

Chopra, A. K. (1995). *Dynamics of Structures: Theory and Applications to Earthquake Engineering*. Upper Saddle River, NJ: Prentice Hall.

Frosch, R., Kreger, M., & Talbott, A. (2009). *Earthquake Resistance of Integral Abutment Bridges*. Rep. JTRP No. 2867, Purdue University, IN.

Garcia, L. E. (1998). *Dinámica Estructural Aplicada al Diseño Sísmico*. Bogotá: Universidad de loa Andes, Facultad de Ingeniería, Departamento de Ingeniería Civil.

IGS (2011). *Predicted Responses of Geologic Materials to Seismically Induced Ground Shaking in Indiana*. Indiana Geological and Water Survey. Retrieved from https://maps.indiana.edu/previewMaps/Geology/Seismic_Shaking_Materials_Response.html

INDOT (2012). *Reinforced-Concrete Encasement for Piles.* Standard Drawing No. E 701-BPIL-01, IN.

INDOT (1940). *Standard Concrete Pile Details*. Bridge Standard P_2, IN.

INDOT (1979). *Structural Plans for Bridge 64-63-03590A.* Pike County, IN.

INDOT (1980). *Structural Plans for Bridge 44-55-06793.* Morgan County, IN.

INDOT (1980). *Structural Plans for Bridge 67-28-00938A.* Greene County, IN.

INDOT (1981). *Structural Plans for Bridge 75-06-04958A.* Boone County, IN.

INDOT (1982). *Structural Plans for Bridge 57-14-06739.* Davies County, IN.

INDOT (1984). *Structural Plans for Bridge 64-19-03723A.* Dubois County, IN.

INDOT (1985). *Structural Plans for Bridge 18-05-06573A.* Blackford County, IN.

INDOT (1985). *Structural Plans for Bridge 252-24-06934.* Franklin County, IN.

INDOT (1991). *Structural Plans for Bridge 24-56-00899B.* Newton County, IN.

INDOT (1992). *Structural Plans for Bridge 55-45-7366.* Lake County, IN.

INDOT (1992). *Structural Plans for Bridge 56-63-7286.* Pike County, IN.

INDOT (1992). *Structural Plans for Bridge 67-55-03831A.* Morgan County, IN.

INDOT (1994). *Structural Plans for Bridge 37-13-07277.* Crawford County, IN.

INDOT (1994). *Structural Plans for Bridge I70-112-05137 DEBL*. Hancock County, IN.

INDOT (1995). *Structural Plans for Bridge 28-79-07672.* Tippecanoe County, IN.

INDOT (1996). *Structural Plans for Bridge 41-56-03828B.* Newton County, IN.

INDOT (1996). *Structural Plans for Bridge 67-42-07298.* Knox County, IN.

INDOT (1997). *Structural Plans for Bridge I69-134-04590B.* Dekalb County, IN.

INDOT (1999). *Structural Plans for Bridge (35) 22-27-04724B.* Grant County, IN.

INDOT (1999). *Structural Plans for Bridge 66-13-05443A.* Crawford County, IN.

INDOT (2009). *Structural Plans for Bridge 41-42-05080 BNBL*. Knox County, IN.

INDOT (2010). *Structural Plans for Bridge I69-26-9187 NB.* Gibson County, IN.

INDOT (2013). *Structural Plans for Bridge 252-55-08713.* Morgan County, IN.

INDOT (2014). *Structural Plans for Bridge 63-86-05970 BNBL*. Warren, IN.

INDOT (2016). *Structural Plans for Bridge 327-17-06419A.* Dekalb County, IN.

Metzger, L.E. (2004). *Vulnerability of Bridges in Southern Indiana to Earthquakes* (Masters thesis).

Nielson, B. G. (2005). *Analytical Fragility Curves for Highway Bridges in Moderate Seismic Zones* (Doctoral dissertation). Retrieved from Georgia Tech Library.

NYSDOT (2004). *Seismic Vulnerability Manual*. New York State Department of Transportation, New York, NY.

Ramirez, J., Frosch, R., Sozen, M., & Turk, A. M. (2000). *Handbook for the Post-Earthquake Safety Evaluation of Bridges and Roads*. Rep. JTRP No. 2377, Purdue University, IN.

Ramirez, J., Peeta, S., & Sozen, M. (2005). *Emergency Earthquake Routes; Part I, Criteria for Selection of Primary Routes; and Part II: Route Seismic Vulnerability Aspects.* Rep. JTRP No. 2480, Purdue University, IN.

USGS (2002). *U.S. Geological Survey FS-131-02.* Publications of the US Geological Survey. Retrieved from https://pubs.usgs.gov/fs/fs-131-02/fs-131-02.html.

U.S. Seismic Design Maps. (n.d.) Retrieved April 29, 2019, from https://seismicmaps.org/

Wight, J. K., & MacGregor, J. G. (2012). *Reinforced Concrete: Mechanics and Design*. Boston: Pearson.

APPENDIX. LEVEL 2 ASSESSMENT RESULTS

1. Bridge Asset Name: (237) 37-13-07277

Table A.5: Specifications and Information on Bridge (237) 37-13-07277

Geographical Information	Asset Name	(237) 37-13-07277
	NBI Number	11840
	County	Crawford
	District	Vincennes
	Year of Construction	1996
	Facility Carried	SR 237
	Feature Intersected	BR Little Blue River
Superstructure Information	Superstructure Type	Continuous Reinforced Concrete Slab
	Number of Spans	3
	Span Lengths	29'-6", 37'-0", 29'-6"
	Deck Width	35'-0"
	Deck Thickness	19"
	Skew	10 degrees
	Concrete Compressive Strength	4000 psi
	Yield Strength of Reinforcement	60000 psi
Substructure Information	Substructure Type	Multi column bent with piles
	Number of Piles per Bent	5
	Pile Type	Concrete encased steel piles
	Pile Size	HP 12 x 53 piles in 24" diameter concrete
	Height of Pile	13'-9"
	Bent Cap Dimensions	30" x 16"
	Abutment Type	Integral
	Concrete Compressive Strength	3500 psi
	Yield Strength of Reinforcement	60000 psi
	Yield Strength of Steel Shape	36000 psi

In Figures A-1 to A-3, the sections and drawings relevant to modeling the bridge are shown.

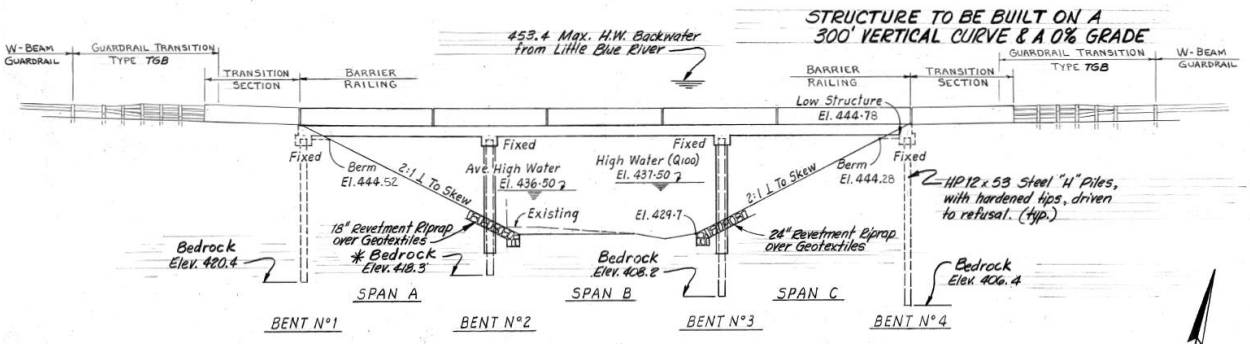

Figure A-2: Elevation View of the Bridge (INDOT, 1994)

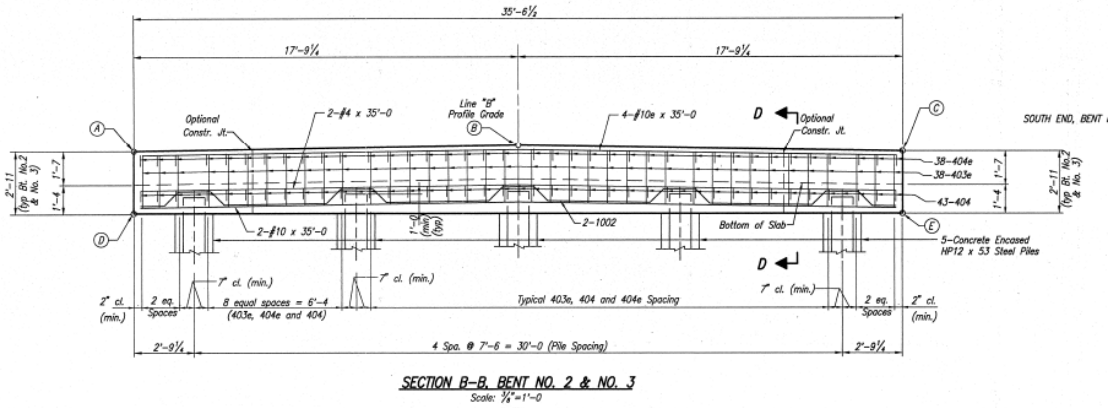

Figure A-3: Transverse Elevation View of the Interior Bents (INDOT, 1994)

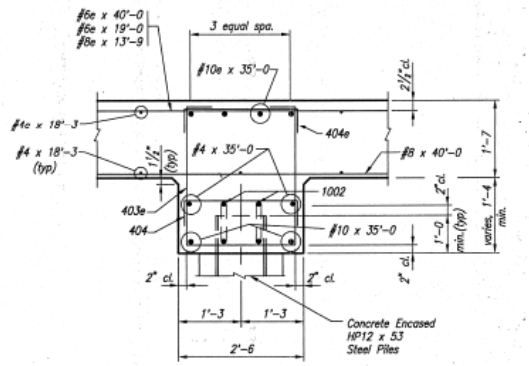

Figure A-4: Section D-D of Figure A-2 (INDOT, 1994)

Results – Transverse Direction

Using the modelling procedure presented in Chapter 3, each bent was modelled as a 4-bay portal frame. Due to the monolithic construction of the deck and bent cap, the deck contributes to the stiffness of the bridge. The mass, stiffness, period, and mode shape of the bridge calculated in the transverse direction are:

$$M = \begin{bmatrix} 0.79 & 0 \\ 0 & 0.79 \end{bmatrix} \frac{kips}{g}$$

$$K = \begin{bmatrix} 30300 & -22200 \\ -22200 & 30300 \end{bmatrix} kips/in$$

$$T = \begin{bmatrix} 0.06 \\ 0.02 \end{bmatrix} seconds$$

$$\Phi = \begin{bmatrix} -0.707 & -0.707 \\ -0.707 & 0.707 \end{bmatrix}$$

Results – Longitudinal Direction

Using the modelling procedure presented in Chapter 3, the piles are acting in parallel and modelled as fixed at the top of the bent cap and at the ground. This assumes that the soil is compacted properly to provide fixity at the base. The bridge is modelled as a single degree of freedom system, so the entire mass is used to obtain the period. The mass, stiffness, and period of the bridge in the longitudinal direction are $2.27\ kips/g$, $520\ kips/in$, and $0.42\ seconds$, respectively.

Due to the use of integral end abutments, the bridge moves together with the ground during earthquakes. Thus, there are no differential displacement or inertial forces on the bridge, and it is not vulnerable.

2. Bridge Asset Name: 55-45-07366

Table A.6: Specifications and Information on Bridge 55-45-07366

Geographical Information	Asset Name	55-45-07366
	NBI Number	019880
	County	Lake
	District	La Porte
	Year of Construction	1993
	Facility Carried	SR 55
	Feature Intersected	Merrillville Turkey Creek
Superstructure Information	Superstructure Type	Continuous Reinforced Concrete Slab
	Number of Spans	3
	Span Lengths	25'-0", 32'-0", 25'-0"
	Deck Width	48'-4"
	Deck Thickness	17"
	Skew	15 degrees
	Concrete Compressive Strength	4000 psi
	Yield Strength of Reinforcement	60000 psi
Substructure Information	Substructure Type	Multi column bent with piles
	Number of Piles per Bent	11
	Pile Type	Concrete encased steel piles
	Pile Size	HP 12 x 53 piles in 24" diameter concrete
	Height of Pile	9'-11"
	Bent Cap Dimensions	30" x 18"
	Abutment Type	Integral
	Concrete Compressive Strength	3500 psi
	Yield Strength of Reinforcement	60000 psi
	Yield Strength of Steel Shape	36000 psi

In Figures A-4 to A-6, the sections and drawings relevant to modeling the bridge are shown.

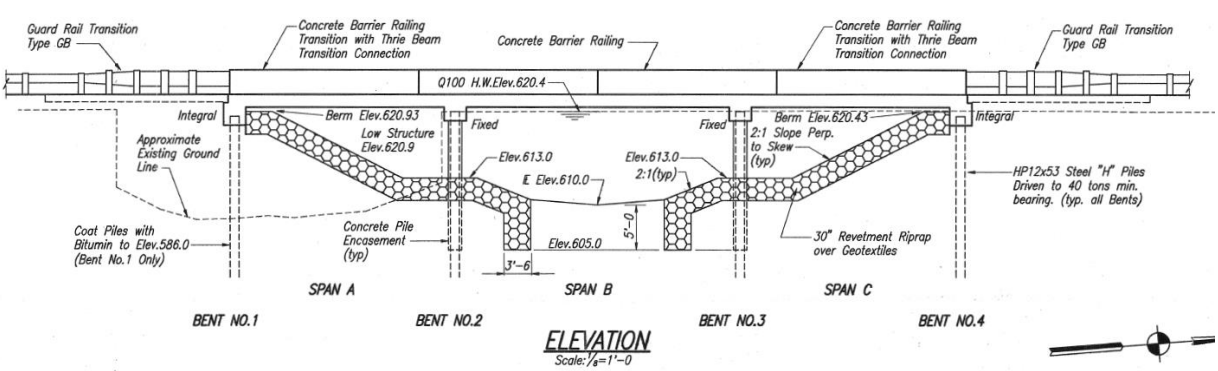

Figure A-5: Elevation View of the Bridge (INDOT, 1992)

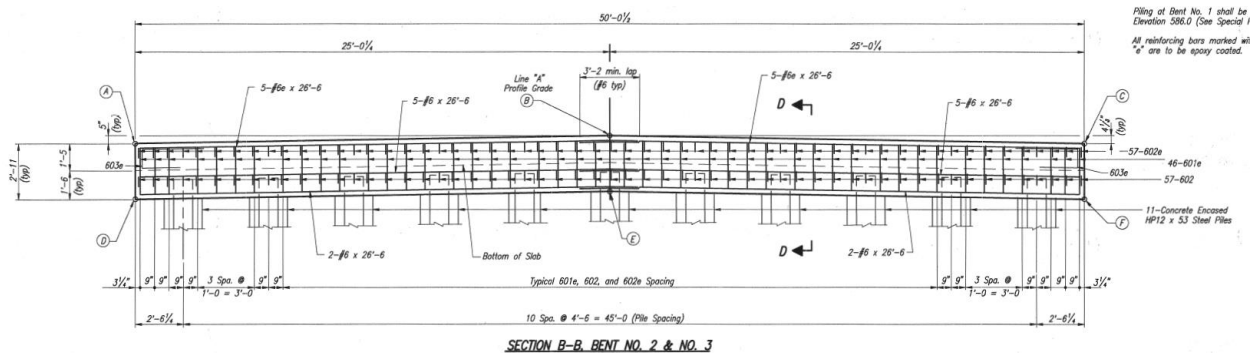

Figure A-6: Transverse Elevation View of the Interior Bents (INDOT, 1992)

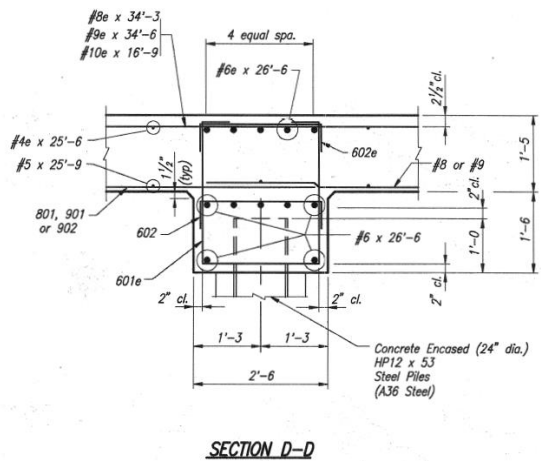

Figure A-7: Section D-D of Figure A.5 (INDOT, 1992)

Results – Transverse Direction

Using the modelling procedure presented in Chapter 3, each bent was modelled as a 10-bay portal frame. Due to the monolithic construction of the deck and bent cap, the deck contributes to the stiffness of the bridge. The mass, stiffness, period, and mode shape of the bridge calculated in the transverse direction are:

$$M = \begin{bmatrix} 0.82 & 0 \\ 0 & 0.82 \end{bmatrix} \frac{kips}{g}$$

$$K = \begin{bmatrix} 61800 & -39000 \\ -39000 & 61800 \end{bmatrix} kips/in$$

$$T = \begin{bmatrix} 0.04 \\ 0.02 \end{bmatrix} seconds$$

$$\Phi = \begin{bmatrix} -0.707 & -0.707 \\ -0.707 & 0.707 \end{bmatrix}$$

Results – Longitudinal Direction

The piles are acting in parallel and modelled as fixed at the top of the bent cap and at the ground. This assumes that the soil is compacted properly to provide fixity at the base. The bridge is modelled as a single degree of freedom system, so the entire mass is used to obtain the period. The mass, stiffness, and period of the bridge in the longitudinal direction are $2.36\ kips/g$, $3040\ kips/in$, and $0.18\ seconds$, respectively.

Due to the use of integral end abutments, the bridge moves together with the ground during earthquakes. Thus, there are no differential displacement or inertial forces on the bridge, and it is not vulnerable.

.

3. Bridge Asset Name: 56-63-07286

Table A.7: Specifications and Information on Bridge 56-63-07286

Geographical Information	Asset Name	56-63-07286
	NBI Number	019933
	County	Pike
	District	Vincennes
	Year of Construction	1993
	Facility Carried	SR 56/57
	Feature Intersected	Pride's Creek
Superstructure Information	Superstructure Type	Continuous Reinforced Concrete Slab
	Number of Spans	3
	Span Lengths	22'-0", 29'-3", 22'-0"
	Deck Width	49'-0"
	Deck Thickness	16"
	Skew	0 degrees
	Concrete Compressive Strength	4000 psi
	Yield Strength of Reinforcement	60000 psi
Substructure Information	Substructure Type	Multi column bent with piles
	Number of Piles per Bent	8
	Pile Type	Concrete encased steel piles
	Pile Size	HP 10 x 42 piles in 21" diameter concrete
	Height of Pile	10'-9.25"
	Bent Cap Dimensions	30" x 18"
	Abutment Type	Integral
	Concrete Compressive Strength	3500 psi
	Yield Strength of Reinforcement	60000 psi
	Yield Strength of Steel Shape	36000 psi

In Figures A-7 to A-9, the sections and drawings relevant to modeling the bridge are shown.

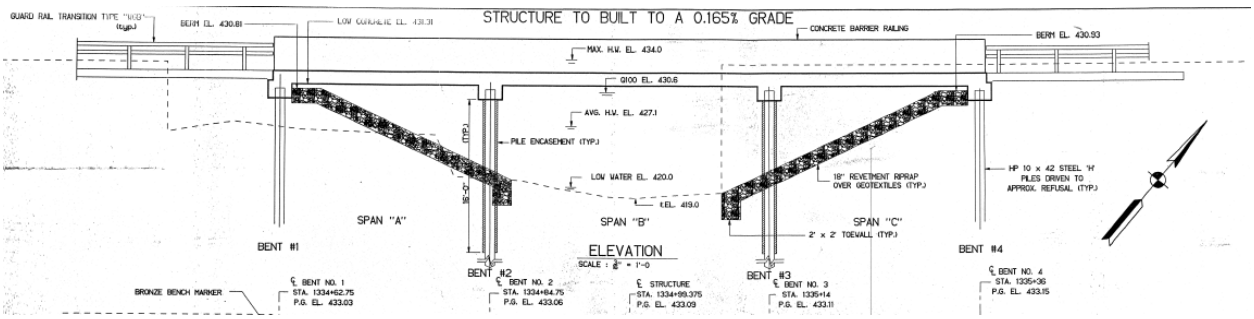

Figure A-8: Elevation View of the Bridge (INDOT, 1992)

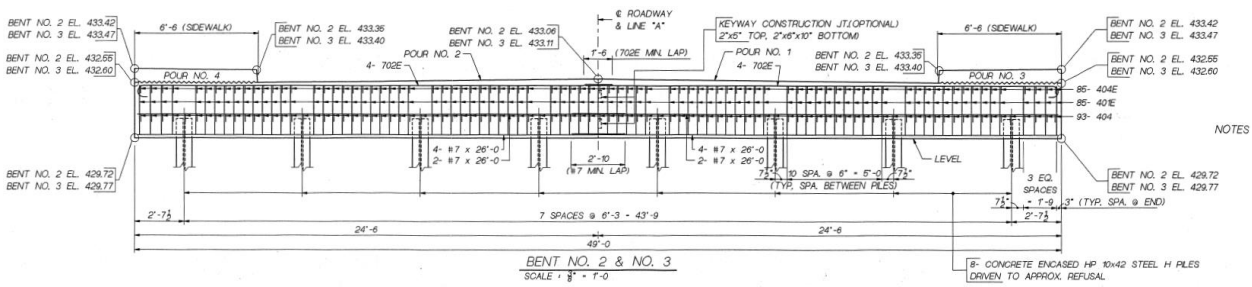

Figure A-9: Transverse Elevation View of the Interior Bents (INDOT, 1992)

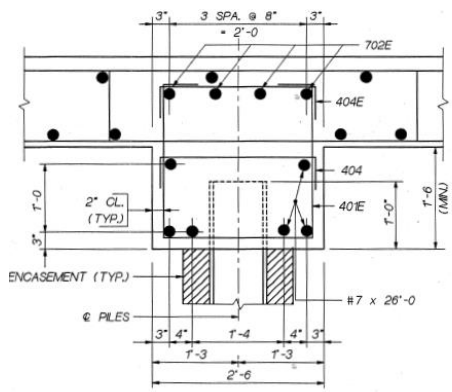

Figure A-10: Section View of Figure A-8 (INDOT, 1992)

Results – Transverse Direction

Using the modelling procedure presented in Chapter 3, each bent was modelled as a 7-bay portal frame. Due to the monolithic construction of the deck and bent cap, the deck contributes to the stiffness of the bridge. The mass, stiffness, period, and mode shape of the bridge calculated in the transverse direction are:

$$M = \begin{bmatrix} 0.70 & 0 \\ 0 & 0.70 \end{bmatrix} \frac{kips}{g}$$

$$K = \begin{bmatrix} 71600 & -43600 \\ -43600 & 71600 \end{bmatrix} kips/in$$

$$T = \begin{bmatrix} 0.03 \\ 0.02 \end{bmatrix} seconds$$

$$\Phi = \begin{bmatrix} -0.707 & -0.707 \\ -0.707 & 0.707 \end{bmatrix}$$

Results – Longitudinal Direction

The piles are acting in parallel and modelled as fixed at the top of the bent cap and at the ground. This assumes that the soil is compacted properly to provide fixity at the base. The bridge is modelled as a single degree of freedom system, so the entire mass is used to obtain the period. The mass, stiffness, and period of the bridge in the longitudinal direction are $2.01\ kips/g$, $1030\ kips/in$, and $0.28\ seconds$, respectively.

Due to the use of integral end abutments, the bridge moves together with the ground during earthquakes. Thus, there are no differential displacement or inertial forces on the bridge, and it is not vulnerable.

.

4. Bridge Asset Name: 252-55-08713

Table A.8: Specifications and Information on Bridge 252-55-08713

Geographical Information	Asset Name	252-55-08713
	NBI Number	030721
	County	Morgan
	District	Seymour
	Year of Construction	2014
	Facility Carried	SR 252
	Feature Intersected	Long Run Creek
Superstructure Information	Superstructure Type	Continuous Reinforced Concrete Slab
	Number of Spans	3
	Span Lengths	35'-0", 46'-0", 35'-0"
	Deck Width	34'-4"
	Deck Thickness	23"
	Skew	56 degrees
	Concrete Compressive Strength	4000 psi
	Yield Strength of Reinforcement	60000 psi
Substructure Information	Substructure Type	Multi column bent with piles
	Number of Piles per Bent	8
	Pile Type	Concrete encased steel piles
	Pile Size	HP 12 x 53 piles in 24" diameter concrete
	Height of Pile	8'-2.75"
	Bent Cap Dimensions	30" x 30"
	Abutment Type	Integral
	Concrete Compressive Strength	3500 psi
	Yield Strength of Reinforcement	60000 psi
	Yield Strength of Steel Shape	50000 psi

In Figures A-10 to A-12, the sections and drawings relevant to modeling the bridge are shown.

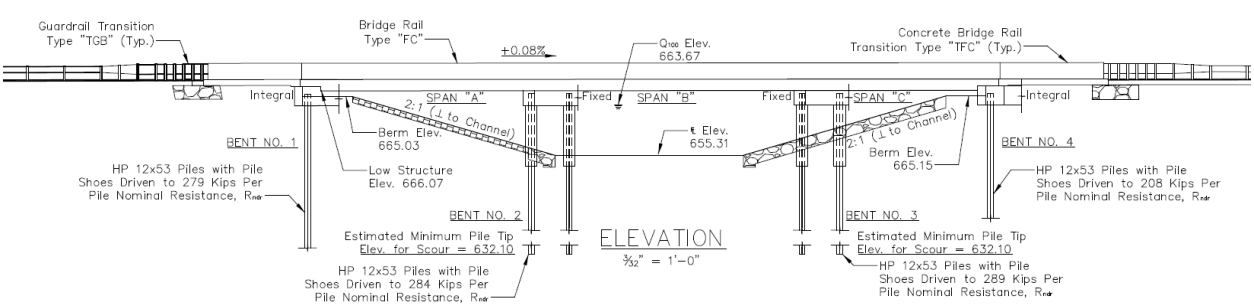

Figure A-11: Elevation View of the Bridge (INDOT, 2013)

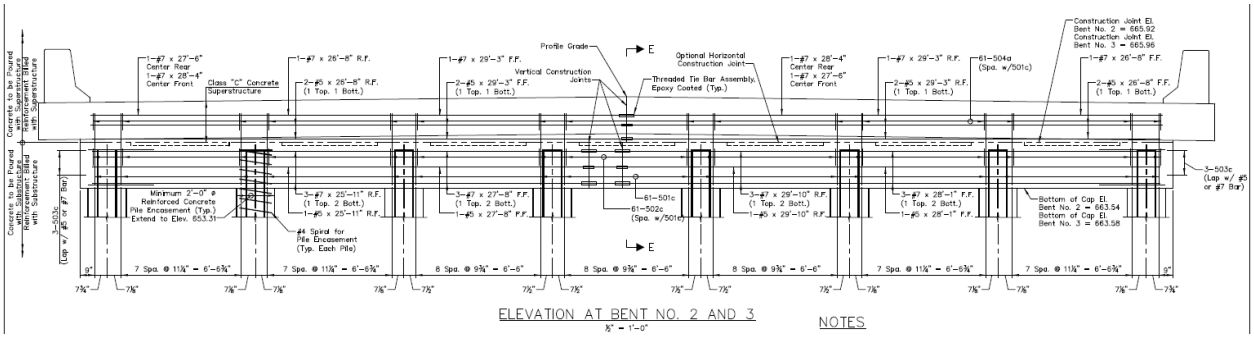

Figure A-12: Transverse Elevation View of the Interior Bents (INDOT, 2013)

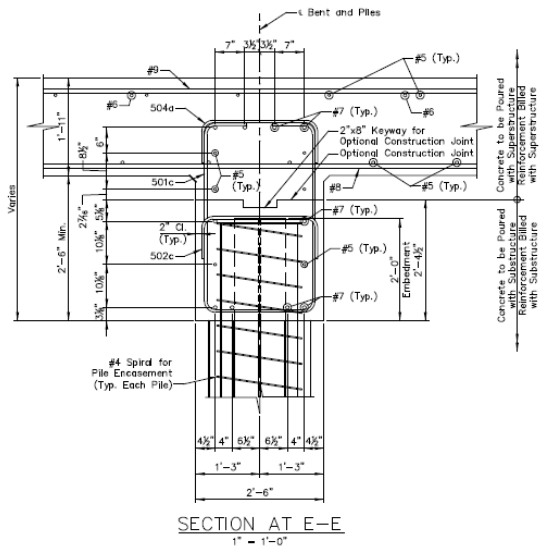

Figure A-13: Section E-E of Figure A-11 (INDOT, 2013)

Results – Transverse Direction

Using the modelling procedure presented in Chapter 3, each bent was modelled as a 7-bay portal frame. Due to the monolithic construction of the deck and bent cap, the deck contributes to the stiffness of the bridge. The mass, stiffness, period, and mode shape of the bridge calculated in the transverse direction are:

$$M = \begin{bmatrix} 1.12 & 0 \\ 0 & 1.12 \end{bmatrix} \frac{kips}{g}$$

$$K = \begin{bmatrix} 15000 & -9950 \\ -9950 & 15000 \end{bmatrix} kips/in$$

$$T = \begin{bmatrix} 0.09 \\ 0.04 \end{bmatrix} seconds$$

$$\Phi = \begin{bmatrix} -0.707 & -0.707 \\ -0.707 & 0.707 \end{bmatrix}$$

Results – Longitudinal Direction

The piles are acting in parallel and modelled as fixed at the top of the bent cap and at the ground. This assumes that the soil is compacted properly to provide fixity at the base. The bridge is modelled as a single degree of freedom system, so the entire mass is used to obtain the period. The mass, stiffness, and period of the bridge in the longitudinal direction are $3.21\ kips/g$, $3890\ kips/in$, and $0.18\ seconds$, respectively.

Due to the use of integral end abutments, the bridge moves together with the ground during earthquakes. Thus, there are no differential displacement or inertial forces on the bridge, and it is not vulnerable.

.

5. Bridge Asset Name: 28-79-07672

Table A.9: Specifications and Information on Bridge 28-79-07672

Geographical Information	Asset Name	28-79-07672
	NBI Number	007640
	County	Tippecanoe
	District	Crawfordsville
	Year of Construction	1996
	Facility Carried	SR 28
	Feature Intersected	Wea Creek
Superstructure Information	Superstructure Type	Continuous Reinforced Concrete Slab
	Number of Spans	3
	Span Lengths	29'-0", 38'-0", 29'-0"
	Deck Width	34'-4"
	Deck Thickness	19"
	Skew	0 degrees
	Concrete Compressive Strength	4000 psi
	Yield Strength of Reinforcement	60000 psi
Substructure Information	Substructure Type	Multi column bent with piles
	Number of Piles per Bent	7
	Pile Type	Concrete filled tubes
	Pile Size	14" diameter steel tube
	Height of Pile	8'-2.75"
	Bent Cap Dimensions	30" x 18"
	Abutment Type	Integral
	Concrete Compressive Strength	3500 psi
	Yield Strength of Reinforcement	60000 psi
	Yield Strength of Steel Shape	60000 psi

In Figures A-13 to A-15, the sections and drawings relevant to modeling the bridge are shown.

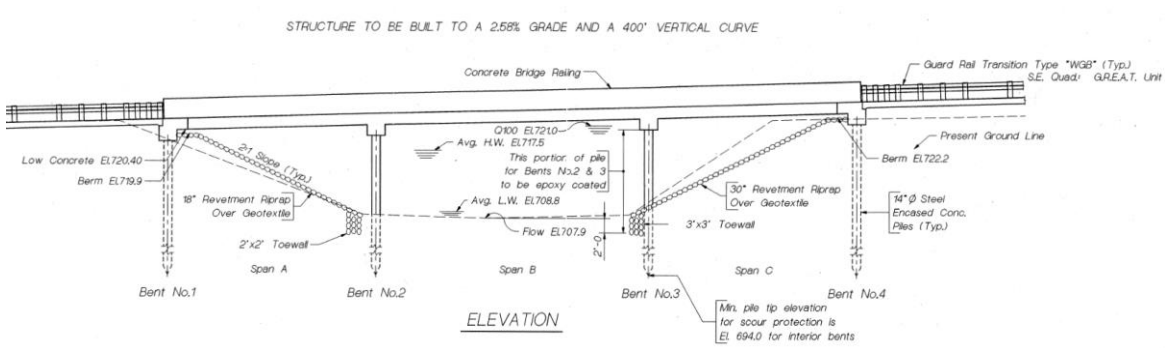

Figure A-14: Elevation View of the Bridge (INDOT, 1995)

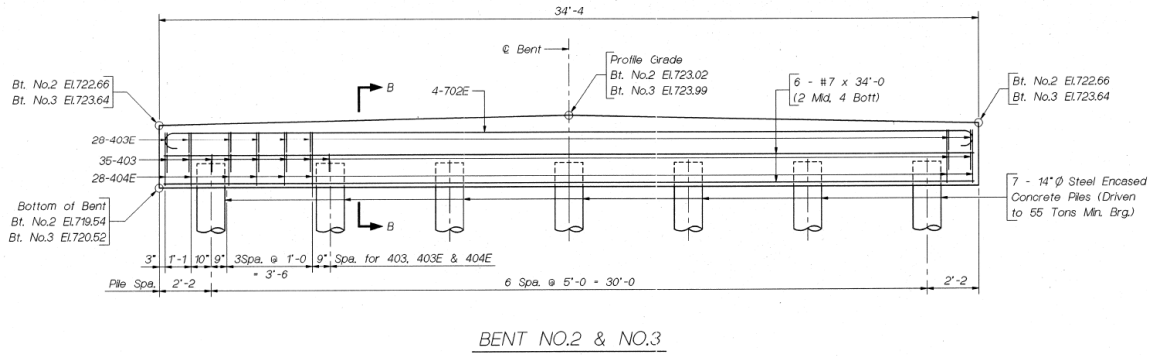

Figure A-15: Transverse Elevation View of the Interior Bents (INDOT, 1995)

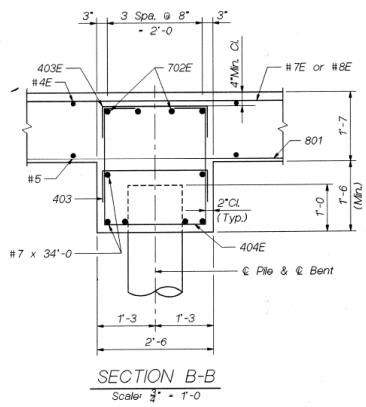

Figure A-16: Section B-B of Figure A-14 (INDOT, 1995)

Results – Transverse Direction

Using the modelling procedure presented in Chapter 3, each bent was modelled as a 6-bay portal frame. Due to the monolithic construction of the deck and bent cap, the deck contributes to the stiffness of the bridge. The mass, stiffness, period, and mode shape of the bridge calculated in the transverse direction are:

$$M = \begin{bmatrix} 0.78 & 0 \\ 0 & 0.78 \end{bmatrix} \frac{kips}{g}$$

$$K = \begin{bmatrix} 28700 & -21000 \\ -21000 & 28700 \end{bmatrix} kips/in$$

$$T = \begin{bmatrix} 0.06 \\ 0.02 \end{bmatrix} seconds$$

$$\varphi = \begin{bmatrix} -0.707 & -0.707 \\ -0.707 & 0.707 \end{bmatrix}$$

Results – Longitudinal Direction

The piles are acting in parallel and modelled as fixed at the top of the bent cap and at the ground. This assumes that the soil is compacted properly to provide fixity at the base. The bridge is modelled as a single degree of freedom system, so the entire mass is used to obtain the period. The mass, stiffness, and period of the bridge in the longitudinal direction are $2.23\ kips/g$, $180\ kips/in$, and $0.70\ seconds$, respectively.

Due to the use of integral end abutments, the bridge moves together with the ground during earthquakes. Thus, there are no differential displacement or inertial forces on the bridge, and it is not vulnerable.

.

6. Bridge Asset Name: 327-17-06419A

Table A.10: Specifications and Information on Bridge 327-17-06419A

Geographical Information	Asset Name	327-17-06419A
	NBI Number	031350
	County	Dekalb
	District	Fort Wayne
	Year of Construction	1984, 2017
	Facility Carried	SR 327
	Feature Intersected	Diehl Ditch
Superstructure Information	Superstructure Type	Continuous Reinforced Concrete Slab
	Number of Spans	3
	Span Lengths	26'-6", 35'-0", 26'-6"
	Deck Width	46'-6"
	Deck Thickness	19"
	Skew	24 degrees
	Concrete Compressive Strength	4000 psi
	Yield Strength of Reinforcement	40000 psi
Substructure Information	Substructure Type	Multi column bent with piles
	Number of Piles per Bent	10
	Pile Type	Concrete filled tubes
	Pile Size	14" diameter steel tube
	Height of Pile	11'-6"
	Bent Cap Dimensions	30" x 23"
	Abutment Type	Integral
	Concrete Compressive Strength	3500 psi
	Yield Strength of Reinforcement	40000 psi
	Yield Strength of Steel Shape	40000 psi

In Figures A-16 to A-18, the sections and drawings relevant to modeling the bridge are shown.

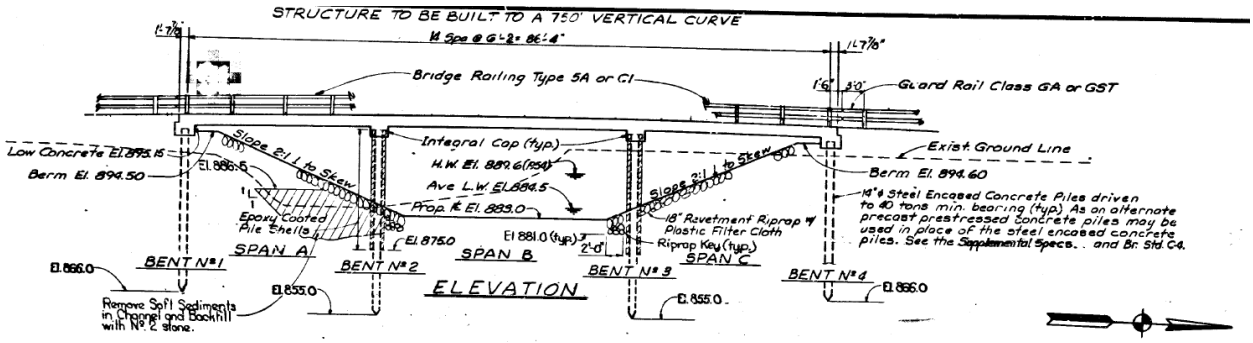

Figure A-17: Elevation View of the Bridge (INDOT, 2016)

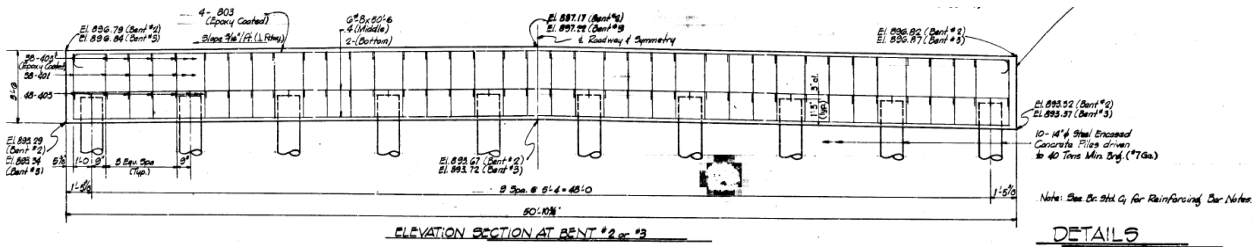

Figure A-18: Transverse Elevation View of the Interior Bents (INDOT, 2016)

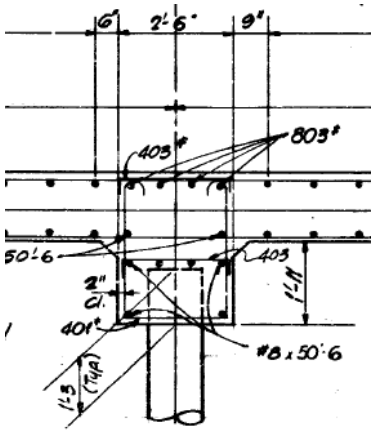

Figure A-19: Section View of Figure A-17 (INDOT, 2016)

Results – Transverse Direction

Using the modelling procedure presented in Chapter 3, each bent was modelled as a 9-bay portal frame. Due to the monolithic construction of the deck and bent cap, the deck contributes to the stiffness of the bridge. The mass, stiffness, period, and mode shape of the bridge calculated in the transverse direction are:

$$M = \begin{bmatrix} 0.94 & 0 \\ 0 & 0.94 \end{bmatrix} \frac{kips}{g}$$

$$K = \begin{bmatrix} 53300 & -35200 \\ -35200 & 53300 \end{bmatrix} kips/in$$

$$T = \begin{bmatrix} 0.05 \\ 0.02 \end{bmatrix} seconds$$

$$\Phi = \begin{bmatrix} -0.707 & -0.707 \\ -0.707 & 0.707 \end{bmatrix}$$

Results – Longitudinal Direction

The piles are acting in parallel and modelled as fixed at the top of the bent cap and at the ground. This assumes that the soil is compacted properly to provide fixity at the base. The bridge is modelled as a single degree of freedom system, so the entire mass is used to obtain the period. The mass, stiffness, and period of the bridge in the longitudinal direction are $2.70\ kips/g$, $290\ kips/in$, and $0.61\ seconds$, respectively.

Due to the use of integral end abutments, the bridge moves together with the ground during earthquakes. Thus, there are no differential displacement or inertial forces on the bridge, and it is not vulnerable.

.

7. Bridge Asset Name: 44-55-06793

Table A.11: Table Specifications and Information on Bridge 44-55-06793

Geographical Information	Asset Name	44-55-06793
	NBI Number	016130
	County	Morgan
	District	Seymour
	Year of Construction	1982
	Facility Carried	SR 44
	Feature Intersected	Fork Clear Creek
Superstructure Information	Superstructure Type	Continuous Reinforced Concrete Slab
	Number of Spans	3
	Span Lengths	28'-0", 37'-0", 28'-0"
	Deck Width	44'-6"
	Deck Thickness	20"
	Skew	45 degrees
	Concrete Compressive Strength	4000 psi
	Yield Strength of Reinforcement	40000 psi
Substructure Information	Substructure Type	Multi column bent with piles
	Number of Piles per Bent	10
	Pile Type	Concrete filled tubes
	Pile Size	14" diameter steel tube
	Height of Pile	9'-11"
	Bent Cap Dimensions	30" x 12"
	Abutment Type	Integral
	Concrete Compressive Strength	3500 psi
	Yield Strength of Reinforcement	40000 psi
	Yield Strength of Steel Shape	40000 psi

In Figures A-19 to A-21, the sections and drawings relevant to modeling the bridge are shown.

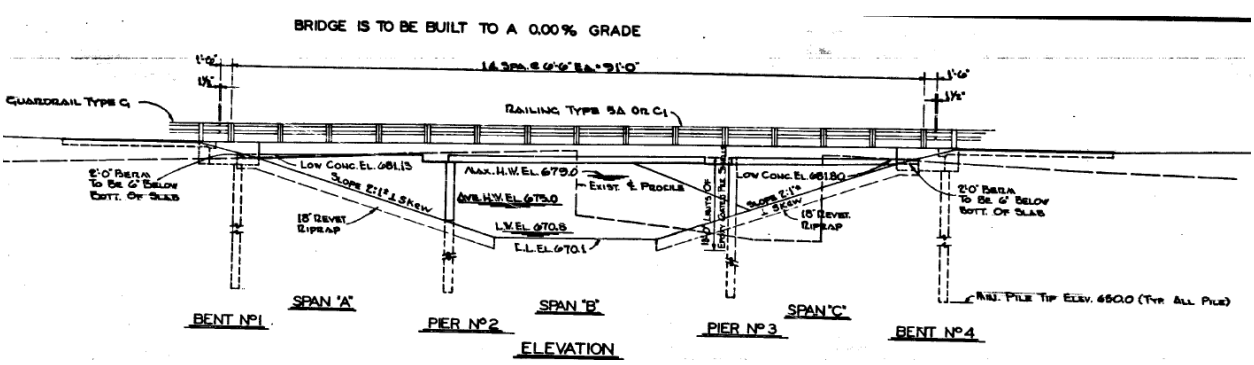

Figure A-20: Elevation View of the Bridge (INDOT, 1980)

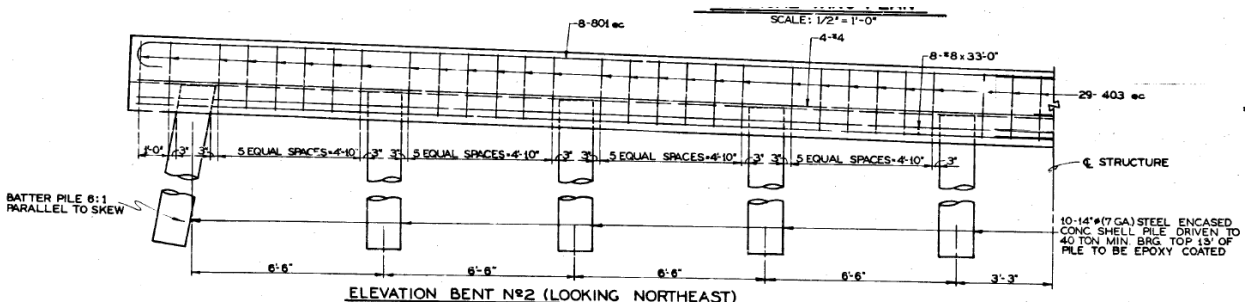

Figure A-21: Transverse Elevation View of the Interior Bents to Center Line (INDOT, 1980)

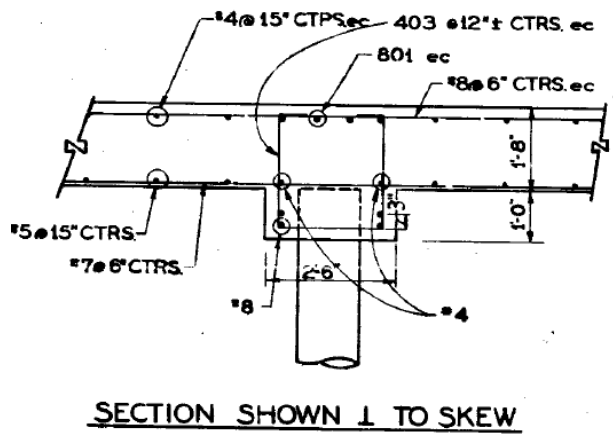

Figure A-22: Section View of Figure A-19 (INDOT, 1980)

Results – Transverse Direction

Using the modelling procedure presented in Chapter 3, each bent was modelled as a 9-bay portal frame. Due to the monolithic construction of the deck and bent cap, the deck contributes to the stiffness of the bridge. The mass, stiffness, period, and mode shape of the bridge calculated in the transverse direction are:

$$M = \begin{bmatrix} 1.0 & 0 \\ 0 & 1.0 \end{bmatrix} \frac{kips}{g}$$

$$K = \begin{bmatrix} 36800 & -24900 \\ -24900 & 36800 \end{bmatrix} kips/in$$

$$T = \begin{bmatrix} 0.06 \\ 0.03 \end{bmatrix} seconds$$

$$\Phi = \begin{bmatrix} -0.707 & -0.707 \\ -0.707 & 0.707 \end{bmatrix}$$

Results – Longitudinal Direction

The piles are acting in parallel and modelled as fixed at the top of the bent cap and at the ground. This assumes that the soil is compacted properly to provide fixity at the base. The bridge is modelled as a single degree of freedom system, so the entire mass is used to obtain the period. The mass, stiffness, and period of the bridge in the longitudinal direction are $2.88\ kips/g$, $470\ kips/in$, and $0.49\ seconds$, respectively.

Due to the use of integral end abutments, the bridge moves together with the ground during earthquakes. Thus, there are no differential displacement or inertial forces on the bridge, and it is not vulnerable.

.

8. Bridge Asset Name: 57-14-06739

Table A.12: Specifications and Information on Bridge 57-14-06739

Geographical Information	Asset Name	57-14-06739
	NBI Number	020690
	County	Daviess
	District	Vincennes
	Year of Construction	1986
	Facility Carried	SR 57
	Feature Intersected	Weaver Ditch
Superstructure Information	Superstructure Type	Continuous Reinforced Concrete Slab
	Number of Spans	3
	Span Lengths	33'-6", 44'-0", 33'-6"
	Deck Width	47'-0"
	Deck Thickness	22"
	Skew	37 degrees
	Concrete Compressive Strength	4000 psi
	Yield Strength of Reinforcement	40000 psi
Substructure Information	Substructure Type	Multi column bent with piles
	Number of Piles per Bent	15
	Pile Type	Concrete filled tubes
	Pile Size	14" diameter steel tube
	Height of Pile	12'-0"
	Bent Cap Dimensions	30" x 18"
	Abutment Type	Integral
	Concrete Compressive Strength	3500 psi
	Yield Strength of Reinforcement	40000 psi
	Yield Strength of Steel Shape	40000 psi

In Figures A-22 to A-24, the sections and drawings relevant to modeling the bridge are shown.

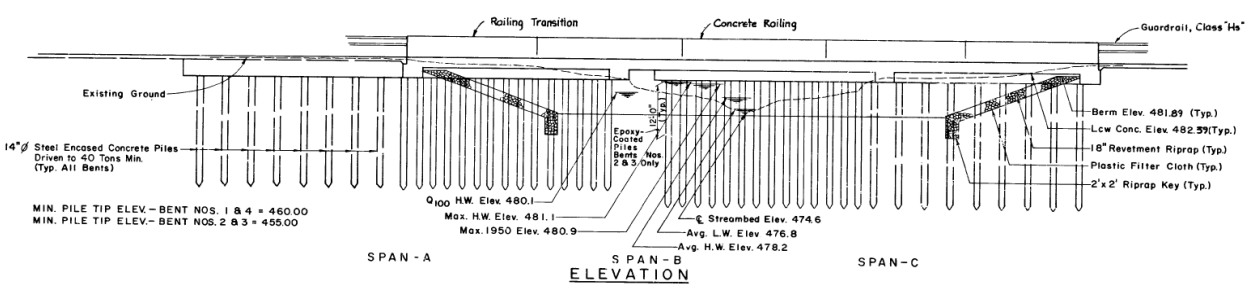

Figure A-23: Elevation View of the Bridge (INDOT, 1982)

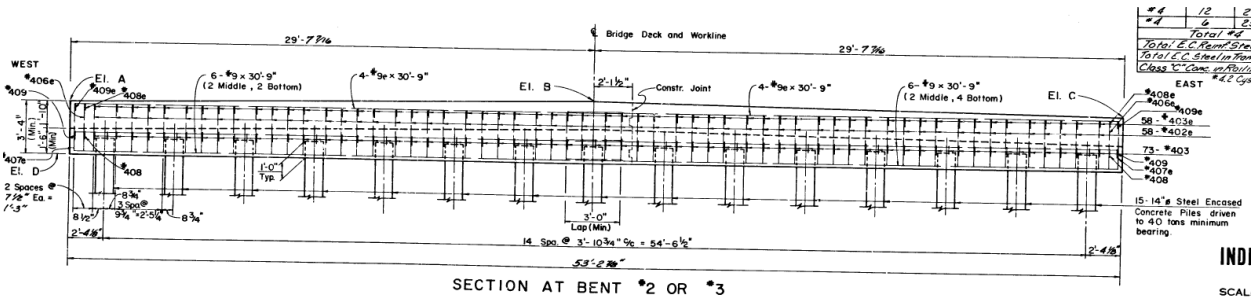

Figure A-24: Transverse Elevation View of the Interior Bents (INDOT, 1982)

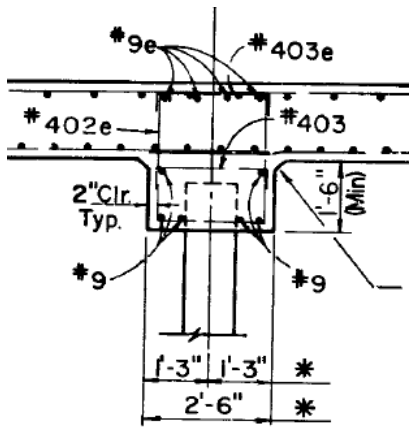

Figure A-25: Section View of Figure A-23 (INDOT, 1982)

Results – Transverse Direction

Using the modelling procedure presented in Chapter 3, each bent was modelled as a 14-bay portal frame. Due to the monolithic construction of the deck and bent cap, the deck contributes to the stiffness of the bridge. The mass, stiffness, period, and mode shape of the bridge calculated in the transverse direction are:

$$M = \begin{bmatrix} 1.38 & 0 \\ 0 & 1.38 \end{bmatrix} \frac{kips}{g}$$

$$K = \begin{bmatrix} 36800 & -25800 \\ -25800 & 38600 \end{bmatrix} kips/in$$

$$T = \begin{bmatrix} 0.07 \\ 0.03 \end{bmatrix} seconds$$

$$\Phi = \begin{bmatrix} -0.707 & -0.707 \\ -0.707 & 0.707 \end{bmatrix}$$

Results – Longitudinal Direction

The piles are acting in parallel and modelled as fixed at the top of the bent cap and at the ground. This assumes that the soil is compacted properly to provide fixity at the base. The bridge is modelled as a single degree of freedom system, so the entire mass is used to obtain the period. The mass, stiffness, and period of the bridge in the longitudinal direction are $3.95\ kips/g$, $390\ kips/in$, and $0.63\ seconds$, respectively.

Due to the use of integral end abutments, the bridge moves together with the ground during earthquakes. Thus, there are no differential displacement or inertial forces on the bridge, and it is not vulnerable.

.

9. Bridge Asset Name: 252-24-06934A

Table A.13: Specifications and Information on Bridge 252-24-06934A

Geographical Information	Asset Name	252-24-06934A
	NBI Number	020690
	County	Franklin
	District	Seymour
	Year of Construction	1988
	Facility Carried	SR 252
	Feature Intersected	Little Cedar Creek
Superstructure Information	Superstructure Type	Continuous Reinforced Concrete Slab
	Number of Spans	3
	Span Lengths	31'-0", 39'-0", 31'-0"
	Deck Width	46'-6"
	Deck Thickness	20"
	Skew	15 degrees
	Concrete Compressive Strength	4000 psi
	Yield Strength of Reinforcement	40000 psi
Substructure Information	Substructure Type	Multi column bent with piles
	Number of Piles per Bent	13
	Pile Type	Concrete filled tubes
	Pile Size	14" diameter steel tube
	Height of Pile	9'-5.5"
	Bent Cap Dimensions	30" x 15"
	Abutment Type	Integral
	Concrete Compressive Strength	3000 psi
	Yield Strength of Reinforcement	40000 psi
	Yield Strength of Steel Shape	40000 psi

In Figures A-25 to A-27, the sections and drawings relevant to modeling the bridge are shown.

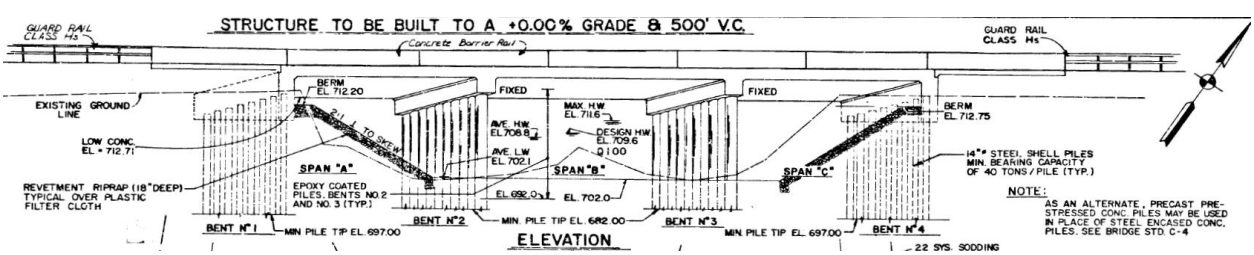

Figure A-26: Elevation View of the Bridge (INDOT, 1985)

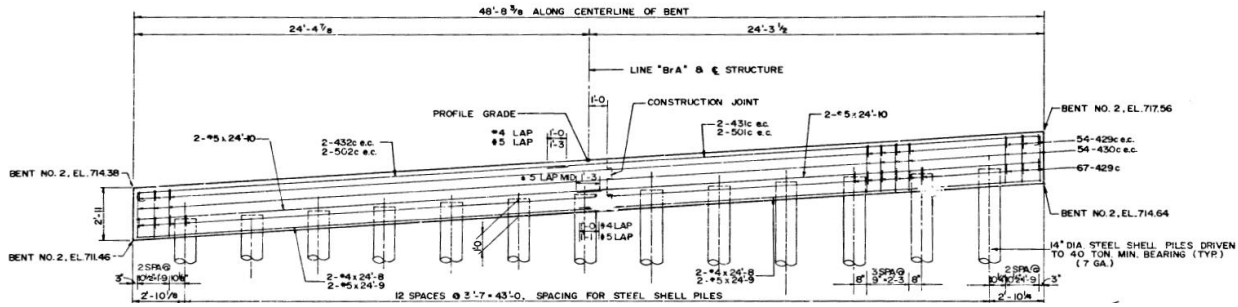

Figure A-27: Transverse Elevation View of the Interior Bents (INDOT, 1985)

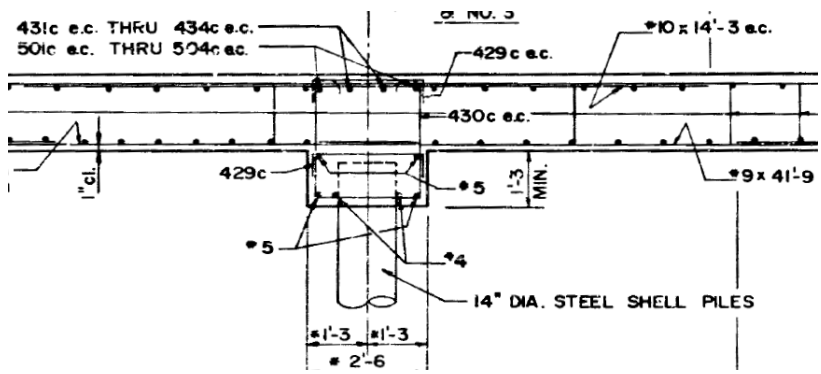

Figure A-28: Section View of Figure A-26 (INDOT, 1985)

Results – Transverse Direction

Using the modelling procedure presented in Chapter 3, each bent was modelled as a 12-bay portal frame. Due to the monolithic construction of the deck and bent cap, the deck contributes to the stiffness of the bridge. The mass, stiffness, period, and mode shape of the bridge calculated in the transverse direction are:

$$M = \begin{bmatrix} 1.13 & 0 \\ 0 & 1.13 \end{bmatrix} \frac{kips}{g}$$

$$K = \begin{bmatrix} 47500 & -32900 \\ -32900 & 47500 \end{bmatrix} kips/in$$

$$T = \begin{bmatrix} 0.06 \\ 0.02 \end{bmatrix} seconds$$

$$\Phi = \begin{bmatrix} -0.71 & -0.71 \\ -0.71 & 0.71 \end{bmatrix}$$

Results – Longitudinal Direction

The piles are acting in parallel and modelled as fixed at the top of the bent cap and at the ground. This assumes that the soil is compacted properly to provide fixity at the base. The bridge is modelled as a single degree of freedom system, so the entire mass is used to obtain the period. The mass, stiffness, and period of the bridge in the longitudinal direction are $3.25\ kips/g$, $680\ kips/in$, and $0.43\ seconds$, respectively.

Due to the use of integral end abutments, the bridge moves together with the ground during earthquakes. Thus, there are no differential displacement or inertial forces on the bridge, and it is not vulnerable.

.

10. Bridge Asset Name: 64-19-03723A

Table A.14: Specifications and Information on Bridge 64-19-03723A

Geographical Information	Asset Name	64-19-03723A
	NBI Number	022960
	County	Dubois
	District	Vincennes
	Year of Construction	1947, 1985
	Facility Carried	SR 64
	Feature Intersected	Rock Creek
Superstructure Information	Superstructure Type	Continuous Reinforced Concrete Slab
	Number of Spans	4
	Span Lengths	22'-4", 28'-0", 28'-0", 22'-4"
	Deck Width	31'-6"
	Deck Thickness	19"
	Skew	45 degrees
	Concrete Compressive Strength	3000 psi
	Yield Strength of Reinforcement	40000 psi
Substructure Information	Substructure Type	Multi column bent with piles
	Number of Piles per Bent	7
	Pile Type	Concrete filled tubes
	Pile Size	14" diameter steel tube
	Height of Pile	8'-6"
	Bent Cap Dimensions	30" x 30"
	Abutment Type	Non-Integral
	Bearing Support Length	2'-6"
	Concrete Compressive Strength	3000 psi
	Yield Strength of Reinforcement	40000 psi
	Yield Strength of Steel Shape	40000 psi

In Figures A-28 to A-31, the sections and drawings relevant to modeling the bridge are shown.

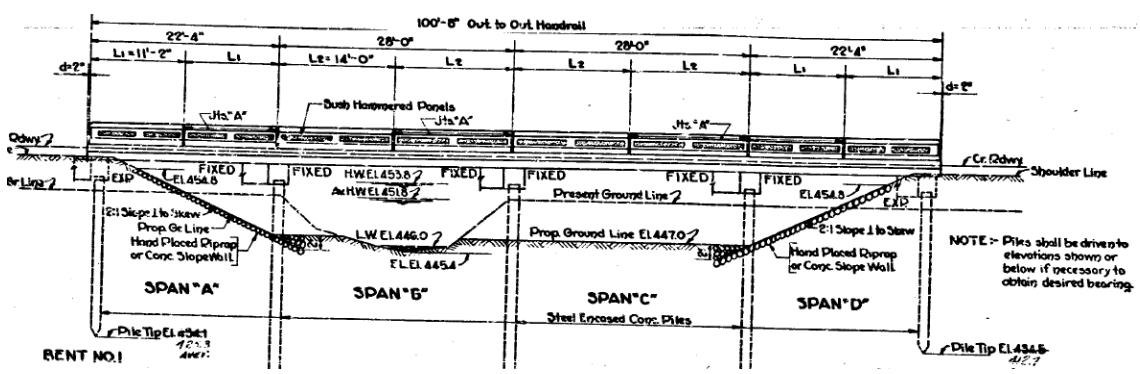

Figure A-29: Elevation View of the Bridge (INDOT, 1984)

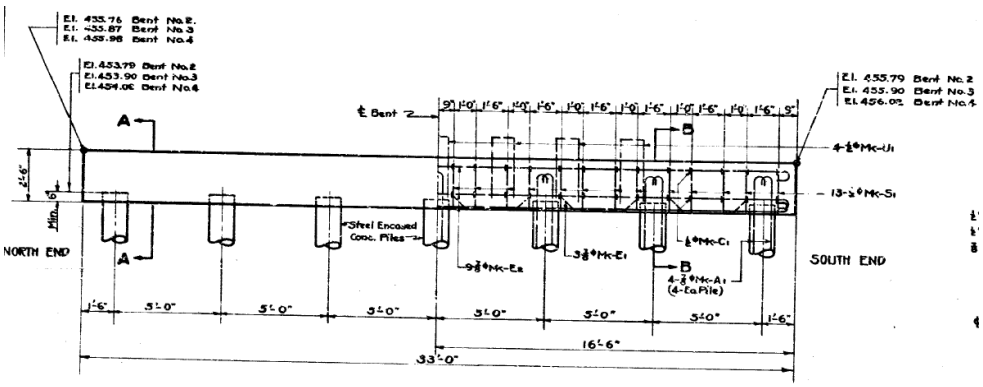

Figure A-30: Transverse Elevation View of the Interior Bents (INDOT, 1984)

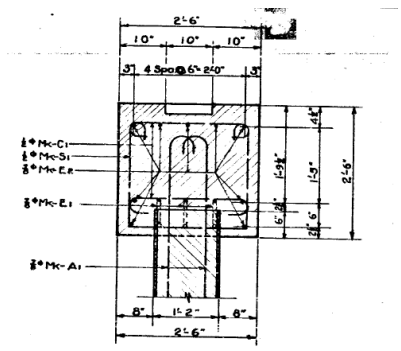

Figure A-31: Section B-B of Figure A-29 (INDOT, 1984)

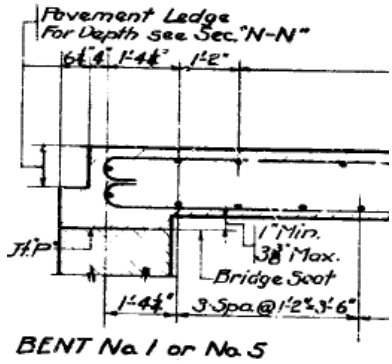

Figure A-32: Bearing Support at Abutments (INDOT, 1984)

Results – Transverse Direction

Using the modelling procedure presented in Chapter 3, each bent was modelled as a 6-bay portal frame. Due to the presence of extended longitudinal bars from the bent cap into the deck, the deck contributes to the stiffness of the bridge. The mass, stiffness, period, and mode shape of the bridge calculated in the transverse direction are:

$$M = \begin{bmatrix} 0.54 & 0 & 0 \\ 0 & 0.60 & 0 \\ 0 & 0 & 0.54 \end{bmatrix} \frac{kips}{g}$$

$$K = \begin{bmatrix} 25700 & -16900 & 3190 \\ -16900 & 24400 & -16900 \\ 3190 & -16900 & 25700 \end{bmatrix} kips/in$$

$$T = \begin{bmatrix} 0.09 \\ 0.03 \\ 0.02 \end{bmatrix} seconds$$

$$\Phi = \begin{bmatrix} 0.47 & 0.71 & -0.55 \\ 0.74 & 0 & 0.63 \\ 0.47 & 0.71 & -0.55 \end{bmatrix}$$

Following the procedure for calculating the strength of the bridge elements in Section 3.5, the plastic moment and shear resultant of each pile are 135 ft-kip, and 32 kips, respectively. Each bent has a shear strength of 735 kips which is greater than the shear resultant (220 kips). Thus, plastic hinges will form prior to collapse. The strength of the shear friction connection between each intermediate bent and the deck is 215 kips. Applying the 100 ground motions generated at this bridge site (site class D) to the bridge model, the shear demand from the ground motions (50 per fault orientation) is plotted against the peak ground acceleration (PGA) of each earthquake. The substructure capacity is shown using threshold values corresponding to the flexural capacity, strength of the shear friction connection and the shear strength, as shown in Figure A-33.

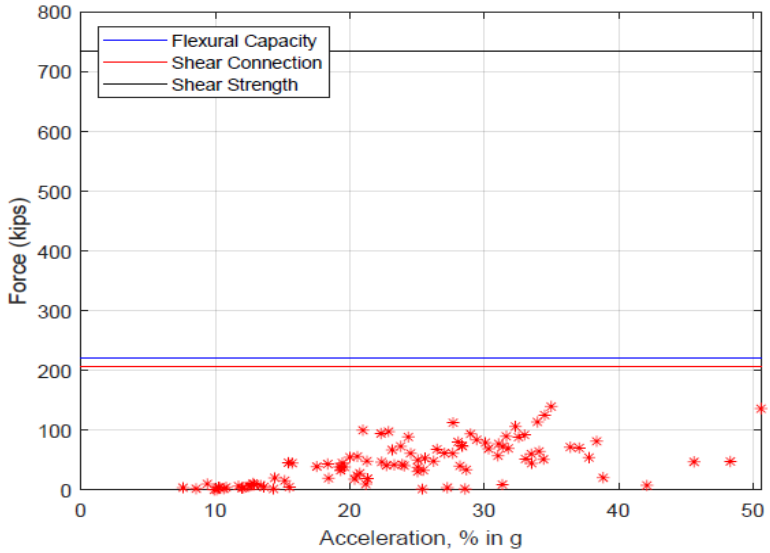

Figure A-33: Shear Demand Due to Applied Ground Motions – Transverse Direction

Based on the plot, the capacity of the substructure is not exceeded by the demand for any ground motions. Additionally, the maximum displacement of the bridge due to the ground motions is less than 0.10”. Therefore, the bridge is not vulnerable in the transverse direction at level of ground motions expected at its location.

Results – Longitudinal Direction

The piles are acting in parallel and modelled as fixed at the top of the bent cap and at the ground. This assumes that the soil is compacted properly to provide fixity at the base. The bridge is modelled as a single degree of freedom system, so the entire mass is used to obtain the period. The mass, stiffness, and period of the bridge in the longitudinal direction are $2.16\ kips/g$, $760\ kips/in$, and $0.34\ seconds$, respectively.

In the longitudinal direction, the plastic moment and shear resultant of each pile are 135 ft-kip, and 12 kips, respectively. The substructure has a total shear strength of 2200 kips which is greater than the total shear resultant (260 kips). The total strength of the shear friction connection between the intermediate bents and the deck is 620 kips. Applying the 100 ground motions generated at this bridge site (site class D) to the bridge model, the shear demand from the ground motions (50 per fault orientation) is plotted against the peak ground acceleration (PGA) of each earthquake. The substructure capacity is shown using threshold values corresponding to the

flexural capacity, strength of the shear friction connection and the shear strength, as shown in Figure A-34.

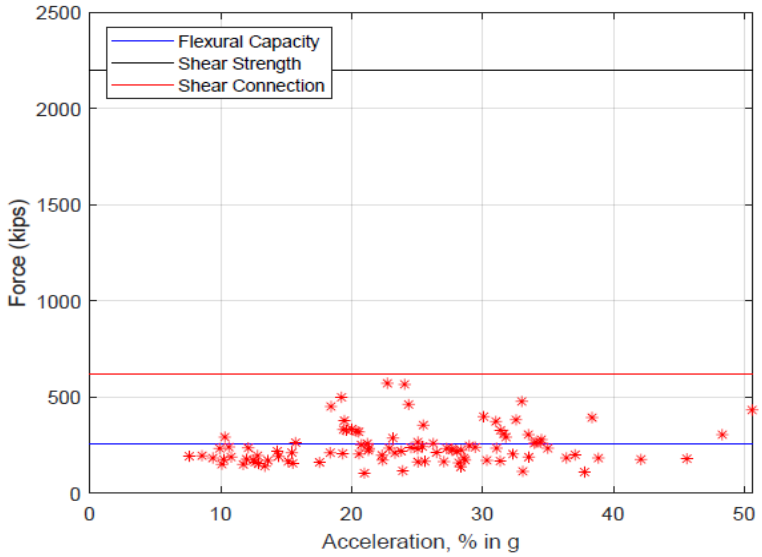

Figure A-34: Shear Demand Due to Applied Ground Motions – Longitudinal Direction

From the plot, the shear demand from the ground motions does exceed the flexural capacity, therefore the longitudinal reinforcement in this direction yields. The maximum displacement of the bridge due to the set of ground motions is 0.76”, which is less than the available bearing support length. Additionally, since the shear strength of the substructure is not exceeded, the bridge is of low vulnerability at the level of ground motions expected at its location.

11. Bridge Asset Name: 67-55-03831ANBL

Table A.15: Specifications and Information on Bridge 67-55-03831ANBL

Geographical Information	Asset Name	67-55-03831ANBL
	NBI Number	024100
	County	Morgan
	District	Crawfordsville
	Year of Construction	1958, 1993
	Facility Carried	SR 67 NB
	Feature Intersected	Mooresville Silon Creek
Superstructure Information	Superstructure Type	Continuous Reinforced Concrete Slab
	Number of Spans	3
	Span Lengths	24'-0", 32'-0", 24'-0"
	Deck Width	43'-2"
	Deck Thickness	15.5"
	Skew	35 degrees
	Concrete Compressive Strength	3500 psi
	Yield Strength of Reinforcement	40000 psi
Substructure Information	Substructure Type	Multi column bent with piles
	Number of Piles per Bent	10
	Pile Type	Concrete encased steel piles
	Pile Size	HP 12 x 53 piles in 24" diameter concrete
	Height of Pile	9'-6"
	Bent Cap Dimensions	30" x 15"
	Abutment Type	Non-Integral
	Bearing Support Length	2'-6"
	Concrete Compressive Strength	3000 psi
	Yield Strength of Reinforcement	40000 psi
	Yield Strength of Steel Shape	36000 psi

In Figures A-34 to A-37, the sections and drawings relevant to modeling the bridge are shown.

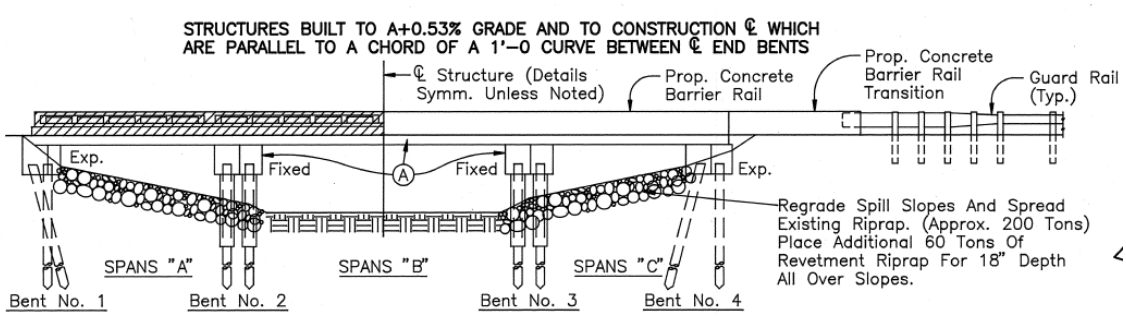

Figure A-35: Elevation View of the Bridge (INDOT, 1992)

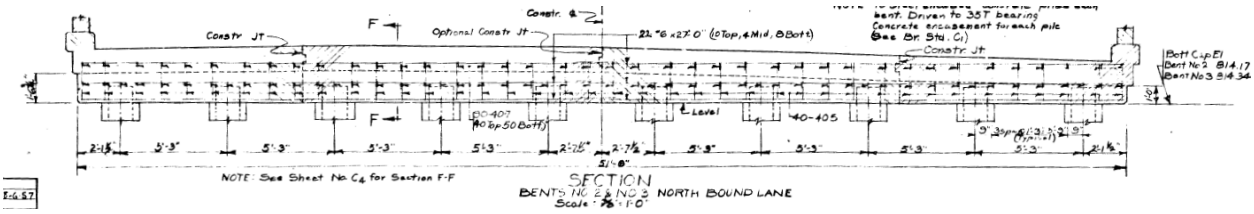

Figure A-36: Transverse Elevation View of Interior Bents (INDOT, 1992)

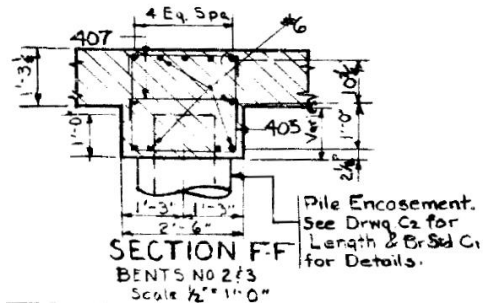

Figure A-37: Section F-F of Figure A-35 (INDOT, 1992)

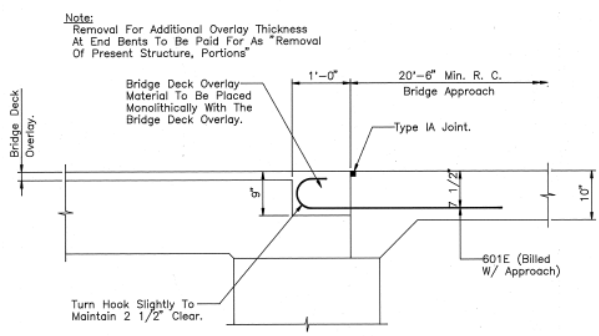

Figure A-38: Bearing Support at Abutments (INDOT, 1992)

Results – Transverse Direction

Using the modelling procedure presented in Chapter 3, each bent was modelled as a 9-bay portal frame. Due to monolithic construction of the bent cap and the deck, the deck contributes to the stiffness of the bridge. The mass, stiffness, period, and mode shape of the bridge calculated in the transverse direction are:

$$M = \begin{bmatrix} 0.67 & 0 \\ 0 & 0.67 \end{bmatrix} \frac{kips}{g}$$

$$K = \begin{bmatrix} 39000 & -24700 \\ -24700 & 39000 \end{bmatrix} kips/in$$

$$T = \begin{bmatrix} 0.04 \\ 0.02 \end{bmatrix} seconds$$

$$\Phi = \begin{bmatrix} -0.71 & -0.71 \\ -0.71 & 0.71 \end{bmatrix}$$

The plastic moment and shear resultant of each pile are 222 ft-kip, and 50 kips, respectively. Each bent has a shear strength of 1100 kips which is greater than the shear resultant (470 kips). Thus, plastic hinges will form prior to collapse. The ultimate inelastic force corresponding to the limiting rotation is 5090 kips. Applying the 100 ground motions generated at this bridge site (site class D) to the bridge model, the shear demand from the ground motions (50 per fault orientation) is plotted against the peak ground acceleration (PGA) of each earthquake. The substructure capacity is shown using threshold values corresponding to the flexural capacity, inelastic force, and the shear strength, as shown in Figure A-39.

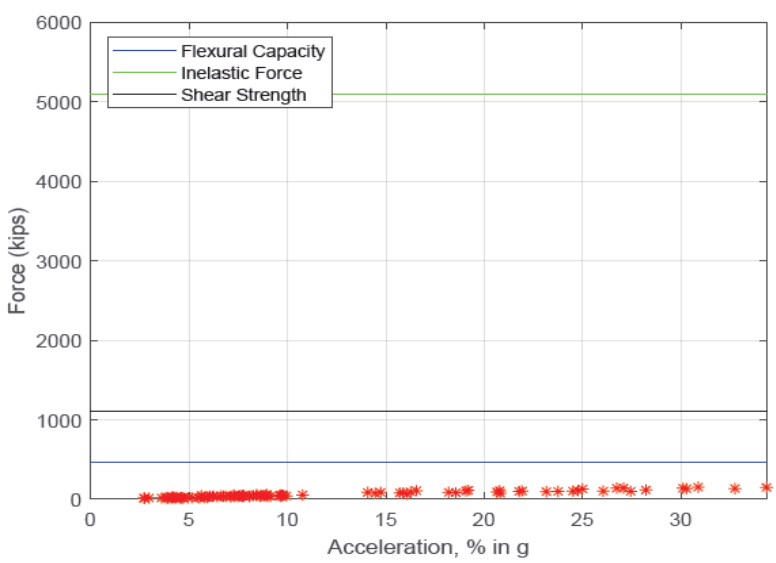

Figure A-39: Shear Demand Due to Applied Ground Motions – Transverse Direction

Based on the plot, the capacity of the substructure is not exceeded by the demand for any ground motions. Additionally, the maximum displacement of the bridge due to the ground motions is less than 0.01”. Therefore, the bridge is not vulnerable in the transverse direction at level of ground motions expected at its location.

Results – Longitudinal Direction

The piles are acting in parallel and modelled as fixed at the top of the bent cap and at the ground. The bridge is modelled as a single degree of freedom system, so the entire mass is used to obtain the period. The mass, stiffness, and period of the bridge in the longitudinal direction are $1.90\ kips/g$, $2940\ kips/in$, and $0.16\ seconds$, respectively.

The plastic moment and shear resultant of each pile are 97 ft-kip, and 9 kips, respectively. The substructure has a total shear strength of 2220 kips which is greater than the total shear resultant (180 kips). The ultimate inelastic force corresponding to the limiting rotation is 2430 kips. Applying the 100 ground motions for this bridge site to the bridge model, the shear demand from the ground motions is plotted against the peak ground acceleration (PGA) of each earthquake. The substructure capacity is shown using threshold values corresponding to the flexural capacity, inelastic force, and the shear strength.

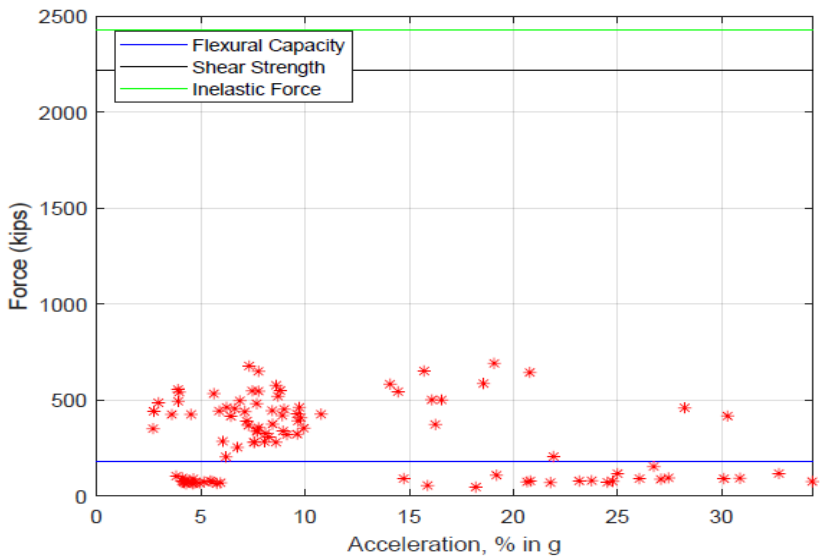

Figure A-40: Shear Demand Due to Applied Ground Motions – Longitudinal Direction

From the plot, the shear demand from the ground motions does exceed the flexural capacity, therefore the longitudinal reinforcement in this direction yields. The maximum displacement of the bridge due to the set of ground motions is less than ¼". Additionally, since the shear strength of the substructure is not exceeded, the bridge is of low vulnerability at the level of ground motions expected at its location.

12. Bridge Asset Name: I69-334-04590BNB

Table A.16: Specifications and Information on Bridge I69-334-04590BNB

Geographical Information	Asset Name	I69-334-04590BNB
	NBI Number	040720
	County	Dekalb
	District	Fort Wayne
	Year of Construction	1963, 1997
	Facility Carried	I-69 NB
	Feature Intersected	Cedar Creek
Superstructure Information	Superstructure Type	Continuous Reinforced Concrete Slab
	Number of Spans	3
	Span Lengths	24'-3", 30'-6", 24'-3"
	Deck Width	56'-9"
	Deck Thickness	16"
	Skew	13 degrees
	Concrete Compressive Strength	4000 psi
	Yield Strength of Reinforcement	40000 psi
Substructure Information	Substructure Type	Multi column bent with piles
	Number of Piles per Bent	10
	Pile Type	Concrete filled tubes
	Pile Size	14" diameter steel tube
	Height of Pile	10'-10"
	Bent Cap Dimensions	30" x 16"
	Abutment Type	Non-Integral
	Bearing Support Length	1'-7"
	Concrete Compressive Strength	3500 psi
	Yield Strength of Reinforcement	40000 psi
	Yield Strength of Steel Shape	36000 psi

In Figures A-40 to A-43, the sections and drawings relevant to modeling the bridge are shown.

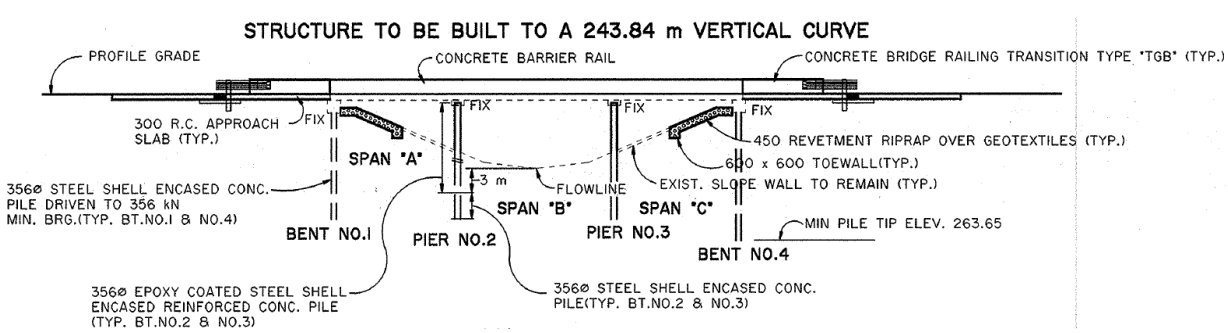

Figure A-41: Elevation View of the Bridge (INDOT, 1997)

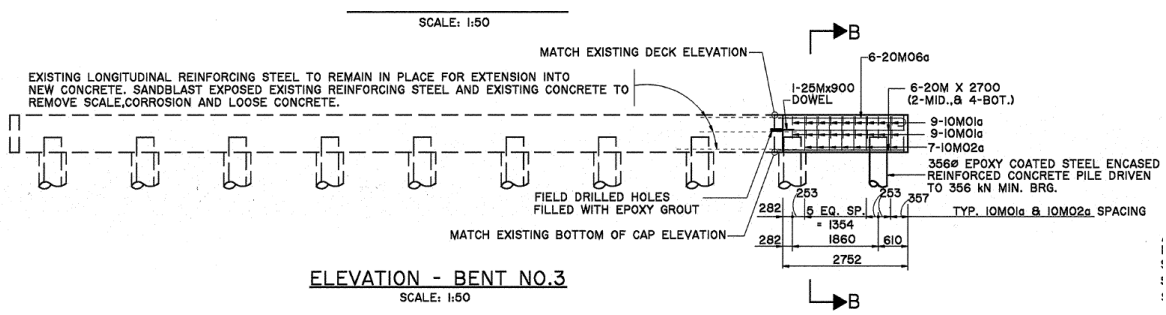

Figure A-42: Transverse Elevation View of Interior Bents (INDOT, 1997)

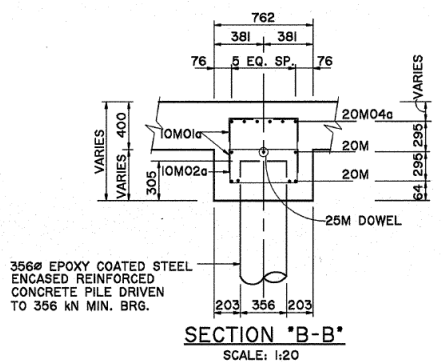

Figure A-43: Section B-B of Figure A-41 (INDOT, 1997)

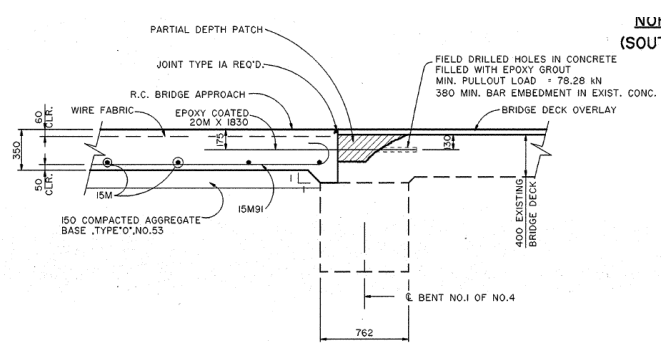

Figure A-44: Bearing Support at Abutments (INDOT, 1997)

Results – Transverse Direction

Each bent was modelled as a 9-bay portal frame. Due to monolithic construction of the bent cap and the deck, the deck contributes to the stiffness of the bridge. The mass, stiffness, period, and mode shape of the bridge calculated in the transverse direction are:

$$M = \begin{bmatrix} 0.86 & 0 \\ 0 & 0.86 \end{bmatrix} \frac{kips}{g}$$

$$K = \begin{bmatrix} 78000 & -47500 \\ -47500 & 78000 \end{bmatrix} kips/in$$

$$T = \begin{bmatrix} 0.03 \\ 0.02 \end{bmatrix} seconds$$

$$\Phi = \begin{bmatrix} -0.71 & -0.71 \\ -0.71 & 0.71 \end{bmatrix}$$

The plastic moment and shear resultant of each pile are 123 ft-kip, and 25 kips, respectively. Each bent has a shear strength of 940 kips which is greater than the shear resultant (230 kips). Thus, plastic hinges will form prior to collapse. Applying the 100 ground motions generated at this bridge site (site class D) to the bridge model, the shear demand from the ground motions (50 per fault orientation) is plotted against the peak ground acceleration (PGA) of each earthquake. The substructure capacity is shown using threshold values corresponding to the flexural capacity, and the shear strength, as shown in Figure A-45.

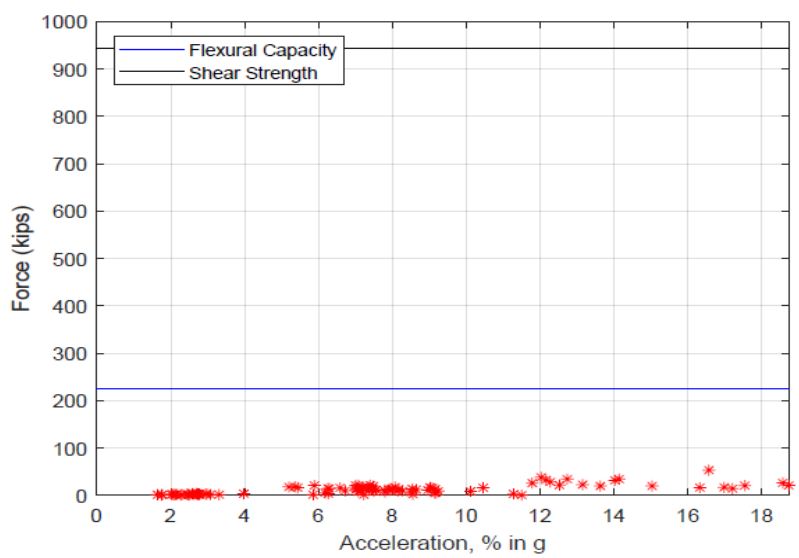

Figure A-45: Shear Demand Due to Applied Ground Motions – Transverse Direction

Based on the plot, the capacity of the substructure is not exceeded by the demand for any ground motions. Additionally, the maximum displacement of the bridge due to the ground motions is approximately zero. Therefore, the bridge is not vulnerable in the transverse direction at level of ground motions expected at its location.

Results – Longitudinal Direction

The piles are acting in parallel and modelled as fixed at the top of the bent cap and at the ground. This assumes that the soil is compacted properly to provide fixity at the base. The bridge is modelled as a single degree of freedom system, so the entire mass is used to obtain the period. The mass, stiffness, and period of the bridge in the longitudinal direction are $2.49\ kips/g$, $360\ kips/in$, and $0.53\ seconds$, respectively.

The plastic moment and shear resultant of each pile are 123 ft-kip, and 10 kips, respectively. The substructure has a total shear strength of 1890 kips which is greater than the total shear resultant (200 kips. Applying the 100 ground motions generated at this bridge site (site class D) to the bridge model, the shear demand from the ground motions (50 per fault orientation) is plotted against the peak ground acceleration (PGA) of each earthquake. The substructure capacity is shown using threshold values corresponding to the flexural capacity, and the shear strength, as shown in Figure A-46.

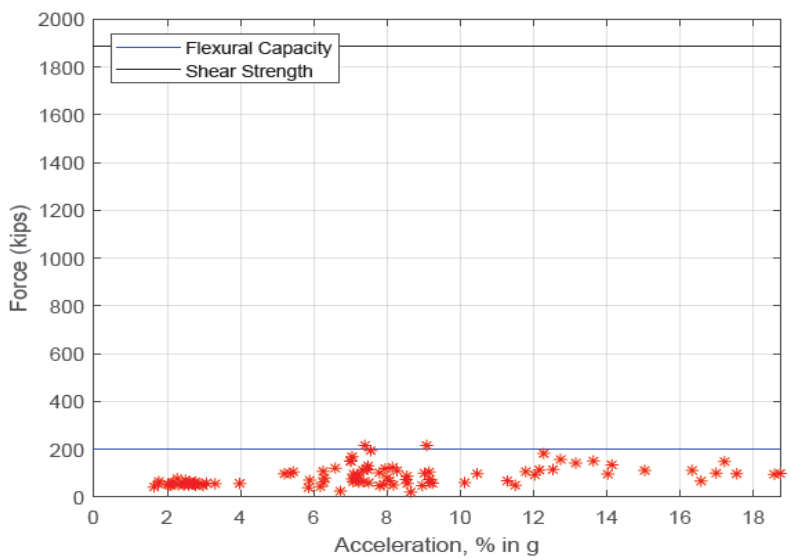

Figure A-46: Shear Demand Due to Applied Ground Motions – Longitudinal Direction

From the plot, the shear demand from the ground motions does exceed the flexural capacity, therefore the longitudinal reinforcement in this direction yields. The maximum displacement of the bridge due to the set of ground motions is less than 0.75”. Additionally, since the shear strength of the substructure is not exceeded, the bridge is of low vulnerability at the level of ground motions expected at its location.

13. Asset Name: 63-86-05970BNBL

Table A.17: Specifications and Information on Bridge 63-86-05970BNBL

Geographical Information	Asset Name	63-86-05970BNBL
	NBI Number	022810
	County	Warren
	District	Crawfordsville
	Year of Construction	1976, 2015
	Facility Carried	SR 63 NB
	Feature Intersected	Fall Creek
Superstructure Information	Superstructure Type	Continuous Reinforced Concrete Slab
	Number of Spans	3
	Span Lengths	28'-0", 36'-0", 28'-0"
	Deck Width	42'-6"
	Deck Thickness	19"
	Skew	15 degrees
	Concrete Compressive Strength	4000 psi
	Yield Strength of Reinforcement	40000 psi
Substructure Information	Substructure Type	Wall
	Height of Wall	14'-0"
	Width of Wall	47'-0"
	Thickness of Wall	2'-0"
	Abutment Type	Non-Integral
	Bearing Support Length	2'-0"
	Concrete Compressive Strength	3500 psi
	Yield Strength of Reinforcement	40000 psi

In Figures A-46 to A-48, the sections and drawings relevant to modeling the bridge are shown.

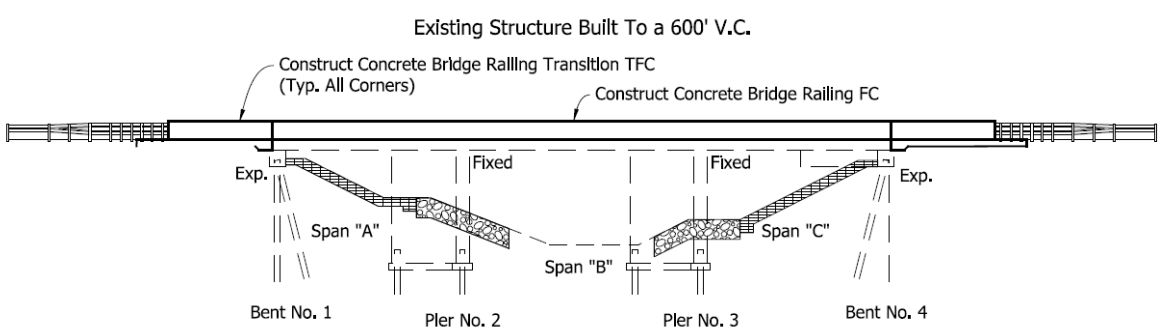

Figure A-47: Elevation View of the Bridge (INDOT, 2014)

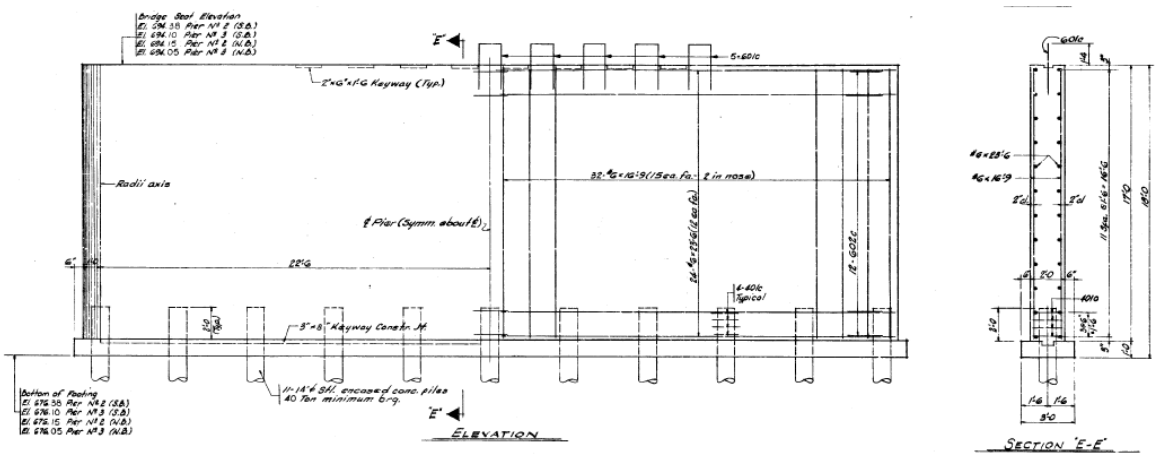

Figure A-48: Transverse Elevation View of Interior Bents (INDOT, 2014)

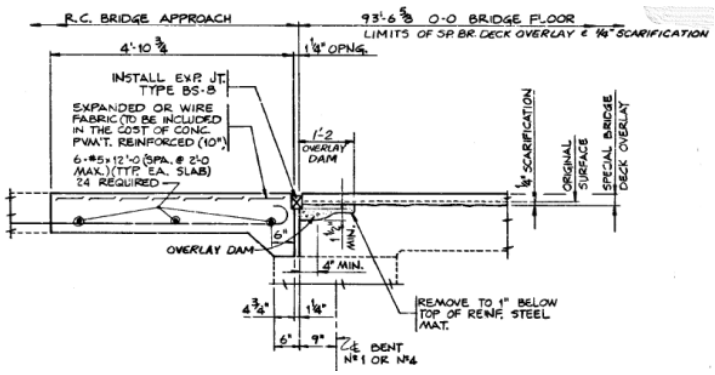

Figure A-49: Bearing Support at Abutments (INDOT, 2014)

Results – Transverse Direction

The bridge is modelled as a three span bridge. Due to the presence of extended longitudinal bars from the bents into the deck, the deck contributes to the stiffness of the bridge. The mass, stiffness, period, and mode shape of the bridge calculated in the transverse direction are:

$$M = \begin{bmatrix} 0.90 & 0 \\ 0 & 0.90 \end{bmatrix} \frac{kips}{g}$$

$$K = \begin{bmatrix} 918500 & -31100 \\ -31100 & 918500 \end{bmatrix} kips/in$$

$$T = \begin{bmatrix} 0.006 \\ 0.006 \end{bmatrix} seconds$$

$$\Phi = \begin{bmatrix} -0.71 & -0.71 \\ -0.71 & 0.71 \end{bmatrix}$$

The plastic moment and shear resultant of each wall are 22470 ft-kip, and 1600 kips, respectively. The wall has a shear strength of 1460 kips which is less than the shear demand. Thus, plastic hinges will not form and the flexural capacity of the bent is limited to the shear strength. The strength of the shear friction connection between each wall and the deck is 500 kips. Applying the 100 ground motions generated at this bridge site (site class D) to the bridge model, the shear demand from the ground motions is plotted against the peak ground acceleration (PGA) of each earthquake. The substructure capacity is shown using threshold values corresponding to the strength of the shear friction connection and the shear strength.

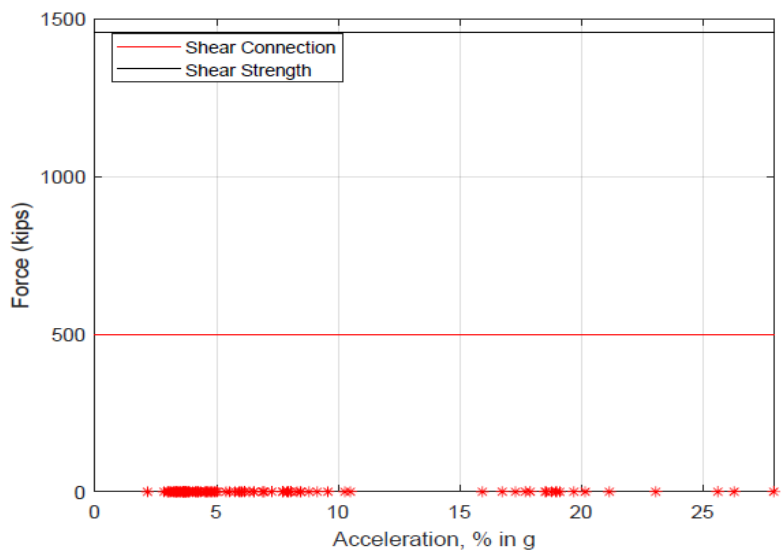

Figure A-50: Shear Demand Due to Applied Ground Motions – Transverse Direction

Based on the plot, the capacity of the substructure is not exceeded by the demand for any ground motions. Additionally, the maximum displacement of the bridge due to the ground motions is approximately zero. Therefore, the bridge is not vulnerable in the transverse direction at level of ground motions expected at its location.

Results – Longitudinal Direction

The wall is modelled as fixed at the footing and at the top. The bridge is modelled as a single degree of freedom system, so the entire mass is used to obtain the period. The mass, stiffness,

and period of the bridge in the longitudinal direction are 2.60 $kips/g$, 11200 $kips/in$, and 0.10 $seconds$, respectively.

The plastic moment and shear resultant of each wall is 860 ft-kip, and 60 kips, respectively. The substructure has a total shear strength of 2910 kips, which is greater than the total shear resultant (125 kips). Thus, plastic hinges will form. The strength of the shear friction connection between the substructure and the deck is 1000 kips. Applying the 100 ground motions generated for this bridge site (site class D) to the bridge model, the shear demand from the ground motions (50 per fault orientation) is plotted against the peak ground acceleration (PGA) of each earthquake. The substructure capacity is shown using three threshold values corresponding to the flexural capacity, strength of the shear friction connection and the shear strength, as shown in Figure A-51.

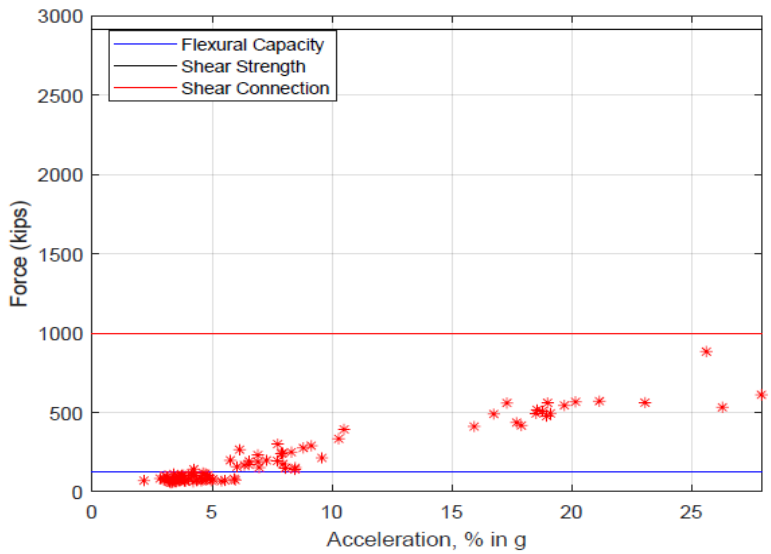

Figure A-51: Shear Demand Due to Applied Ground Motions – Longitudinal Direction

From the plot, the shear demand from the ground motions does exceed the flexural capacity, therefore the longitudinal reinforcement in this direction yields. The maximum displacement of the bridge due to the set of ground motions is less than 0.1”. Additionally, since the shear strength of the substructure is not exceeded, the bridge is of low vulnerability at the level of ground motions expected at its location.

14. Asset Name: I70-112-05137 DEBL

Table A.18: Specifications and Information on Bridge I70-112-05137 DEBL

Geographical Information	Asset Name	I70-112-05137 DEBL
	NBI Number	042960
	County	Hancock
	District	Greenfield
	Year of Construction	1964, 2017
	Facility Carried	I 70 EB
	Feature Intersected	Six Mile Creek
Superstructure Information	Superstructure Type	Continuous Reinforced Concrete Slab
	Number of Spans	3
	Span Lengths	24'-0", 32'-0", 24'-0"
	Deck Width	43'-0"
	Deck Thickness	16"
	Skew	0 degrees
	Concrete Compressive Strength	4000 psi
	Yield Strength of Reinforcement	40000 psi
Substructure Information	Substructure Type	Wall
	Height of Wall	11'-2.5"
	Width of Wall	43'-0"
	Thickness of Wall	2'-0"
	Abutment Type	Non-Integral
	Bearing Support Length	1'-6"
	Concrete Compressive Strength	3000 psi
	Yield Strength of Reinforcement	40000 psi

In Figures A-51 to A-53, the sections and drawings relevant to modeling the bridge are shown.

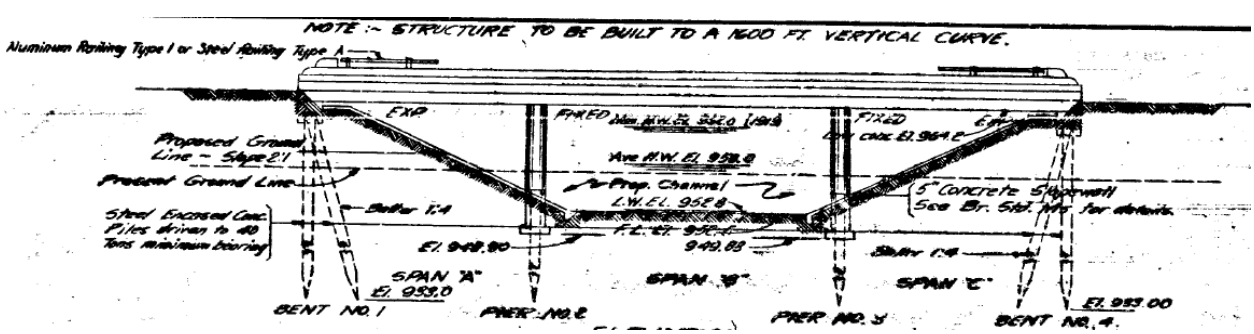

Figure A-52: Elevation View of the Bridge (INDOT, 1994)

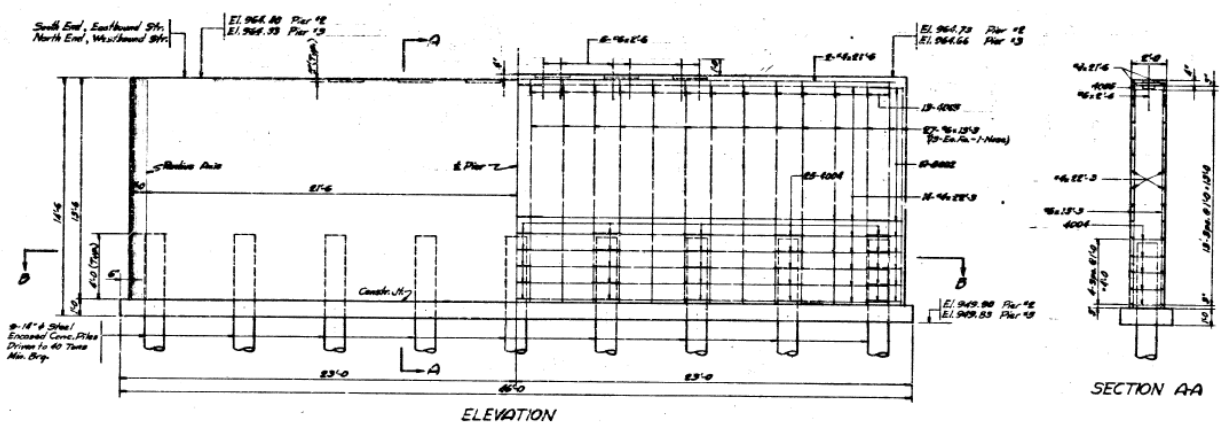

Figure A-53: Transverse Elevation View of Interior Bents (INDOT, 1994)

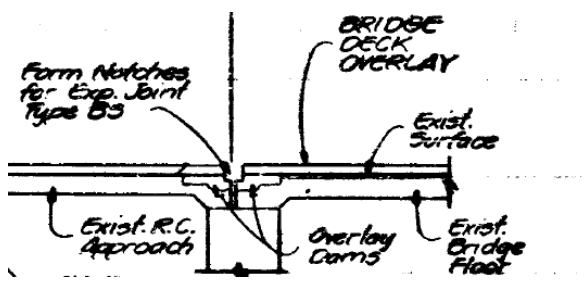

Figure A-54: Bearing Support at Abutments (INDOT, 1994)

Results – Transverse Direction

The bridge is modelled as a three span bridge. Due to the presence of extended longitudinal bars from the walls into the deck, the deck contributes to the stiffness of the bridge. The mass, stiffness, period, and mode shape of the bridge calculated in the transverse direction are:

$$M = \begin{bmatrix} 0.68 & 0 \\ 0 & 0.68 \end{bmatrix} \frac{kips}{g}$$

$$K = \begin{bmatrix} 1212000 & -33100 \\ -33100 & 1212000 \end{bmatrix} kips/in$$

$$T = \begin{bmatrix} 0.005 \\ 0.005 \end{bmatrix} seconds$$

$$\Phi = \begin{bmatrix} -0.71 & -0.71 \\ -0.71 & 0.71 \end{bmatrix}$$

The plastic moment and shear resultant of each wall is 17800 ft-kip, and 1580 kips, respectively. The wall has a shear strength of 1350 kips which is less than the shear demand. Thus, plastic hinges will not form and the flexural capacity of the bent is limited to the shear strength. The strength of the shear friction connection between each wall and the deck is 335 kips. Applying the 100 ground motions generated at this bridge site (site class D) to the bridge model, the shear demand from the ground motions (50 per fault orientation) is plotted against the peak ground acceleration (PGA) of each earthquake. The substructure capacity is shown using threshold values corresponding to the strength of the shear friction connection and the shear strength, as shown in Figure A-55.

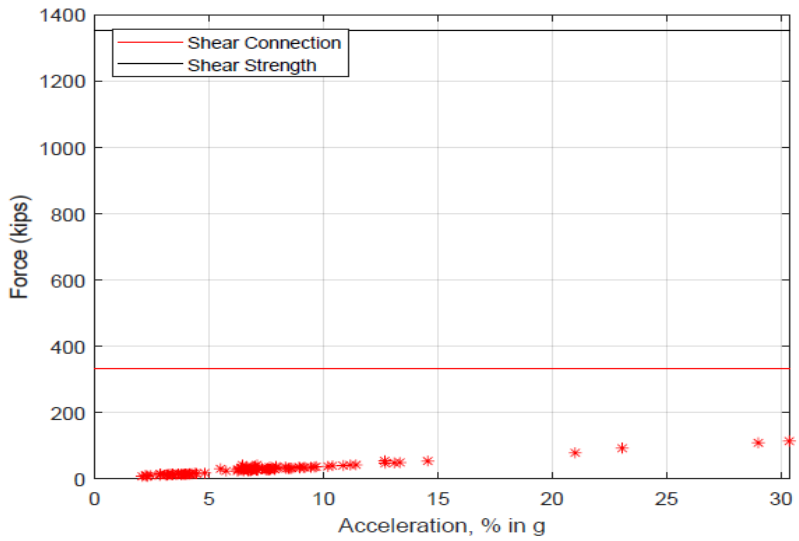

Figure A-55: Shear Demand Due to Applied Ground Motions – Transverse Direction

Based on the plot, the capacity of the substructure is not exceeded by the demand for any ground motions. Additionally, the maximum displacement of the bridge due to the ground motions is approximately zero. Therefore, the bridge is not vulnerable in the transverse direction at level of ground motions expected at its location.

Results – Longitudinal Direction

The wall is modelled as fixed at the footing and at the top. This assumes that the footing and the extended longitudinal bars into the deck were designed properly to provide fixity. The bridge is modelled as a single degree of freedom system, so the entire mass is used to obtain the period.

The mass, stiffness, and period of the bridge in the longitudinal direction are 1.95 $kips/g$, 18300 $kips/in$, and 0.06 $seconds$, respectively.

In the longitudinal direction, the plastic moment and shear resultant of each wall is 760 ft-kip, and 70 kips, respectively. The substructure has a total shear strength of 2710 kips, which is greater than the total shear resultant (135 kips). Thus, plastic hinges will form. The strength of the shear friction connection between the substructure and the deck is 670 kips. Applying the 100 ground motions generated for this bridge site (site class D) to the bridge model, the shear demand from the ground motions (50 per fault orientation) is plotted against the peak ground acceleration (PGA) of each earthquake. The substructure capacity is shown using three threshold values corresponding to the flexural capacity, strength of the shear friction connection and the shear strength, as shown in Figure A-56.

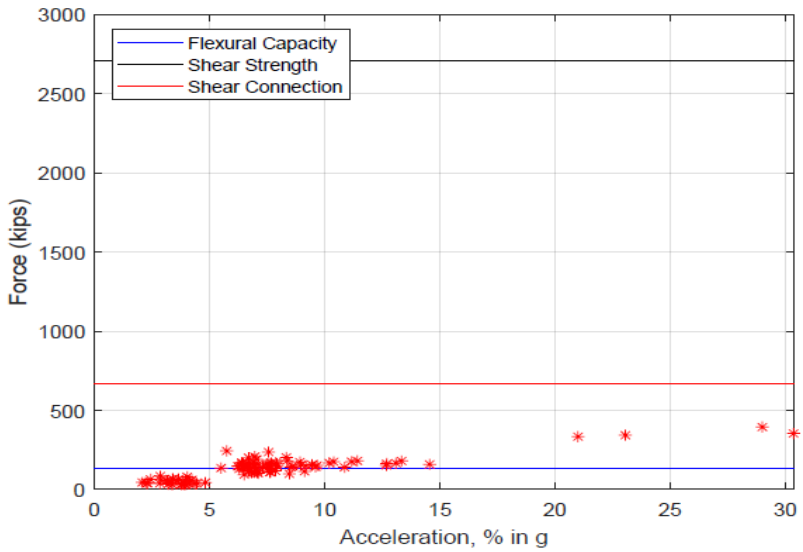

Figure A-56: Shear Demand Due to Applied Ground Motions – Longitudinal Direction

From the plot, the shear demand from the ground motions does exceed the flexural capacity, therefore the longitudinal reinforcement in this direction yields. The maximum displacement of the bridge due to the set of ground motions is less than 0.05”. Additionally, since the shear strength of the substructure is not exceeded, the bridge is of low vulnerability at the level of ground motions expected at its location.

15. Asset Name: 18-05-06573

Table A.19: Specifications and Information on Bridge 18-05-06573

Geographical Information	Asset Name	18-05-06573
	NBI Number	004880
	County	Blackford
	District	Fort Wayne
	Year of Construction	1976, 2016
	Facility Carried	SR 18
	Feature Intersected	Praire Creek
Superstructure Information	Superstructure Type	Continuous Reinforced Concrete Slab
	Number of Spans	3
	Span Lengths	30'-6", 41'-0", 30'-6"
	Deck Width	47'-0"
	Deck Thickness	16"
	Skew	30 degrees
	Concrete Compressive Strength	4000 psi
	Yield Strength of Reinforcement	40000 psi
Substructure Information	Substructure Type	Wall
	Height of Wall	10'-5"
	Width of Wall	57'-0"
	Thickness of Wall	2'-0"
	Abutment Type	Non-Integral
	Bearing Support Length	2'-0"
	Concrete Compressive Strength	3500 psi
	Yield Strength of Reinforcement	40000 psi

In Figures A-56 to A-58, the sections and drawings relevant to modeling the bridge are shown.

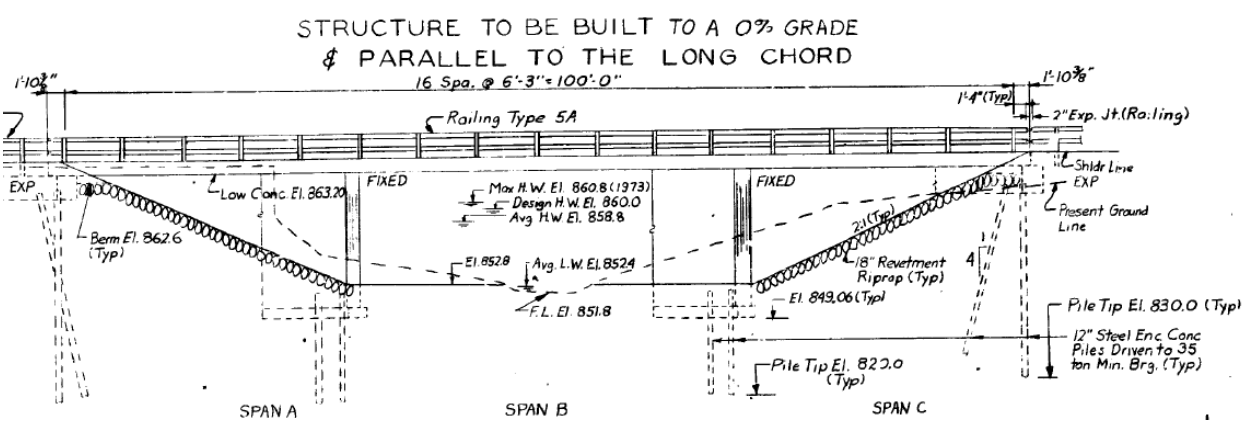

Figure A-57: Elevation View of the Bridge (INDOT, 1985)

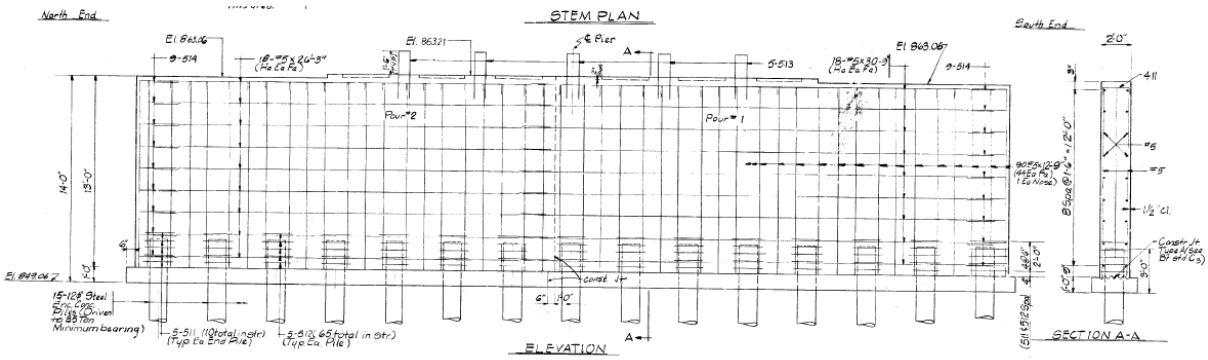

Figure A-58: Transverse Elevation View of Interior Bents (INDOT, 1985)

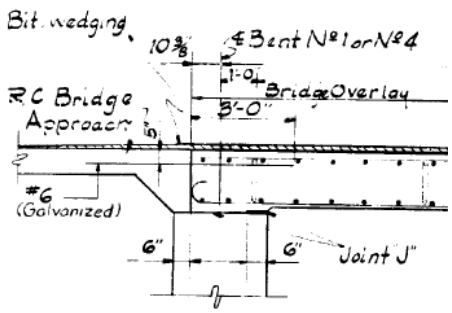

Figure A-59: Bearing Support at Abutments (INDOT, 1985)

Results – Transverse Direction

The bridge is modelled as a three span bridge. Due to the presence of extended longitudinal bars from the walls into the deck, the deck contributes to the stiffness of the bridge. The mass, stiffness, period, and mode shape of the bridge calculated in the transverse direction are:

$$M = \begin{bmatrix} 0.95 & 0 \\ 0 & 0.95 \end{bmatrix} \frac{kips}{g}$$

$$K = \begin{bmatrix} 3564000 & -22900 \\ -22900 & 3564000 \end{bmatrix} kips/in$$

$$T = \begin{bmatrix} 0.003 \\ 0.003 \end{bmatrix} seconds$$

$$\Phi = \begin{bmatrix} -0.71 & -0.71 \\ -0.71 & 0.71 \end{bmatrix}$$

Following the procedure for calculating the strength of the bridge elements in Section 3.5, the plastic moment and shear resultant of each wall is 30800 ft-kip, and 2970 kips, respectively. The wall has a shear strength of 1800 kips which is less than the shear demand. Thus, plastic hinges will not form and the flexural capacity of the bent is limited to the shear strength. The strength of the shear friction connection between each wall and the deck is 345 kips. Applying the 100 ground motions generated at this bridge site (site class D) to the bridge model, the shear demand from the ground motions (50 per fault orientation) is plotted against the peak ground acceleration (PGA) of each earthquake. The substructure capacity is shown using threshold values corresponding to the strength of the shear friction connection and the shear strength, as shown in Figure A-60.

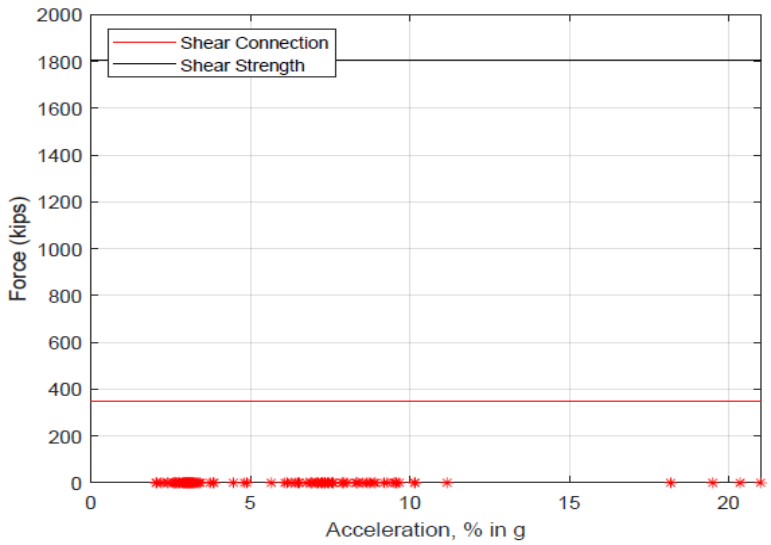

Figure A-60: Shear Demand Due to Applied Ground Motions – Transverse Direction

Based on the plot, the capacity of the substructure is not exceeded by the demand for any ground motions. Additionally, the maximum displacement of the bridge due to the ground motions is approximately zero. Therefore, the bridge is not vulnerable in the transverse direction at level of ground motions expected at its location.

Results – Longitudinal Direction

The wall is modelled as fixed at the footing and at the top. The bridge is modelled as a single degree of freedom system, so the entire mass is used to obtain the period. The mass, stiffness,

and period of the bridge in the longitudinal direction are 2.70 $kips/g$, 33200 $kips/in$, and 0.06 $seconds$, respectively.

The plastic moment and shear resultant of each wall is 1000 ft-kip, and 95 kips, respectively. The substructure has a total shear strength of 3600 kips, which is greater than the total shear resultant (190 kips). Thus, plastic hinges will form. The strength of the shear friction connection between the substructure and the deck is 690 kips. Applying the 100 ground motions generated for this bridge site (site class D) to the bridge model, the shear demand from the ground motions is plotted against the peak ground acceleration (PGA) of each earthquake. The substructure capacity is shown using three threshold values corresponding to the flexural capacity, strength of the shear friction connection and the shear strength, as shown in Figure A-61.

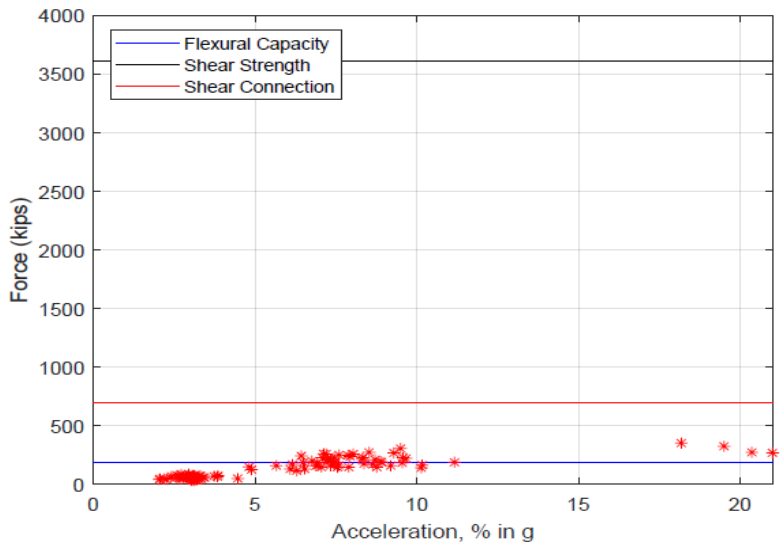

Figure A-61: Shear Demand Due to Applied Ground Motions – Longitudinal Direction

From the plot, the shear demand from the ground motions does exceed the flexural capacity, therefore the longitudinal reinforcement in this direction yields. The maximum displacement of the bridge due to the set of ground motions is less than 0.01”. Additionally, since the shear strength of the substructure is not exceeded, the bridge is of low vulnerability at the level of ground motions expected at its location.

16. Asset Name: 22-27-04724

Table A.20: Specifications and Information on Bridge 22-27-04724

Geographical Information	Asset Name	22-27-04724
	NBI Number	011170
	County	Grant
	District	Fort Wayne
	Year of Construction	1964, 1999
	Facility Carried	US 35, SR 22
	Feature Intersected	Mississinewa River
Superstructure Information	Superstructure Type	Continuous Reinforced Concrete Girder
	Number of Main Spans	4
	Span Lengths	58'-0", 87'-0", 87'-0", 58'-0"
	Deck Width	64'-6"
	Skew	15 degrees
	Concrete Compressive Strength	3000 psi
	Yield Strength of Reinforcement	40000 psi
	Substructure Type	Hammerhead Wall
Substructure Information	Height of Wall	31'-6"
	Width of Wall	52'-0"
	Thickness of Wall	3'-4"
	Abutment Type	Non-Integral
	Bearing Support Length	1'-10"
	Concrete Compressive Strength	3000 psi
	Yield Strength of Reinforcement	40000 psi

In Figures A-61 to A-65, the sections and drawings relevant to modeling the bridge are shown.

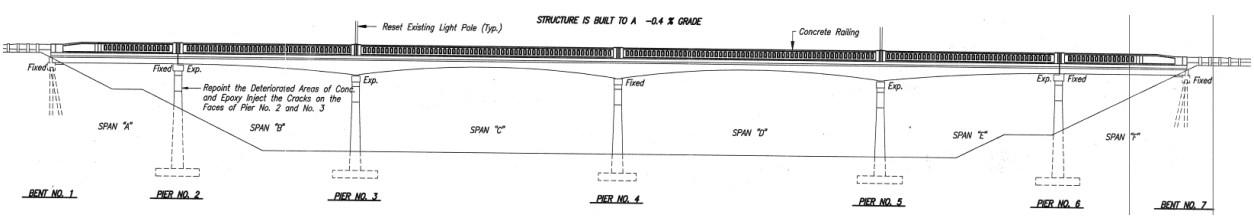

Figure A-62: Elevation View of the Bridge (INDOT, 1999)

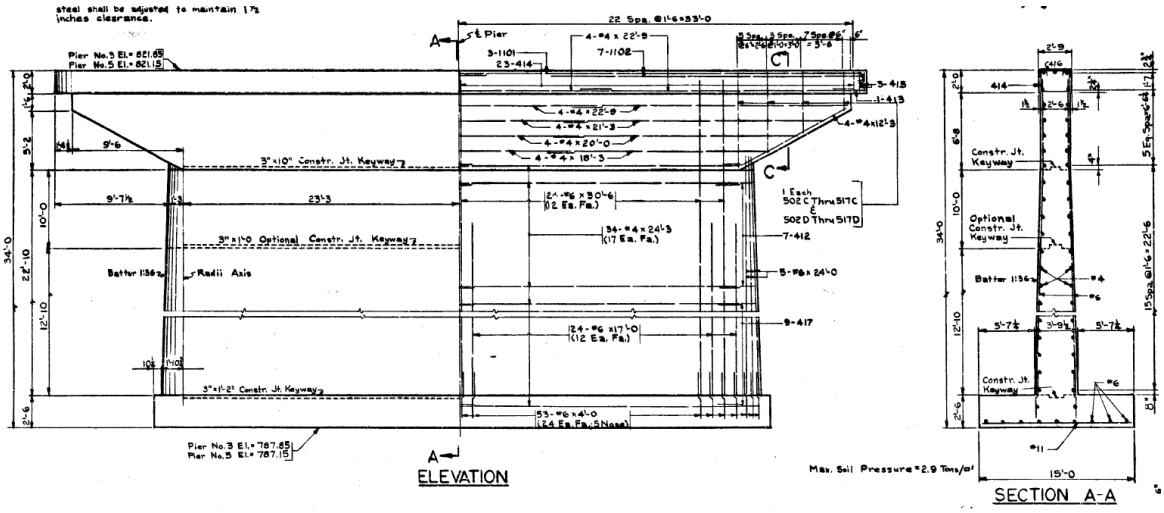

Figure A-63: Transverse Elevation View of Interior Bents #3 and #5 (INDOT, 1999)

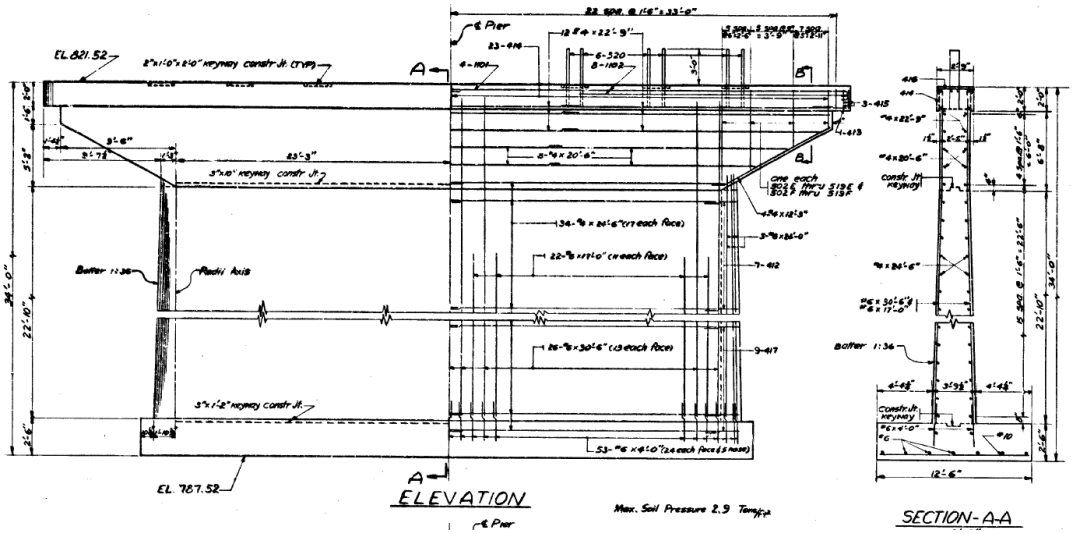

Figure A-64: Transverse Elevation View of Interior Bent #4 (INDOT, 1999)

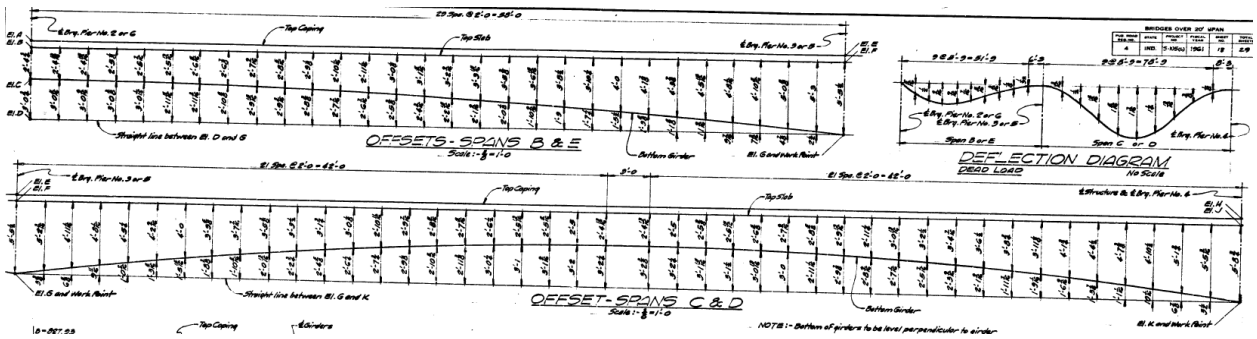

Figure A-65: Elevation of Girder Section (INDOT, 1999)

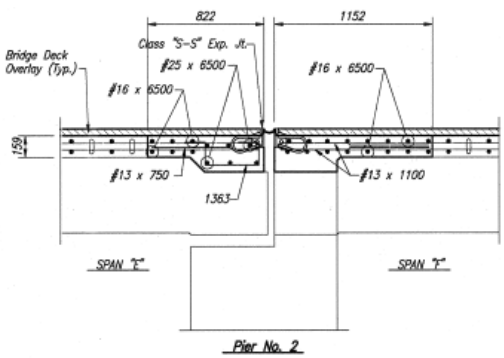

Figure A-66: Bearing Support at Abutments (INDOT, 1999)

Results – Transverse Direction

The bridge is a six span bridge with a 4 main spans. The two adjacent spans are treated as single span bridges, while the main span is analyzed. Due to the lack of extended longitudinal bars between the walls at piers #3 and #5, the bridge is modelled as a two span bridge using the modelling technique discussed in Chapter 3. Due to the presence of extended longitudinal bars from the bent #4 into the deck, the deck contributes to the stiffness of the bridge. The mass, stiffness, and period of the bridge calculated in the transverse direction are $12.7\ \frac{kips}{g}$, $2.13 \times 10^5\ kips/in$, and $0.03\ seconds$ respectively.

The plastic moment and shear resultant of each wall is 43800 ft-kip, and 1390 kips, respectively. The wall has a shear strength of 2750 kips which is greater than the shear demand. Thus, plastic hinges will form. The strength of the shear friction connection between each wall and the deck is 355 kips. Applying the 100 ground motions generated at this bridge site (site class D) to the bridge model, the shear demand from the ground motions (50 per fault orientation) is plotted against the peak ground acceleration (PGA) of each earthquake. The substructure capacity is shown using threshold values corresponding to the strength of the shear friction connection, flexural capacity, and the shear strength, as shown in Figure A-67.

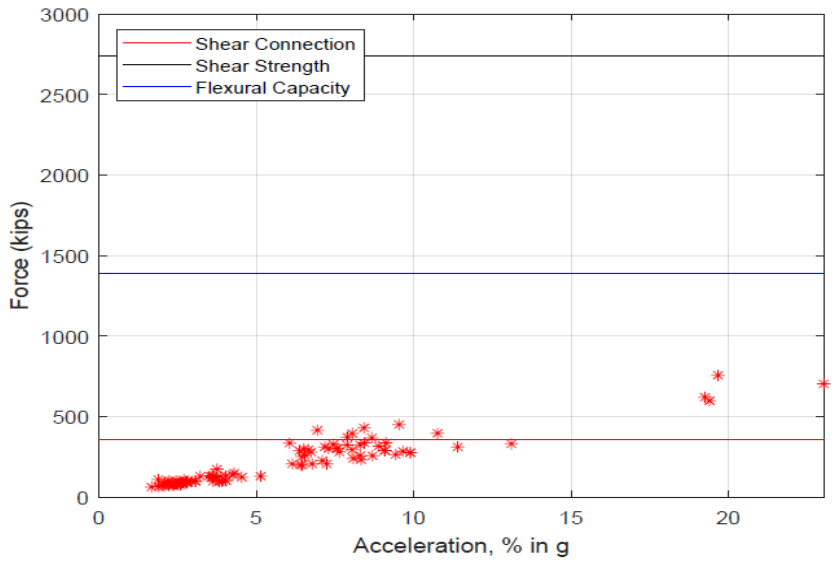

Figure A-67: Shear Demand Due to Applied Ground Motions – Transverse Direction

Based on the plot, the strength of the shear friction connection is by the demand from a few ground motions. Additionally, the maximum displacement of the bridge due to the ground motions is less than 0.005”. Therefore, the bridge is slightly vulnerable in the transverse direction at level of ground motions expected at its location.

Results – Longitudinal Direction

The bridge is also modelled as a two span bridge in this direction. The wall is modelled as fixed at the footing and at the top. This assumes that the footing and the extended longitudinal bars into the deck were designed properly to provide fixity. The bridge is modelled as a single degree of freedom system, so the entire mass is used to obtain the period. The mass, stiffness, and period of the bridge in the longitudinal direction are $6.40\ kips/g$, $2160\ kips/in$, and $0.03\ seconds$, respectively.

In the longitudinal direction, the plastic moment and shear resultant of each wall is 2600 ft-kip, and 85 kips, respectively. The substructure has a total shear strength of 2750 kips, which is greater than the total shear resultant (85 kips). Thus, plastic hinges will form. The strength of the shear friction connection between the substructure and the deck is 355 kips. Applying the 100 ground motions generated for this bridge site (site class D) to the bridge model, the shear demand from the ground motions (50 per fault orientation) is plotted against the peak ground

acceleration (PGA) of each earthquake. The substructure capacity is shown using three threshold values corresponding to the flexural capacity, strength of the shear friction connection and the shear strength, as shown in Figure A-68.

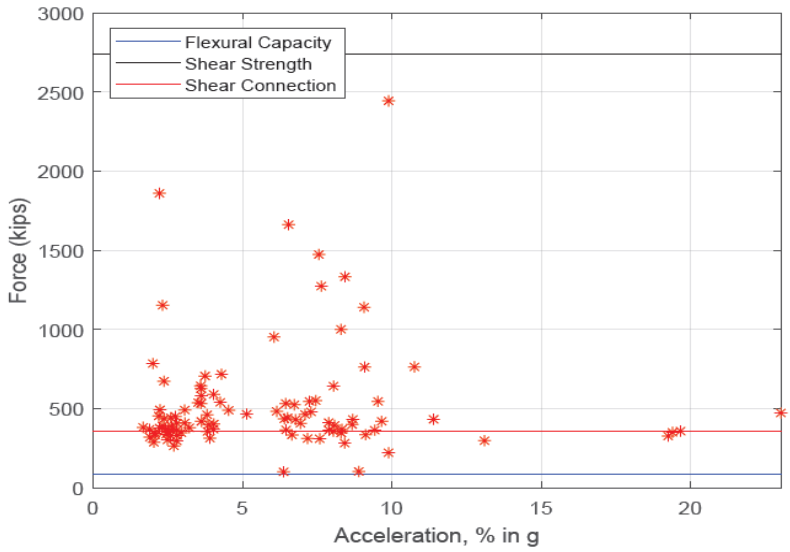

Figure A-68: Shear Demand Due to Applied Ground Motions – Longitudinal Direction

From the plot, the shear demand from the ground motions does exceed the flexural capacity and the strength of the shear friction connection. The maximum displacement of the bridge due to the set of ground motions is less than 1.25”. Therefore, the bridge is of marginal vulnerability at the level of ground motions expected at its location.

17. Bridge Asset Name: 75-06-04958A

Table A.21: Specifications and Information on Bridge 75-06-04958A

Geographical Information	Asset Name	75-06-04958A
	NBI Number	024860
	County	Boone
	District	Crawfordsville
	Year of Construction	1963, 1983
	Facility Carried	SR 75
	Feature Intersected	I-74 EW/WB
Superstructure Information	Superstructure Type	Continuous Reinforced Concrete Girder
	Number of Spans	4
	Span Lengths	43'-0", 75'-0", 75'-0", 43'-0"
	Deck Width	36'-4"
	Skew	26 degrees
	Concrete Compressive Strength	3000 psi
	Yield Strength of Reinforcement	40000 psi
Substructure Information	Substructure Type	Multi column bent with RC Columns
	Number of Piles per Bent	5
	Column Dimensions	36" x 24"
	Height of Pile	7'-9"
	Bent Cap Dimensions	30" x 30"
	Abutment Type	Non-Integral
	Bearing Support Length	2'-9"
	Concrete Compressive Strength	3000 psi
	Yield Strength of Reinforcement	40000 psi

In Figures A-68 to A-72, the sections and drawings relevant to modeling the bridge are shown.

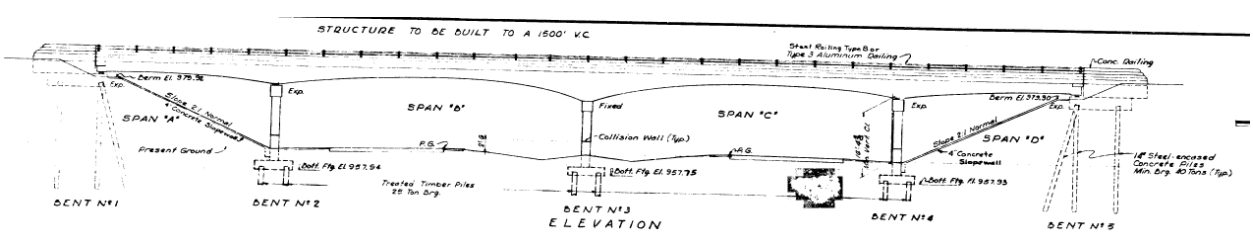

Figure A-69: Elevation View of the Bridge (INDOT, 1981)

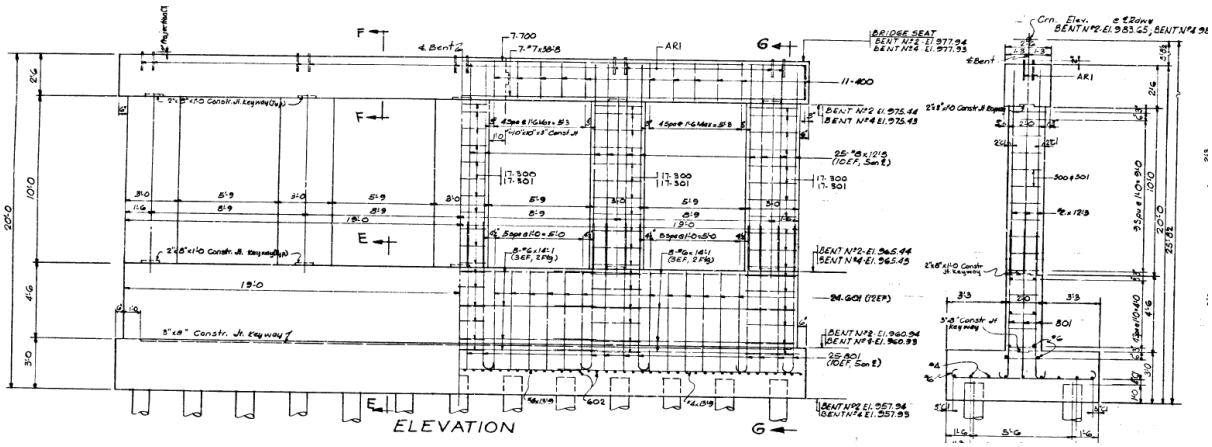

Figure A-70: Transverse Elevation View of Interior Bents #2 and #4 (INDOT, 1981)

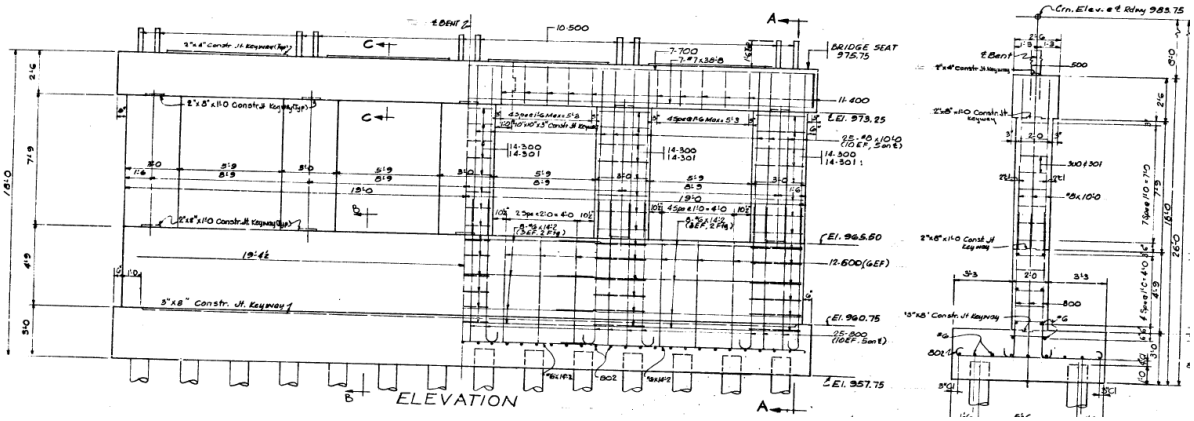

Figure A-71: Transverse Elevation View of Interior Bents #3 (INDOT, 1981)

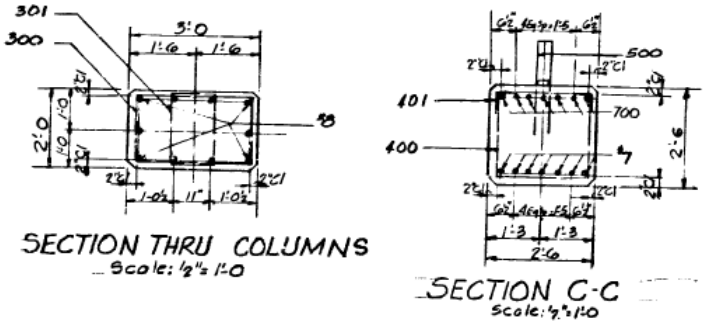

Figure A-72: Cross-Section of the Column Members and Bent Cap (INDOT, 1981)

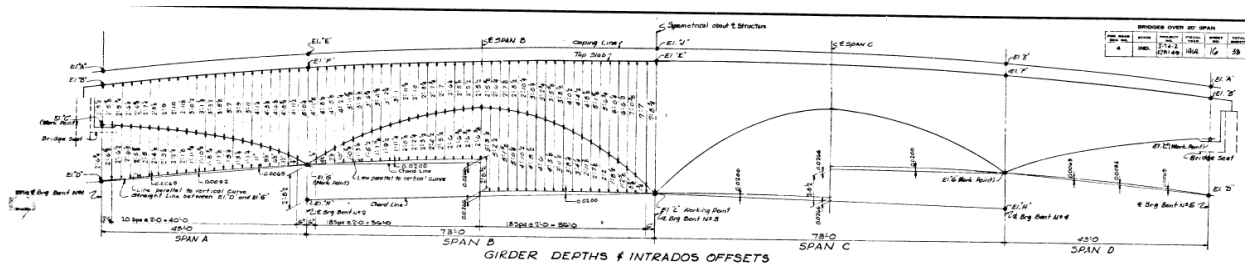

Figure A-73: Elevation View of Girders (INDOT, 1981)

Results – Transverse Direction

Due to the lack of extended longitudinal bars from bents #2 and #4, the bridge is modelled as a two span bridge. The extended longitudinal bars from the bent cap in bent #3 into the deck, the deck contributes to the stiffness of the bridge. The mass, stiffness, and period of the bridge calculated in the transverse direction are 2.70 $\frac{kips}{g}$, 16950 $kips/in$, and 0.08 $seconds$ respectively.

The plastic moment and shear resultant of each column are 440 ft-kip, and 115 kips, respectively. Each bent has a shear strength of 560 kips which is less than the shear resultant (575 kips). Thus, plastic hinges will not form, and the flexural capacity is limited to the shear strength. The strength of the shear friction connection between each bent and the deck is 210 kips. Applying the 100 ground motions generated at this bridge site (site class D) to the bridge model, the shear demand from the ground motions (50 per fault orientation) is plotted against the peak ground acceleration (PGA) of each earthquake. The substructure capacity is shown using threshold values corresponding to the strength of the shear friction connection, and the shear strength, as shown in Figure A-74.

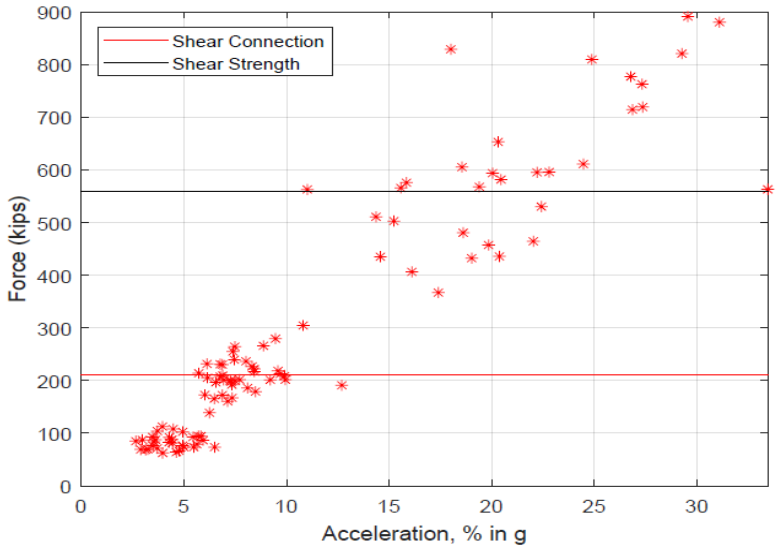

Figure A-74: Shear Demand Due to Applied Ground Motions – Transverse Direction

Based on the plot, the capacity of the substructure is exceeded by the demand from the ground motions. The maximum displacement of the bridge due to the ground motions is less than 0.05”. However, since the capacity of the shear strength is exceeded, the bridge is vulnerable in the transverse direction at level of ground motions expected at its location.

Results – Longitudinal Direction

The columns are acting in parallel and modelled as fixed at the top of the bent cap and at the crash wall. This assumes that the connection between the columns and the crash wall were designed properly to provide fixity. The bridge is modelled as a single degree of freedom system, so the entire mass is used to obtain the period. The mass, stiffness, and period of the bridge in the longitudinal direction are 5.40 $kips/g$, 9760 $kips/in$, and 0.15 $seconds$, respectively.

The plastic moment and shear resultant of each column are 325 ft-kip, and 30 kips, respectively. The substructure has a total shear strength of 1060 kips which is greater than the total shear resultant (300 kips). The strength of the shear friction connection between the substructure and the deck is 210 kips. Applying the 100 ground motions generated at this bridge site (site class D) to the bridge model, the shear demand from the ground motions (50 per fault orientation) is plotted against the peak ground acceleration (PGA) of each earthquake. The

substructure capacity is shown using threshold values corresponding to the flexural capacity, strength of the shear friction connection, and the shear strength, as shown in Figure A-75.

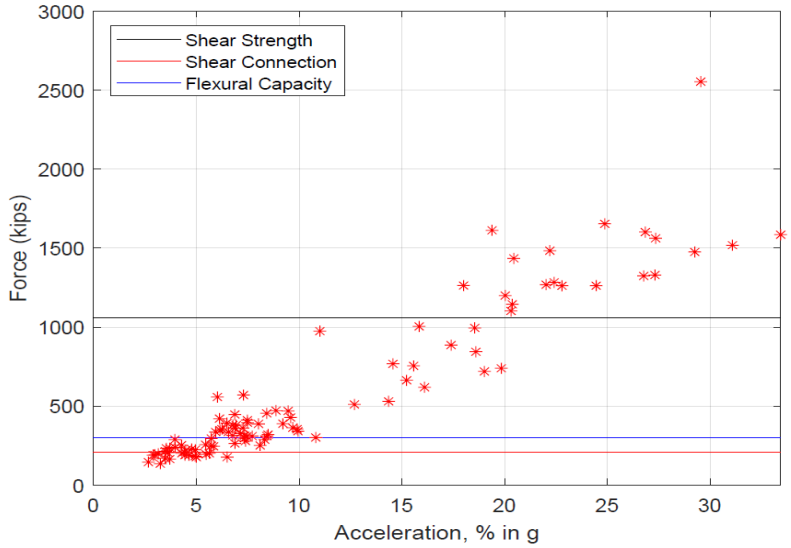

Figure A-75: Shear Demand Due to Applied Ground Motions – Longitudinal Direction

From the plot, the shear demand from the ground motions exceeds the flexural capacity, and shear strength of the substructure. The maximum displacement of the bridge due to the set of ground motions is less than 0.5”. Additionally, since the shear strength of the substructure is exceeded, the bridge is vulnerable at the level of ground motions expected at its location.

18. Bridge Asset Name: 64-63-03590A

Table A.22: Specifications and Information on Bridge 64-63-03590A

Geographical Information	Asset Name	64-63-03590A
	NBI Number	022950
	County	Pike
	District	Vincennes
	Year of Construction	1950, 1980
	Facility Carried	SR 64
	Feature Intersected	Cup Creek
Superstructure Information	Superstructure Type	Reinforced Concrete Girder
	Number of Spans	3
	Span Lengths	32'-0", 40'-0", 32'-0"
	Deck Width	32'-4"
	Skew	10 degrees
	Concrete Compressive Strength	3000 psi
	Yield Strength of Reinforcement	40000 psi
Substructure Information	Substructure Type	Multi column bent with RC Precast Piles
	Number of Precast Piles per Bent	8
	Pile Dimensions	12" x 12"
	Height of Pile	12'-7"
	Bent Cap Dimensions	36" x 36"
	Abutment Type	Non-Integral
	Bearing Support Length	1'-10"
	Concrete Compressive Strength	3000 psi
	Yield Strength of Reinforcement	40000 psi

In Figures A-75 to A-79, the sections and drawings relevant to modeling the bridge are shown.

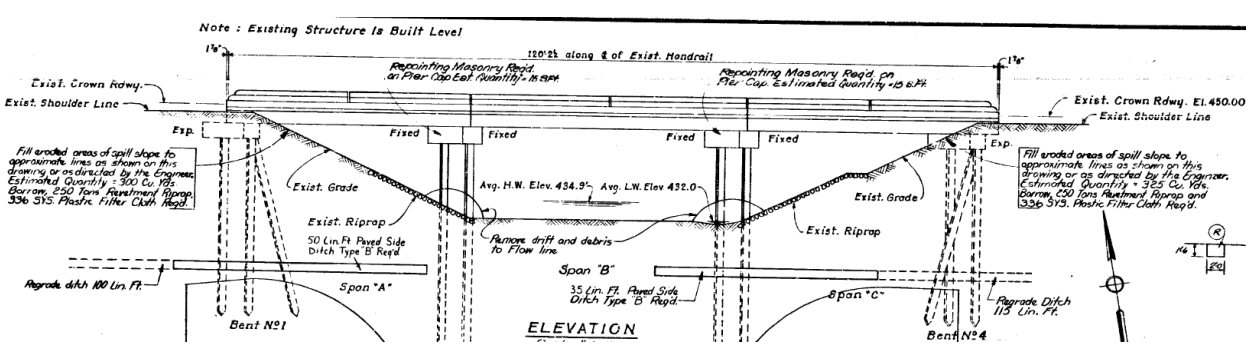

Figure A-76: Elevation View of the Bridge (INDOT, 1979)

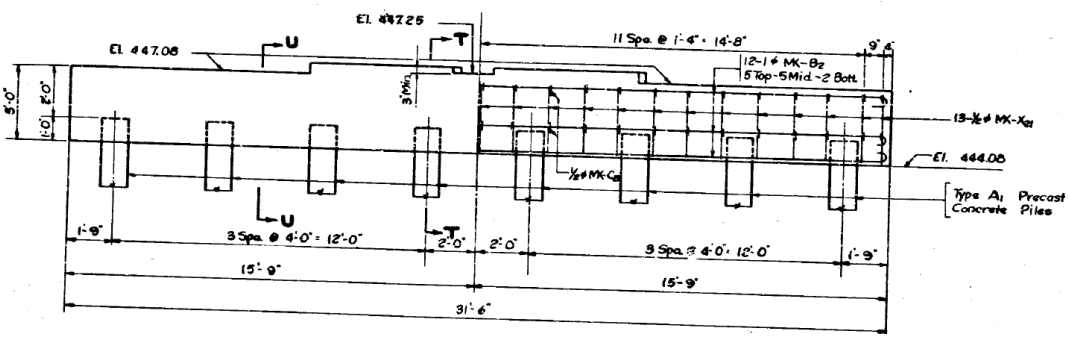

Figure A-77: Transverse Elevation View of Interior Bents (INDOT, 1979)

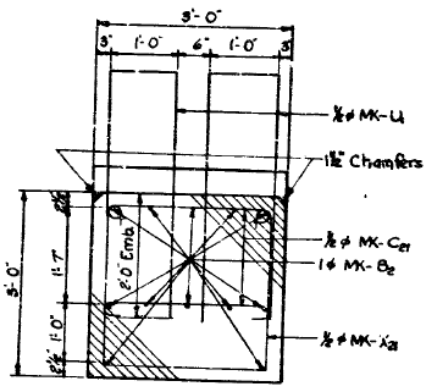

Figure A-78: Section U-U of Figure A-76 (INDOT, 1979)

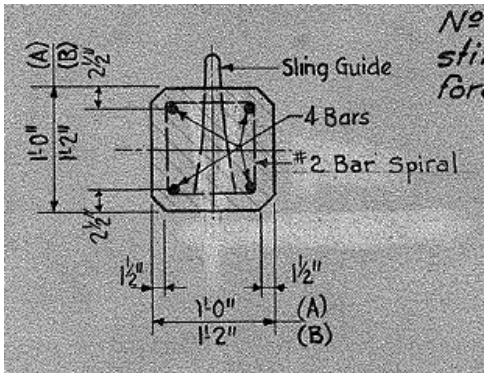

Figure A-79:Cross-Section of Precast Concrete Piles (INDOT, 1940)

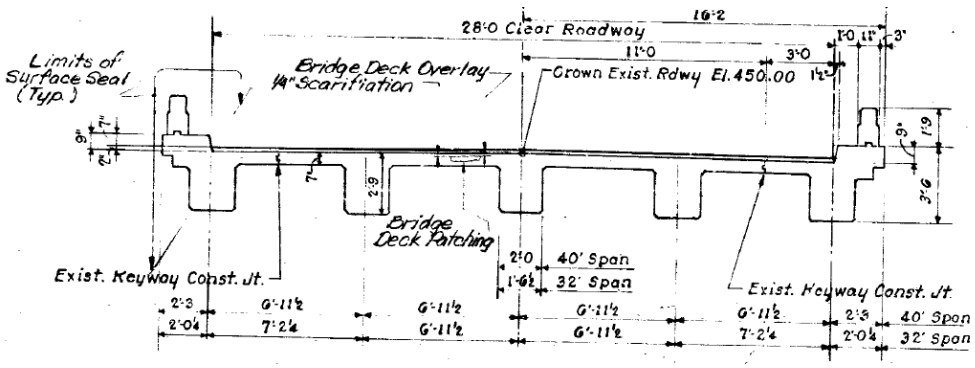

Figure A-80: Cross-Section of Bridge Superstructure (INDOT, 1979)

Results – Transverse Direction

Using the modelling procedure presented in Chapter 3, each bent was modelled as a 7-bay portal frame. Due to presence of extended longitudinal bars from the bent cap into the deck, the deck contributes to the stiffness of the bridge. The mass, stiffness, period, and mode shape of the bridge calculated in the transverse direction are:

$$M = \begin{bmatrix} 0.95 & 0 \\ 0 & 0.95 \end{bmatrix} \frac{kips}{g}$$

$$K = \begin{bmatrix} 6980 & -5200 \\ -5200 & 6980 \end{bmatrix} kips/in$$

$$T = \begin{bmatrix} 0.14 \\ 0.06 \end{bmatrix} seconds$$

$$\Phi = \begin{bmatrix} -0.71 & -0.71 \\ -0.71 & 0.71 \end{bmatrix}$$

The plastic moment and shear resultant of each precast pile are 45 ft-kip, and 8 kips, respectively. Each bent has a total shear strength of 150 kips which is greater than the shear resultant (64 kips). Thus, plastic hinges will form prior to collapse. The strength of the shear friction connection between each bent and the deck is 250 kips. Applying the 100 ground motions generated for this bridge site (site class D) to the bridge model, the shear demand from the ground motions is plotted against the PGA of each earthquake. The substructure capacity is

shown using threshold values corresponding to the flexural capacity, strength of the shear friction connection, and the shear strength, as shown in Figure A-81.

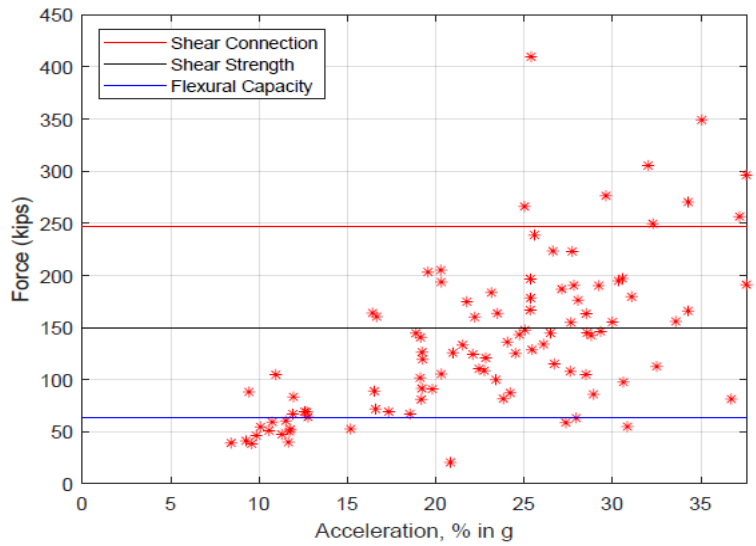

Figure A-81: Shear Demand Due to Applied Ground Motions – Transverse Direction

Based on the plot, the capacity of the substructure is exceeded by the demand from the ground motions. The maximum displacement of the bridge due to the ground motions is less than ¼". Since the capacity of the shear strength is exceeded, the bridge is vulnerable in the transverse direction at level of ground motions expected at its location.

Results – Longitudinal Direction

The piles are acting in parallel and modelled as fixed at the top of the bent cap and at the ground. This assumes that the ground provides adequate fixity at the base of the piles. The bridge is modelled as a single degree of freedom system, so the entire mass is used to obtain the period. The mass, stiffness, and period of the bridge in the longitudinal direction are 2.73 $kips/g$, 305 $kips/in$, and 0.60 $seconds$, respectively.

In the longitudinal direction, the plastic moment and shear resultant of each pile are 45 ft-kip, and 6 kips, respectively. The substructure has a total shear strength of 300 kips which is greater than the total shear resultant (95 kips). The strength of the shear friction connection between the substructure and the deck is 495 kips. Applying the 100 ground motions generated at this bridge site (site class D) to the bridge model, the shear demand from the ground motions (50

per fault orientation) is plotted against the peak ground acceleration (PGA) of each earthquake. The substructure capacity is shown using threshold values corresponding to the flexural capacity, strength of the shear friction connection, inelastic force, and the shear strength, as shown in Figure A-82.

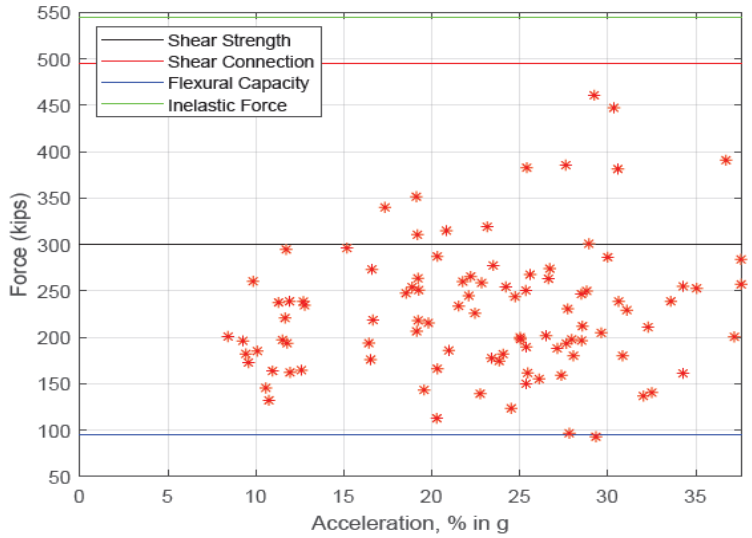

Figure A-82: Shear Demand Due to Applied Ground Motions – Longitudinal Direction

From the plot, the shear demand from the ground motions exceeds the flexural capacity, and shear strength of the substructure. The maximum displacement of the bridge due to the set of ground motions is greater than 1.5”. Additionally, since the shear strength of the substructure is exceeded, the bridge is vulnerable at the level of ground motions expected at its location.

19. Bridge Asset Name: 41-56-03828 BSBL

Table A.23: Specifications and Information on Bridge 41-56-03828 BSBL

Geographical Information	Asset Name	41-56-03828 BSBL
	NBI Number	015440
	County	Newton
	District	La Porte
	Year of Construction	1950, 1997
	Facility Carried	US 41 SB
	Feature Intersected	Montgomery Ditch
Superstructure Information	Superstructure Type	Continuous Reinforced Concrete Girder
	Number of Spans	3
	Span Lengths	32'-0", 40'-0", 32'-0"
	Deck Width	32'-4"
	Skew	5 degrees
	Concrete Compressive Strength	3000 psi
	Yield Strength of Reinforcement	40000 psi
Substructure Information	Substructure Type	Multi column bent with RC Precast Piles
	Number of Precast Piles per Bent	10
	Pile Dimensions	12" x 12"
	Height of Pile	9'-7", 3'-7"
	Bent Cap Dimensions	36" x 36"
	Abutment Type	Non-Integral
	Bearing Support Length	1'-10"
	Concrete Compressive Strength	3000 psi
	Yield Strength of Reinforcement	40000 psi

In Figures A-82 to A-86, the sections and drawings relevant to modeling the bridge are shown.

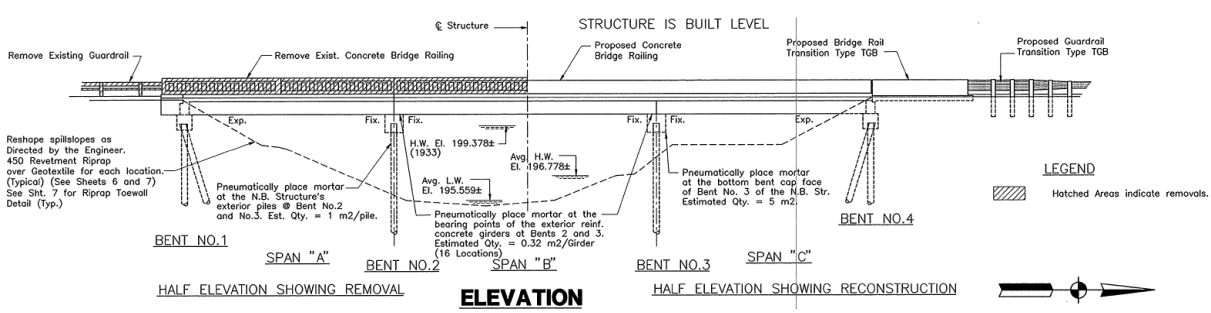

Figure A-83: Elevation View of the Bridge (INDOT, 1996)

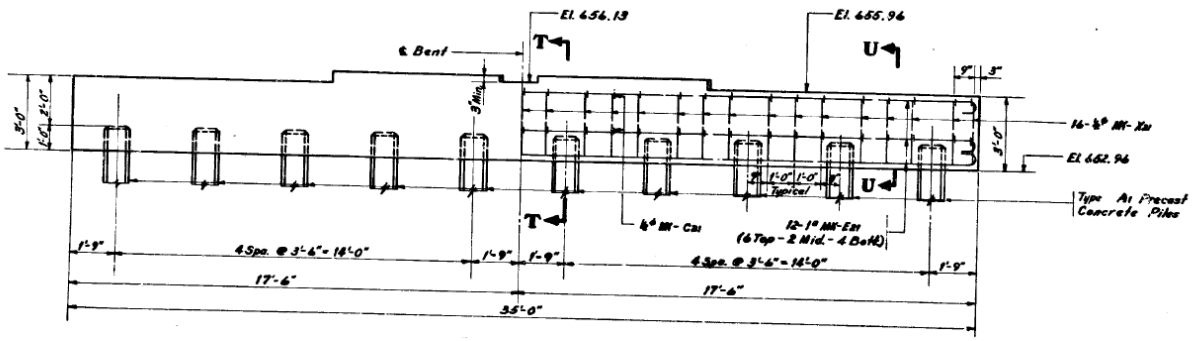

Figure A-84: Transverse Elevation View of Interior Bents (INDOT, 1996)

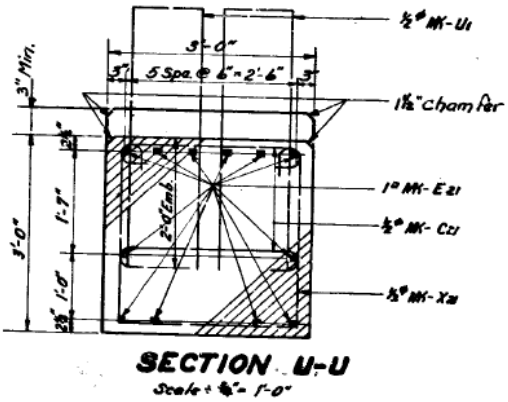

Figure A-85: Section U-U of Figure A-89 (INDOT, 1996)

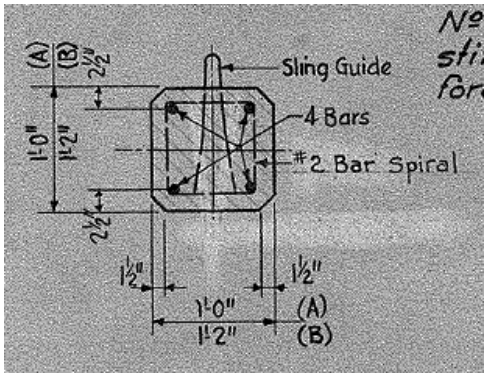

Figure A-86:Cross-Section of Precast Concrete Piles (INDOT, 1940)

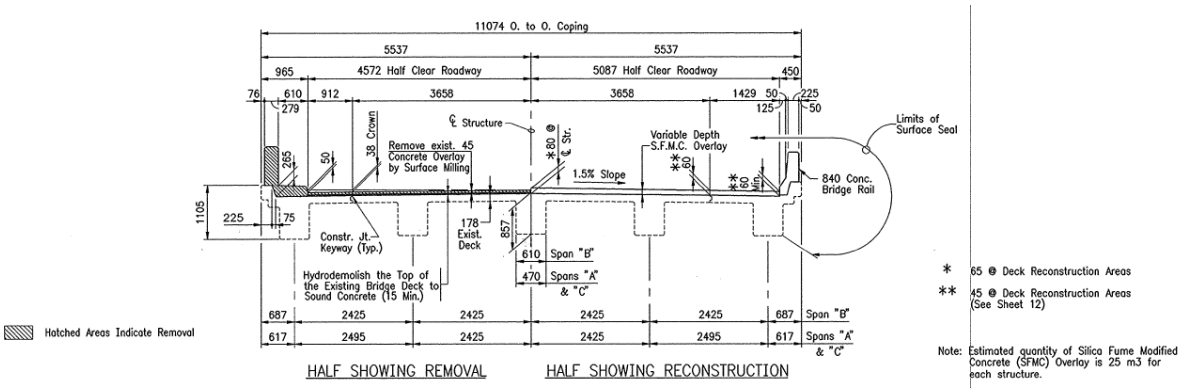

Figure A-87: Cross-Section of Bridge Superstructure (INDOT, 1996)

Results – Transverse Direction

Using the modelling procedure presented in Chapter 3, each bent was modelled as a 9-bay portal frame. Due to presence of extended longitudinal bars from the bent cap into the deck, the deck contributes to the stiffness of the bridge. The mass, stiffness, period, and mode shape of the bridge calculated in the transverse direction are:

$$M = \begin{bmatrix} 0.68 & 0 \\ 0 & 0.68 \end{bmatrix} \frac{kips}{g}$$

$$K = \begin{bmatrix} 9200 & -6550 \\ -6550 & 16700 \end{bmatrix} kips/in$$

$$T = \begin{bmatrix} 0.07 \\ 0.03 \end{bmatrix} seconds$$

$$\Phi = \begin{bmatrix} -0.86 & -0.50 \\ -0.50 & 0.86 \end{bmatrix}$$

The plastic moment and shear resultant of each precast pile in bent #2 are 45 ft-kip, and 10 kips, respectively. Bent #2 has a total shear strength of 190 kips which is greater than the shear resultant (100 kips for bent #2). Thus, plastic hinges will form prior to collapse. In bent #3, the plastic moment and shear resultant of each precast are 45 ft-kip, and 25 kips, respectively. The total shear strength of bent #3 is 190 kips which is less than the shear resultant (210 kips). Thus, plastic hinges will not form and the flexural capacity is limited to the shear strength. The strength of the shear friction connection between each bent and the deck is 250 kips. Applying

the 100 ground motions generated for this bridge site (site class D) to the bridge model, the shear demand from the ground motions is plotted against the PGA of each earthquake. The substructure capacity is shown using threshold values corresponding to the flexural capacity, strength of the shear friction connection, and the shear strength, as shown in Figure A-88.

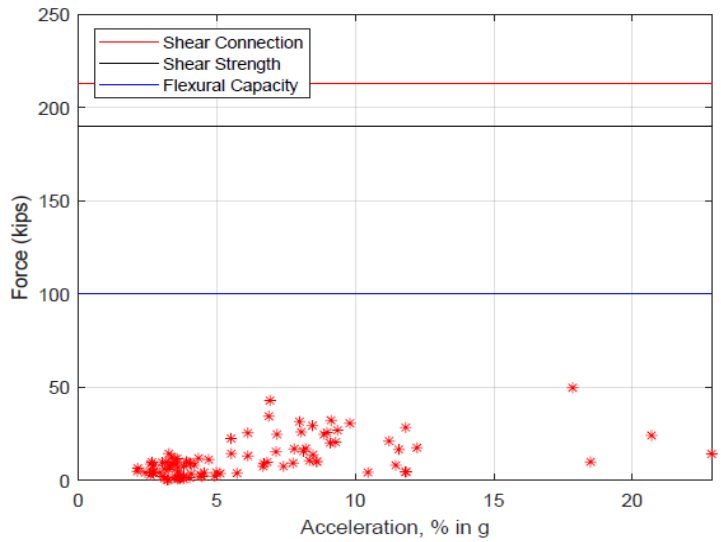

Figure A-88: Shear Demand Due to Applied Ground Motions – Transverse Direction

Based on the plot, the capacity of the substructure is not exceeded by the demand from the ground motions. The maximum displacement of the bridge due to the ground motions is less than 0.05”. Thus, the bridge is not vulnerable in the transverse direction at level of ground motions expected at its location.

Results – Longitudinal Direction

The piles are acting in parallel and modelled as fixed at the top of the bent cap and at the ground. This assumes that the ground provides adequate fixity at the base of the piles. The bridge is modelled as a single degree of freedom system, so the entire mass is used to obtain the period. The mass, stiffness, and period of the bridge in the longitudinal direction are 1.95 $kips/g$, 8340 $kips/in$, and 0.10 $seconds$, respectively.

In the longitudinal direction, the plastic moment and shear resultant of each pile in bent #2 are 45 ft-kip, and 8 kips, respectively. In bent #3, the plastic moment and shear resultant of each precast are 45 ft-kip, and 14 kips, respectively. The substructure has a total shear strength of

380 kips which is greater than the total shear resultant (220 kips). The strength of the shear friction connection between the substructure and the deck is 425 kips. Applying the 100 ground motions generated at this bridge site (site class D) to the bridge model, the shear demand from the ground motions (50 per fault orientation) is plotted against the peak ground acceleration (PGA) of each earthquake. The substructure capacity is shown using threshold values corresponding to the flexural capacity, strength of the shear friction connection, and the shear strength, as shown in Figure A-89.

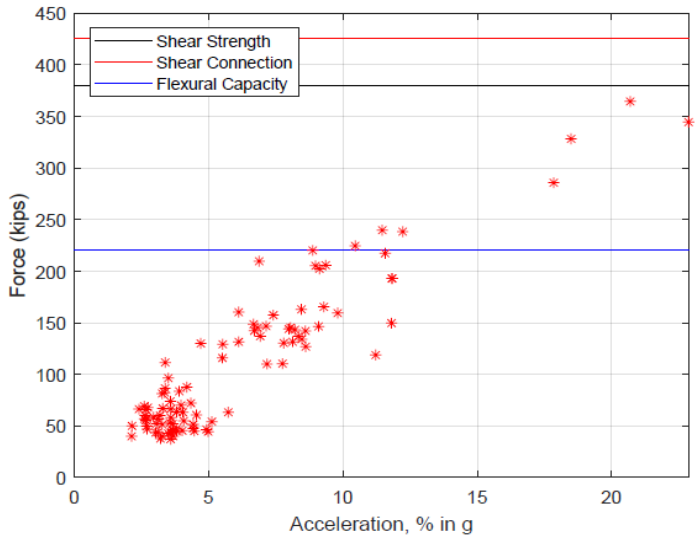

Figure A-89: Shear Demand Due to Applied Ground Motions – Longitudinal Direction

From the plot, the shear demand from the ground motions exceeds the flexural capacity of the substructure. The maximum displacement of the bridge due to the set of ground motions is greater than 0.05”. Additionally, since the shear strength of the substructure is not exceeded, the bridge is not vulnerable at the level of ground motions expected at its location.

20. Bridge Asset Name: 24-56-00899B

Table A.24: Specifications and Information on Bridge 24-56-00899B

Geographical Information	Asset Name	24-56-00899B
	NBI Number	005880
	County	Newton
	District	La Porte
	Year of Construction	1929, 1991
	Facility Carried	US 24
	Feature Intersected	Hunter Ditch
Superstructure Information	Superstructure Type	Reinforced Concrete Girder
	Number of Spans	1
	Span Lengths	28'-0"
	Deck Width	48'-6"
	Skew	0 degrees
	Concrete Compressive Strength	4000 psi
	Yield Strength of Reinforcement	60000 psi
	Abutment Type	Non-Integral
	Bearing Support Length	6"

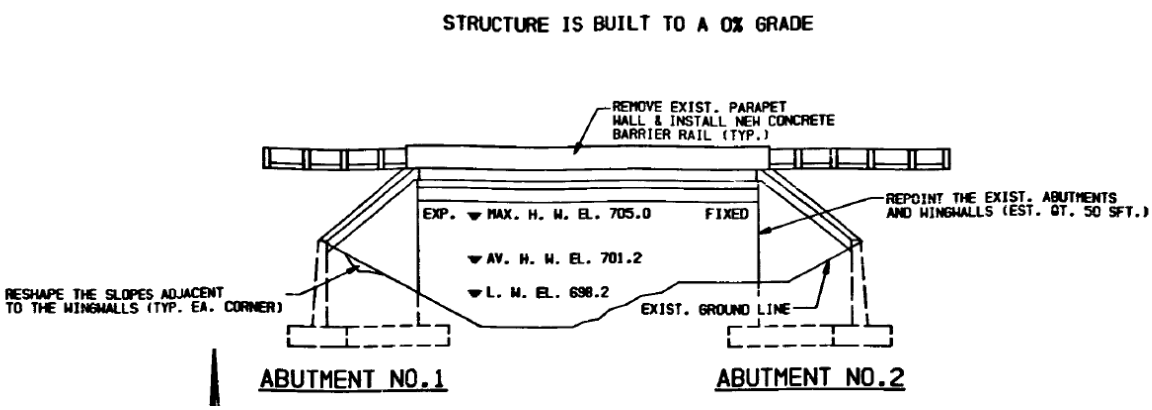

Figure A-90: Elevation View of the Bridge (INDOT, 1991)

According to Section 3-3, single span bridges are highly resistant to seismic demands, and have been excluded from the analysis in this thesis.

21. Bridge Asset Name: 67-28-00938A

Table A.25: Specifications and Information on Bridge 67-28-00938A

Geographical Information	Asset Name	67-28-00938A
	NBI Number	023770
	County	Greene
	District	Vincennes
	Year of Construction	1930, 1984
	Facility Carried	SR 67
	Feature Intersected	Brewer Ditch
Superstructure Information	Superstructure Type	Reinforced Concrete Slab
	Number of Spans	1
	Span Lengths	25'-0"
	Deck Width	46'-6"
	Skew	15 degrees
	Concrete Compressive Strength	4000 psi
	Yield Strength of Reinforcement	40000 psi
	Abutment Type	Non-Integral
	Bearing Support Length	1'-0"

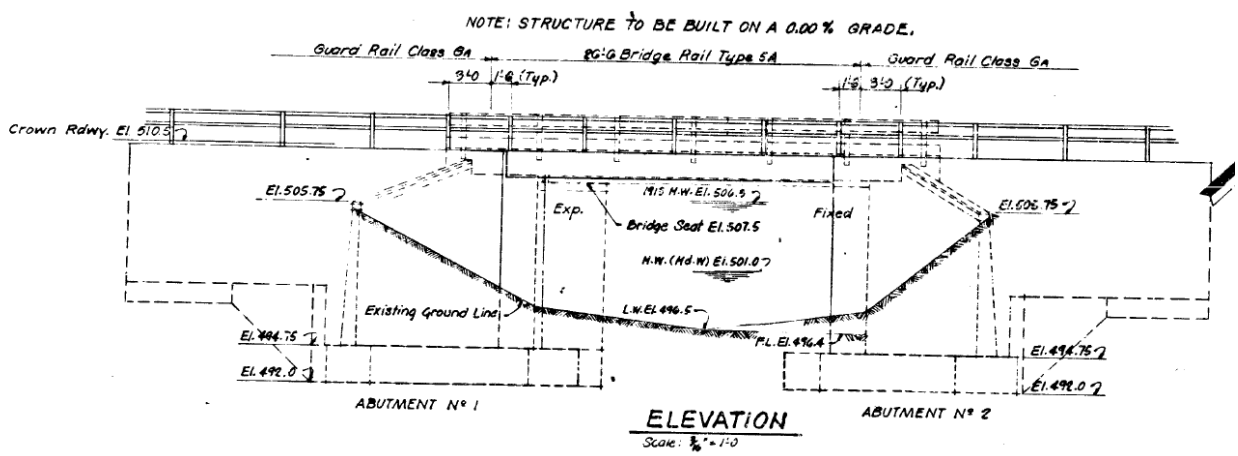

Figure A-91: Elevation View of the Bridge (INDOT, 1980)

According to Section 3-3, single span bridges are highly resistant to seismic demands, and have been excluded from the analysis in this thesis.

22. Bridge Asset Name: I69-30-9187NB

Table A.26: Specifications and Information on Bridge I69-30-9187NB

Geographical Information	Asset Name	I69-30-9187NB
	NBI Number	080114
	County	Gibson
	District	Vincennes
	Year of Construction	2012
	Facility Carried	I69 NB
	Feature Intersected	Wildlife Undercrossing
Superstructure Information	Superstructure Type	Reinforced Concrete Slab
	Number of Spans	1
	Span Lengths	29'-0"
	Deck Width	43'-4"
	Skew	0 degrees
	Concrete Compressive Strength	4000 psi
	Yield Strength of Reinforcement	60000 psi
	Abutment Type	Integral

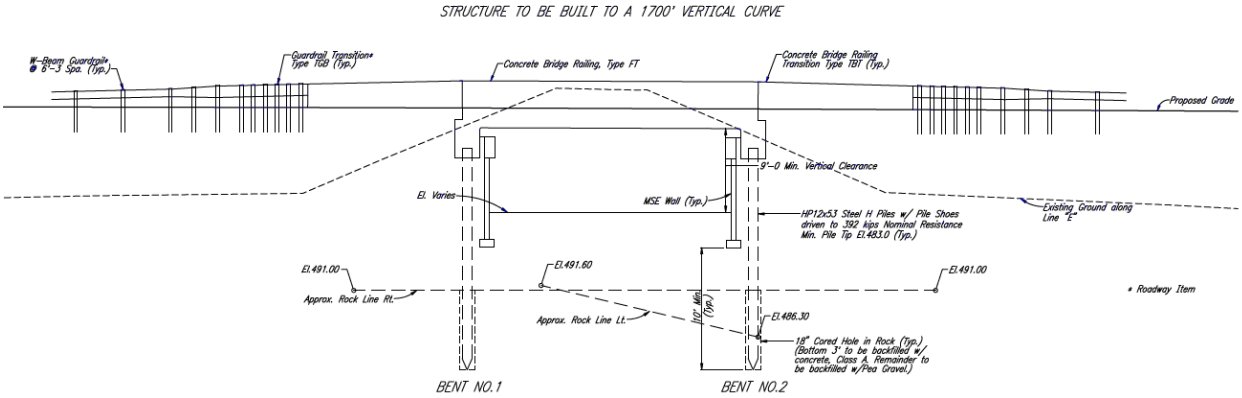

Figure A-92: Elevation View of the Bridge (INDOT, 2010)

According to Section 3-3, single span bridges are highly resistant to seismic demands, and have been excluded from the analysis in this thesis.